WAVELENGTH-DEPENDENCE OF HORSERADISH PEROXIDASE INACTIVATION BY SOFT X-RAYS

Peter Paraskevoudakis

A dissertation submitted in partial fulfillment

of the requirements for the degree of

Doctor of Philosophy in The

University of Michigan

1964

Doctoral Committee:

Professor G. Hoyt Whipple, Chairman
Assistant Professor Charles H. Burns
Assistant Professor Adon A. Gordus
Assistant Professor James F. Hogg
Professor William Kerr

TO TOULA

ACKNOWLEDGEMENTS

The author owes a great measure of gratitude to many people. First, it is a pleasure to acknowledge the patience, advice and assistance of each of the Committee members, and particularly, of the chairman. Special mention is due to Doctor A. H. Emmons who introduced me to this field, and to Doctor H. J. Gomberg for the original ideas and continuous encouragement which led to this investigation. The assistance in the laboratory of Messrs. R. Siemon B. Frisinger, J. Glore and S. Hasapoglou was invaluable. Many other members of the Phoenix Laboratory staff rendered expert assistance. Discussions of this research problem with a fellow student working on a similar problem, J. W. Baum, and his constructive criticisms were indispensable.

The untiring patience and constant encouragement of my wife have been a genuine contribution to the completion of this research. To my wife and my children I wish to express my deepest appreciation.

The support of this work by the U. S. Atomic Energy Commission and the Michigan Memorial Phoenix Project (Contract No. AT(11-1)-1205) is gratefully acknowledged.

TABLE OF CONTENTS

		Page
ACKNOWLEDGEMENTS		iii
LIST OF TABLES		vii
LIST OF FIGURES		viii
ABSTRACT		x
I.	INTRODUCTION	1
	A. Purpose of Study	1
	B. Experimental Approach	2
II.	BACKGROUND AND THEORY	5
	A. Review of Pertinent Literature	5
	B. The Biochemical System	13
	C. Mechanism of Horseradish Peroxidase Action	15
	1. Introduction	15
	2. Basis of Activity Determination	16
III.	EXPERIMENTAL PROCEDURES	20
	A. Horseradish Peroxidase Assay	20
	1. Materials Used	20
	2. Procedure of Beckman Analysis	21
	3. Determination of Horseradish Peroxidase Activity	21
	a. Measurements	21
	b. Calculations	23
	B. Radiation Sources Available	26
	1. Co^{60} γ-Ray Source	26
	2. Monochromatic X-Ray Source	27

TABLE OF CONTENTS (Continued)

		Page
	C. Irradiation Procedures.....	35
	1. Construction of Radiators and Filters	35
	2. Construction of Irradiation Cells.....	35
	3. Sample-Source Alignment.....	40
	4. Sample Irradiations.....	42
	D. Dosimetry.....	43
	1. Introduction.....	43
	2. The Absolute Dosimeter.....	45
	3. Calorimetric Measurements.....	50
	4. The Fricke Dosimeter.....	56
	5. Determination of Dose Rates Delivered in Sample.....	60
IV.	IRRADIATION EFFECTS ON HORSERADISH PEROXIDASE	65
	A. Bragg Spectrometer Technique.....	65
	B. Fluorescent X-Radiation Technique.....	67
	1. Dose-Effect Relation.....	67
	2. Energy Dependent Effect.....	69
	3. Effect of Dose Rate.....	74
	4. Some Useful Computations.....	77
	C. Absorption Spectrum of Horseradish Peroxidase	83
	D. Consideration of Errors.....	85
	1. Introduction.....	85
	2. Error of Measurements.....	86
V.	DISCUSSION.....	87
	A. Summary of Conclusions.....	87
	B. Discussion.....	88
	1. Modes of Horseradish Peroxidase Inactivation.....	88
	2. Energy Dependence Phenomena.....	90
APPENDIX 1	HORSERADISH PEROXIDASE KINETICS.....	94
	A. Introduction.....	94
	B. The "Theorell and Chance" Mechanism.....	95

TABLE OF CONTENTS (Continued)

		Page
	C. Experimental Studies of the Over-all Reaction.....	97
	D. The Alberty Mechanism	100
APPENDIX 2		108
	A. G Value Determination	108
	B. Dose Rate Determination	109
	1. LiF Crystal Spectrometer Technique	109
	2. Fluorescent Radiation Technique.	110
BIBLIOGRAPHY	.....	112

LIST OF TABLES

Table		Page
I	CALIBRATION OF THE CALORIMETER BY ELECTRICAL POWER.	54
II	A. X-RAY BEAM MEASUREMENTS AND G VALUE EVALUATIONS.	54
III	COMPARISON OF THE THREE SETS OF DATA AVAILABLE	59
IV	DETERMINATION OF THE DOSE RATES ABSORBED IN THE SAMPLE	59
V	DETERMINATION OF THE NUMBER OF MOLECULES PRESENT IN THE SAMPLE.	80
VI	STATISTICAL VARIATION OF HRP INACTIVATION BY FLUORESCENT X-RAY FOR AN ABSORBED DOSE OF 30 KRADS	81
VII	HRP G VALUES DETERMINATION	82

LIST OF FIGURES

Figure		Page
1	Over-all reaction rate versus enzyme concentration.....	25
2	Photograph of crystal diffraction assembly; the multi-slit collimator, the crystal, and the sample supporting gauge are in place.....	30
3	Crystal spectrometer calibration, Bragg angle versus energy.....	31
4	Photograph of fluorescent technique assembly: a) a Plexiglas dry box was made to prevent moisture collection on sample's surface b) sample and fluorescent box drawer in position.	33
5	Schematic representation of production of fluorescent x-ray beam.....	34
6	Photograph of radiators; one of them is mounted in the fluorescent box drawer at 45°.....	36
7	Schematic representation of typical sample of holder used.....	38
8	Photograph of sample holders.....	39
9	Relative optical density of fluorescent x-ray photographic image.....	41
10	Photograph of calorimeter, showing location of x-ray machine.....	46
11	Photograph of gold target for calorimeter.....	48
12	Schematic diagram of x-ray calorimeter.....	49
13	Schematic representation of calorimeter Wheatstone bridge and heater control circuit.....	51
14	Photograph of typical plot of data output from calorimeter.....	53

LIST OF FIGURES (Continued)

Figure		Page
15	Power calibration of the calorimeter; net slope vs. heat power input.....	55
16	Fe^{++} -Fe^{+++} calorimeter absorber; absorbance change vs. radiation exposure time.....	58
17	Fe^{++} -Fe^{+++} Dosimetry; absorbance change vs. radiation exposure time.....	61
18	The energy dependence of Fricke's dosimeter; G values between 5 and 9 Kev.....	63
19	LiF Crystal spectrometer irradiation; % HRP inactivation vs. photon energy for $3x10^{13}$ photons absorbed per sample.....	66
20	Dose effect curves; % HPR remaining activity vs. absorbed dose.....	70
21	Dose effect curves; % HRP remaining activity vs. absorbed dose.....	71
22	Dose effect curves; % HRP remaining activity vs. absorbed dose.....	72
23	X-ray fluorescent irradiations; % inactivation of HRP vs. photon energy at fixed doses.....	73
24	X-ray fluorescent irradiation; % HRP inactivation vs. photon energy at 30 Krads.....	75
25	Possible ways of representing the energy dependent effect; % HRP inactivation vs. photon energy at 30 Krads.....	76
26	Nickel fluorescent irradiation; % HRP remaining activity vs. absorbed dose at constant dose rate.....	78
27	Nickel fluorescent irradiation; % HRP remaining activity vs. absorbed dose at constant dose rate.....	79
28	HRP absorption spectrum; absorbance vs. wave length.....	84
29	HRP Kinetics at Constant (H_2O_2).....	101
30	HRP Kinetics at Infinite (G).....	102
31	HRP Kinetics at Constant (G).....	103
32	HRP Kinetics at Infinite (S).....	104

ABSTRACT

WAVELENGTH DEPENDENCE OF HORSERADISH PEROXIDASE INACTIVATION BY SOFT X-RAYS

Peter Paraskevoudakis

The purpose of this work was to determine if the inactivation of dilute solutions of horseradish peroxidase (HRP) by x-rays is energy dependent in the photon energy range from 5 to 9 Kev, and thus, to suggest that the energy dependence, found by Emmons,[#] was not a peculiar phenomenon displayed by catalase, but could be a general property of metalloproteins.

HRP solutions with protein concentration of 3.3×10^{-7} M were irradiated by monochromatic x-rays of 5 to 9 Kev photon energy. The results indicated that the HRP inactivation is energy dependent at fixed dose levels. The type of dependency is best described by a step curve. A photon with energy above 6.9 Kev is capable of producing twice as much radiation damage as a photon with energy below 6.9 Kev. Furthermore, the experimental error of an average value of 10 runs is less than ± 10 of per cent activity remaining at the 95 per cent confidence level.

The above HRP solutions were irradiated with nickel fluorescent radiations as a function of dose rate. The results indicated that the HRP inactivation is dose rate independent in the range from 645 to 64,000 rads/hr.

[#]A. H. Emmons, "Resonance Radiation Effects of Low Energy Monochromatic X-Rays on Catalase," Ph.D. Thesis, The University of Michigan, 1959.

A dose of 3×10^5 rads of mixed energy soft x-rays, delivered to a 2.5×10^{-5}M HRP solution resulted in a marked reduction of the peak at 403 mμ of the absorption spectrum of HRP. This reduction suggests destruction of the porphyrin ring.

It is concluded from these results that 1) HRP solutions exhibit an energy dependence in the region of the iron K-absorption edge, 2) this effect is not due to experimental error or dose rate dependence, and 3) the porphyrin ring is destroyed by radiation. To explain this effect, the author postulates the possibility of the existence of the HRP molecule as a whole in an excited state for a finite time interval. Afterwards the excited molecule splits into fragments. Since these fragments are highly reactive, they serve as connecting bridges between other HRP molecules. The data suggest that an amount of energy above 6.4 Kev is required to excite the HRP molecule. The iron atom and the porphyrin ring help in the absorption and localization of this large amount of energy in the HRP molecule because the absorption cross section of iron is considerably higher than the absorption cross section of carbon or oxygen in the energy range of 5 to 9 Kev.

I. INTRODUCTION

A. Purpose of Study

It is the purpose of this study to determine whether the radiation damage spectrum induced in horseradish peroxidase (HRP) in solution is photon energy dependent, and to contribute to the extremely sparse information on the energy dependence of biologically important effects of ionizing radiation.

The term "radiation damage spectrum" is equivalent to the term "action spectrum" extensively used by workers in the field of ultraviolet radiation effects except that it corresponds to photons in the soft x-ray region. In graphing action spectra, it is common to plot the ordinate as effect per photon absorbed. However, in graphing radiation damage spectra, it is common to plot the effect produced per unit energy absorbed as a function of the incoming photon energy.

The per cent HRP inactivation per unit[#] of energy absorbed in solution has been determined for various x-ray wave lengths in the region of the iron K-edge discontinuity. This region has been chosen because of the importance of the iron atom with respect to HRP enzymatic activity. In general, it might be expected that if energy dependence phenomena did occur they

---

[#]The word "unit" is used here to mean some arbitrary fixed absorbed dose rather than any conventional unit.

might be in the low energy x-ray region where absorption cross-sections are changing rapidly and where some (important in enzymatic activity) elements have large discontinuities in absorption. If the effect exists, it will be of particular importance in the porphyrin ring and in the iron atom. Furthermore, the prophyrin ring may be the key to energy transfer processes. But in order to explain the effect, more information will be required about the mechanism of enzyme inactivation which itself is very important in enzyme chemistry.

The present study was motivated by some very interesting and largely unexpected results from studies with monochromatic x-rays at this University.[43,4,29,37,103,10] In general, not only have there been very few experiments reported in the literature on the energy dependence of the effects of ionizing radiation, but also the techniques for making such experiments have not been well developed.

B. Experimental Approach

This thesis was designed 1) to confirm the results on catalase found by Emmons[37] and, 2) to prove that the energy dependence, found by Emmons, was not a peculiar phenomenon displayed by catalase, but a general property of metalloproteins. A number of improvements upon methods and techniques previously used were found to be necessary in order to investigate more definitively the question of energy dependence. Attention was directed to the following:

1) Selection of a better enzyme system, similar to catalase if possible, but less complex, less sensitive to tempera-

ture and light and, more sensitive to radiation, than catalase; moreover, an easy and accurate method of detection of radiation damage should exist or be developed.

2) Pursuit of better dosimetry than that applied in the catalase study. The uncertainty of dose measurement is a major factor of the uncertainty of the energy dependence effect. It is possible that an uncertainty of 25 per cent can mask the energy dependence effect.

3) Avoidance of introducing other factors which might affect the radiation sensitivity of the enzyme system. For example, organics or free radicals can be released by substances in contact with the enzyme solution during irradiation.

The enzyme horseradish peroxidase (HRP) meets all the mentioned specifications and is selected as the most suitable system for the investigation of the energy dependence effect (see Part II B). The ability of HRP to catalyze a specific chemical reaction was chosen for the measure of radiation effects on HRP. Any loss of the ability of the enzyme HRP to decompose H_2O_2 is designated as damage or inactivation. Radiation damage is defined as any loss of enzymatic activity produced by radiation with respect to the H_2O_2 decomposition. This method is the most sensitive and accurate method available (see Part II C).

A dosimetric technique, combining a total absorption calorimeter[49] especially designed for soft x-rays, with the ferrous-ferric dosimeter, was developed in order to determine absorbed dosages as accurately as possible (see Part III D).

A plexiglas sample holder with a thin mylar window was developed in order to avoid the scotch tape window used by Emmons. Plexiglas and mylar are known to be materials chemically inert. This sample holder was also used for the ferrous-ferric dosimetry (see Part III C).

II. BACKGROUND AND THEORY

A. Review of Pertinent Literature

The amount of reported research on energy dependence forms a very small part of the voluminous literature on radiation effects. The literature contains only a few x-ray energy dependence curves in which a great deal of confidence can be placed. Two major obstacles to definitive work in this area have been, 1) the unavailability of monochromatic x-ray beams of sufficient intensity and 2) the unreliable dosimetry. The relevant literature has been reviewed recently[3,7,9] and will not be repeated here. However, prior to describing the test system used in this study, it seems pertinent to review briefly some other studies completed at this Laboratory which motivated this thesis.

S. Manoylov,[69,70] summarizing a series of experiments in the USSR, concluded that x-radiation acted directly upon the iron atoms of iron-containing enzyme systems during whole body or isolated organ irradiation by filtered x-radiation from tubes with iron, copper, nickel, and cobalt anodes. Moreover, he reported that a difference did exist on the biological effect for x-rays emitted from tubes with iron or cobalt and nickel or copper anodes at the same dosages. In fact, Manoylov and Ivanov found that radiations from nickel and copper anodes were much more efficient in producing biological damage than radiations from

iron and cobalt, in other words, they found a wave length dependence. Manoylov attributed these effects to the absorption of photons by the K-electrons of the iron atom.

Analysis of Manoylov's speculations is difficult because he did not use monochromatic radiation; he measured the dose in roentgens and does not mention any conversion to rads or where and how the dose was measured. Thus, it is possible that more energy per unit mass was absorbed in his samples in the case of copper and nickel anodes although the exposure in roentgens was the same. Finally, he did not prove that the effect was due to the enzyme system destruction. Thus, the question of a wave length dependence remained open.

J. Garsou[43] studied organic halides dissolved in plastic films using a crystal spectrometer for the production of monochromatic x-radiation. The quantity of crystal violet produced during irradiation was determined spectrophotometrically and was used to compute the radiation yield per photon absorbed. Garsou reported that high radiation yield occurred at specific energies near the K edge of the target halide atom, but reproducibility difficulties introduced large uncertainties and the question of a wave length dependence still remained unresolved.

W. Clendinning[29] studied purified 1-bromobutane containing DPPH (diphenyl-picryl-hydrazyl) using fluorescent characteristic radiation (K_α and K_β of different elements). The radiation effect was determined spectrophotometrically from the disappearance of DPPH during irradiation, since DPPH reacts quantitatively with

1-bromobutane radicals produced by radiation. Clendinning did not observe any wave length dependence around the bromine K absorption edge.

M. Atkins[4] studied an organic compound of mercury (α-acetoxymercuri-β-methoxy hydrocinuamic ethyl ester) using fluorescent characteristic radiation and came to the same conclusion. The radiation effect was determined as the quantity of inorganic mercury released during irradiation per unit energy absorbed. Atkins reported no energy dependence around the mercury L edge.

A. Emmons[37] studied an isolated enzyme, namely catalase, using both techniques, the fluorescent and the crystal spectrometer, for the production of monochromatic x-radiation. The radiation effect was measured as the percentage of enzyme inactivation by radiation with respect to H_2O_2 decomposition. He reported a strong energy-dependent effect in three types of experiments: 1) photons of energies just above the energy of the iron K-absorption edge produced much more inactivation of catalase in solution than photons of any other energy, 2) the iron characteristic radiations (K_α and K_β) were much more efficient in producing damage of the enzyme in solution than the nickel and manganese characteristic radiations, and 3) the nickel and chromium characteristic radiations were more efficient than the iron and manganese characteristic radiations when the dry enzyme was irradiated. Moreover, the shape of the inactivation curve was a straight line on semi-log paper in the case of nickel and chromium characteristic

radiations and a curve indicating a multi-hit effect in the case of iron and manganese characteristic radiations.

In order to explain his results, Emmons suggested the possibility that some type of preferential energy transfer from catalase molecule to catalase molecule might account for the high number of inactivations observed per initial photon absorbed. He was not able to explain his results, but was forced to recognize the possibility of the existence of some new process.

A number of imperfections in experimental techniques could alter the results, but not appreciably change the energy dependence effect, e.g., the use of scotch tape, the dose rate measurements by a proportional photon counter, the extrapolation of the reaction rate vs. concentration curve to lower concentrations than the ones for which the reaction rate was determined experimentally. Thus, it was important to repeat the experiments with catalase solutions not only for the above reasons, but also because these effects were unique and this was the first thorough study of the effects of monochromatic radiations on a biologically important system.

I have duplicated these experiments.[#] My results[47,75] were somewhat different from Emmons' and indicated the following:

1) Using the crystal spectrometer, I found an energy dependence, but the total number of 7.5 Kev photons absorbed per ml to produce 50 per cent inactivation,

---

[#]My experiments on catalase were terminated prior to the beginning of the present investigation.

was higher by a factor of 6 than that found by Emmons.

2) Investigating the activity measurements for different enzyme preparations, I found[75] that large amounts of impurities or inactive catalase molecules were present in preparations made by Nutritional Biochemicals Corporation[#] which were not considered by Emmons. As a result, the number of active enzyme molecules per ml of solution was lower by a factor of 35 than the number reported by Emmons and, therefore, his statement that 23 molecules were inactivated per 6.9 Kev photon absorbed in solution is not correct.

3) The inactivation of catalase solutions by fluorescent radiation showed that the iron characteristic radiation was slightly more effective than the nickel and manganese characteristic radiations. Comparing the 50 per cent inactivation dosages, I found that the $LD_{50\%}^{Fe}$ was less by 20 per cent than $LD_{50\%}^{Ni}$ and less by 40 per cent than $LD_{50\%}^{Mn}$, while Emmons reported 500 and 700 per cent respectively.

After these results (note that the same technique and the same imperfections were followed in both cases), it can be stated that there is a wave length dependence, but that the number of molecules inactivated per photon absorbed is less than 1.0 and that the relative effectiveness of the iron fluorescent radiation is not as high as reported by Emmons, but of the order of 30 per cent higher than the nickel and manganese.

[#]Cleveland, Ohio.

Now one can ask the question, "How valid are these results and how much confidence can be put on them?" My opinion (especially of my own results) is that one cannot be certain about the effect for a number of reasons.

a) The dosimetry was not accurate enough in either case.

b) Scotch tape adhesive was in contact with the solution during irradiation in both cases and, therefore, release of organics or free radicals could alter the results.

c) High uncertainties existed in activity measurements in both cases.

d) High sensitivity of the enzyme could be due to other factors (temperature, light, etc.).

e) Control activity was low compared with sample kept in refrigerator.

f) The dose rate[#] was considerably higher at the front side than at the back side of the sample.

g) Protection against radiation could come from impurities present.

Thus, the work on catalase not only left the question open, but also made it more interesting and it is more important now to reinvestigate the problem more accurately with another biological system or even the same from a different point of view.

If the energy dependence effect exists, then it must be a new phenomenon and one can ask, "Is this phenomenon a property of the prophyrin ring or a general property of large protein molecules containing metal atoms?"

[#]Catalase inactivation is dose rate dependent.[37,6]

In view of all these questions, I selected another biochemical system to investigate the problem of wave length dependence which will be discussed in Section (IIB).

W. Wegst[103] studied mouse fibroblast cells designated as strain L, clone 929, using fluorescent characteristic radiation. The radiation effect was determined by two types of measurements: 1) the gross survival of the cells as a function of radiation dose at different wave lengths, and 2) the effect on glucose metabolism as a function of photon energy for a fixed dose. The glucose metabolism was determined through the production of carbon dioxide (aerobic metabolism).

Wegst reported that the survival of L strain cells, as measured by the dose in rads necessary to kill 25 per cent of the cells, varied by a factor of approximately 3, between 5.41 and 5.90 Kev. Also, the survival of the cells as measured by the dose in rads necessary to reduce the surviving fraction by 63 per cent along the exponential part of the survival curve varied by a factor of approximately 3.5, between 5.90 and 7.48 Kev. Finally, the production of carbon dioxide per milligram of precipitable cellular protein per unit dose varied by a factor of approximately 2, between 6.40 and 7.48 Kev.

Wegst concluded that certain metallic trace elements in the tissue cells are involved in producing the observed discontinuities in the radiation damage spectrum. In particular, the relative magnitudes of the depression of carbon dioxide production as a function of energy appear to parallel the relative magnitudes of the mass absorption cross section of the element iron. This may

indicate that the cytochrome enzymes are involved in the radiation induced depression of carbon dioxide production. Also, the relative magnitudes of the various methods of expressing cell survival as a function of energy seem to parallel the relative magnitudes of the mass absorption cross section of the element manganese.

Wegst did not postulate any hypothesis to explain the relation between x-ray absorption and cell death.

Finally, Baum[10] restudied the biochemical system catalase in an attempt to confirm or explain the effect found by Emmons. In his latest progress report, Baum reported that his results indicate that the energy dependence for inactivation of catalase by low energy x-rays is less than 31 per cent in the energy region from 5 to 7.5 Kev. This statement can be made with 95 per cent confidence and is based on statistical evaluation of 16 sets of data obtained with dose rates from 80 rad/hr to 51,600 rad/hr. Also, both crystalline and lyophilized catalase exhibited a dose rate dependence in the range 80 to 1600 rad/hr. The dose rate dependence curves were linear with slopes 31 rad/(rad/hr) and 60 rad(rad/hr) respectively.

Baum concluded[10] that the inactivation of catalase does not exhibit photon energy dependent phenomena. His results indicated a small effect which could not be distinguished from experimental error. Furthermore, Baum claims that experimental artifacts caused Emmons' energy dependence findings, e.g.,

1) Release of organics from scotch tape windows.

2) Change of enzyme sensitivity from one experiment to another.

3) Differences in heat exposure at different x-ray energies.

If the effect is due to free radicals released by the scotch tape adhesive, then the adhesive must be energy dependent. The enzyme sensitivity may change from one experiment to another, but this change is included in the experimental error. Differences in heat exposures are possible, since the x-ray tube is operated at a different current for each radiator, but the highest temperature is received for the manganese radiator and not the iron radiator.

B. The Biochemical System

On the one hand, horseradish peroxidase (designated by HRP) was selected for studying the energy dependence phenomena because of its similarities to catalase. On the other hand, it was of utmost importance that the new system be less complex and more stable in order to furnish reliable data. It was anticipated that the energy dependence displayed by catalase was a phenomenon occuring in metalloproteins and that its magnitude was not large enough to permit accurate and indubitable measurements with the catalase system.

HRP has a molecular weight of 40,000 and contains one atom of iron per molecule, while catalase with a molecular weight of 225,000, contains four iron atoms per molecule. Thus, the fractional iron content of the two enzymes is about the same. Moreover, the prosthetic group hematin containing the iron atom is the same for both enzymes. Hematin is a complex formed between protoporphyrin IX and ferric ion, and its chloride derivative is called hemin. In general, porphyrins (for more details see re: 42)

form complexes with metal ions of iron, copper, manganese, magnesium and zinc, of which the most common are the iron complexes called hemes. Catalase and peroxidase are heme proteins in which the iron is in the ferric state. The mode of linkage between the ferriheme moiety and the protein portion of these enzymes has not been elucidated yet, but studies on crystalline HRP suggest that carboxylic groups of the protein may be involved. In any event, the participation of imidazole groups appears to be unlikely.[42]

In general, the peroxidases are conjugated proteins found largely in plant tissues. The type of reaction catalyzed by these enzymes may be written:

$$AH_2 + H_2O_2 \xrightarrow{\text{enzyme}} A + 2\ H_2O$$

where AH_2 is a hydrogen donor, e.g., a phenol or ascorbic acid. The peroxidase that has been studied most closely is horseradish peroxidase which has been crystallized by Theorell.[96,98] This conjugated protein contains 1.47 per cent hemin[42] and its protein fraction is inactive catalytically. Peroxidase is a protein comparable to methemoglobin in which the iron is in the ferric state, as it is in HRP. The composition of HRP is:[24]

Carbon	47.00%
Oxygen	32.00
Nitrogen	13.20
Hydrogen	7.25
Sulfur	0.43
Iron	0.127

Other properties of HRP are:

Isoelectric point:	7.2
Solubility:	5 g/100 ml of water
Thermal stability of solutions used:	stable for weeks at 25°C

An advantage of HRP over catalase is its far greater stability in water solutions.

A technique has been developed[24,26] which permits one to measure the reaction rate at which the donor oxidation occurs, and, thus in turn, to determine the HRP concentration.

C. Mechanism of Horseradish Peroxidase Action

1. Introduction

Both catalase and peroxidase combine with their substrate to form more than one enzyme-substrate complex. The specificity for the substrate is high; only H_2O_2 and monoalcylhydroperoxides are able to combine with these enzymes.[26]

Some of these enzyme-substrate complexes, in a second reaction sequence, can oxidize a hydrogen donor molecule. If this donor happens to be H_2O_2, we speak of catalatic activity and if other hydrogen donors are oxidized, of peroxidatic activity. Catalase can exhibit both activities, whereas peroxidase can act only peroxidatically, therefore, only the peroxidatic mode of enzyme action will be considered here.

Four enzyme complexes with H_2O_2 are known for protohemin-containing peroxidases and catalases: complex (I) green, complex (II) pale red, complex (III) bright red, and complex (IV) light green.

The kinetics of enzyme-substrate compounds of catalase are distinguished from those of HRP by the fact that the former require only the green compound (I) whereas the latter require both the green and the pale red complexes (I) and (II); complexes (III) and (IV) are apparently unnecessary for either. Under the usual experimental conditions for the catalytic function of peroxidase, the

values of the various velocity constants involved in the reaction have such magnitudes that the pale red complex (II) is the Michaelis or rate-limiting enzyme-substrate compound in peroxidase action. The same is true for the green complex (I) in catalase action. The kinetics of both enzyme-substrate compounds follow a mathematical solution of an extension of the theory of Michaelis over a wide range of experimental conditions and with considerable accuracy. Thus, the mechanism of peroxidatic action can be explained by the following formulation:

$$E + S \underset{k_2}{\overset{k_1}{\rightleftarrows}} [ES]_I \qquad \text{complex (I) green}$$

$$[ES]_I + AH_2 \overset{k_3}{\rightleftarrows} [ES]_{II} \qquad \text{complex (II) red} \qquad (1)$$

$$[ES]_{II} + AH_2 \xrightarrow{k_4} E + 2A + P$$

where: E = enzyme

S = substrate (H_2O_2)

P = other products (H_2O)

AH_2 = hydrogen donor

A = hydrogen donor oxidized

Any sound procedure for activity determination should depend, if possible, on the measurement of only one reaction velocity constant of the enzymic mechanism (k_4 for example).

2. Basis of Activity Determination

One of the most favorable assay methods for peroxidases involves the oxidation of guaiacol. This compound, catechol monomethyl ether, serves as the hydrogen donor and, on oxidation

with peroxidase and H_2O_2, forms tetraguaiacol. Tetraguaiacol solutions have a red-brown (rather orange) color which begins to fade a few minutes after its formation. The concentrations of such solutions can easily be determined colorimetrically or spectrophotometrically if the measurements are made within a few minutes.

The rate of utilization of H_2O_2, $\frac{\Delta [S]}{\Delta t}$, to form the colored reaction product, as measured at 470 mμ, depends on the respective concentrations of substrate and donor as follows:

$$\frac{\Delta [S]}{\Delta t} = \frac{[E]}{\frac{1}{k_1[S_o]} + \frac{1}{k_4[G_o]}} \qquad (2)$$

where: $[E]$ = enzyme concentration

$[S_o]$ = initial substrate concentration

$[G_o]$ = AH_2 = initial donor concentration

k_1 = reaction rate constant for the combination of the enzyme with the substrate

k_3 = reaction rate constant for the transition of enzyme-substrate complex (I) to complex (II)

k_4 = reaction rate constant for the combination of the enzyme-substrate complex (II) with the donor

(Equations (1) and (2) have been derived by Chance,[24] full description is given in Appendix 1).

Because the rate constants of the opposing reactions are very small compared with k_1, k_3, and k_4, the initial conditions of $[G_o]$ and

$[S_o]$ can be chosen so that one of the denominator terms is very small compared to the other.

If $k_4 [G_o] \gg k_1 [S_o]$, then the H_2O_2 utilization rate is independent of donor concentration, and,

$$\frac{\Delta [S]}{\Delta t} \approx k_1 [S_o][E] \qquad (3)$$

Therefore, k_1 can be evaluated. If, on the other hand, $k_4[G_o] \ll k_1[S_o]$ then the H_2O_2 utilization rate is independent of substrate concentration, and,

$$\frac{\Delta [S]}{\Delta t} \approx k_4[G_o][E] \qquad (4)$$

In this case k_4 can be evaluated. The latter is a highly desirable condition for peroxidase assay, because convenient zero-order[#] kinetics with respect to H_2O_2 and a high value of the turnover number are obtained with a low substrate concentration; high substrate concentrations inactivate peroxidase more than do high donor concentrations.

A single number representing the figure of merit[##] for HRP following the mechanism described above may be defined as either k_1 or k_4, but the total merit should be specified by both k_1 and k_4. The Michaelis constant K_m for such a system is not a true constant, for it is proportional to the donor concentration.

[#]Actually the over-all reaction is second order, because it depends on both the substrate and donor concentration.

[##]By figure of merit, I mean the ability of HRP to catalyze a specific chemical reaction.

The activity increases linearly with the donor concentration provided that the substrate concentration is sufficient, that is

$$[S] >> \frac{k_4[G] + k_2}{k_1} = K_m^{\#} \qquad (5)$$

Thus, "optimum" activity would be found at infinite concentrations of substrate and donor. This optimum activity can be defined as the total figure of merit for HRP (see Appendix 1 for more details).

$^{\#}K_m$ is defined as the dissociation constant of $[ES]_{II}$ under the assumption that $k_1 \gg k_4$ which is valid for HRP. However, the substrate concentration required for the attainment of half-maximal velocity is a characteristic constant of an enzyme catalyzed reaction and equals K_m. This property has been used extensively as definition of K_m since K_m is expressed in concentration units M.
Chance[20-24] found the following values:

$k_1 = 0.9 \times 10^7\ M^{-1}\ sec^{-1}$
$k_2 = 5\ sec^{-1}$
$k_4 = 2.5 \times 10^5\ M^{-1}\ sec^{-1}$
$K_m = 12 \times 10^{-6}\ M$

III. EXPERIMENTAL PROCEDURES

A. Horseradish Peroxidase Assay

1. Materials used

a) dry HRP preparation from Nutritional Biochemicals Corporation, Cleveland 28, Ohio.

b) Guaiacol from Eastman Organic Chemicals of Rochester, New York.

c) A 3% analytical reagent solution of hydrogen peroxide.

d) Reagent grade of phosphate salts.

e) Deionized double distilled water.

Stock solutions[#] were prepared as follows:

a) 13.6 mg/l of dry enzyme preparation in $\frac{1}{15}$M phosphate buffer pH = 6.9, i.e., 3.3×10^{-7}M.

b) 0.22 ml guaiacol in 100 ml double distilled water, i.e., $\sim 2 \times 10^{-2}$M.

c) 1 ml 3% reagent hydrogen peroxide in 100 ml buffer, i.e., 8.8×10^{-3}M.

The stock solutions were placed in the deep freeze at 20°C and for routine analysis were further diluted by a factor of 60 in the Beckman cuvette so that at the moment the reaction was started the initial concentrations[#] were:

[#]The initial concentrations of substrate $[S_o]$ and hydrogen donor $[G_o]$ were adjusted so that zero order kinetics were obtained ($k_4[G_o] \ll k_1[S_o]$ and were kept constant throughout this study.

a) enzyme [E] $\approx 5.6 \times 10^{-9}$M or 0.225 mg/l

b) guaiacol [G_o] $\approx 3.3 \times 10^{-4}$M

c) hydrogen peroxide [S_o] $\approx 1.4 \times 10^{-4}$M

2. Procedure of Beckman spectrophotometer analysis

An amount of enzyme stock solution equal to 50 μl was placed in a Beckman cell together with 50 μl of guaiacol stock solution in 2.85 ml of 0.01 M phosphate buffer solution of pH = 7. After positioning the cell in the DU spectrophotometer, the % transmission was adjusted at 470 mμ so that the recorder indicates 0% with the shutter closed and 100% with the shutter open. Thus, the absorption due to the enzyme, other protein impurities, guaiacol, and possible dirt present on optical surfaces of the cell was eliminated. Then 50 μl of the H_2O_2 stock solution was added to make a total volume of 3 ml, the mixed solution was stirred and the Beckman housing which was kept at 25°C (by circulating water from a constant temperature bath) was closed. Then the shutter was opened and the reaction could be followed continuously by recording the % transmission, T, as a function of time. The absorption of H_2O_2 at 470 mμ is negligible. This record plot was replotted on one cycle semi-log paper with time on the linear scale. The over-all reaction rate K was evaluated according to Equation (9).

3. Determination of horseradish peroxidase activity

a. Measurements. The rate constants for all the intermediate reactions between horseradish peroxidase and its substrate have been measured by Chance, and since $k_1 >> k_4$, as derived by Chance,[24] [G_o] and [S_o] can be chosen so that condition $k_4[G_o] << k_1[S_o]$ holds, in which case we get

$$\frac{\Delta [S]}{\Delta t} = k_4 [G_o] [E] \qquad \text{(See Eq. 4, page 18)}$$

where: $\Delta [S] = H_2O_2$ utilized in time Δt

$\Delta [S]$ may be evaluated from the formation of tetraguaiacol. Measurements of tetraguaiacol concentrations can be made, for example, using the Beckman DU spectrophotometer at 470 mμ. The extinction coefficient of tetraguaiacol at 470 mμ is $\epsilon = 26.6\ mM^{-1}cm^{-1}$ (24) and since 4 moles of H_2O_2 are required to form 1 mole of tetraguaiacol:

$$\Delta [S] = \Delta [H_2O_2] = 4x \frac{\Delta A}{\epsilon}$$

where: ΔA = change of absorbance in time Δt due to tetraguaiacol formation per 1 cm. light path

A = Absorbance = $\log \frac{1}{T} = -\log T$ where T is the % transmission.

ϵ = the absorbance of a molar concentration at a certain wave length per cm of light path,

if the absorbance at time t_o is A_o and at time t is A where $t - t_o = \Delta t$ then

$$\Delta [S] = \frac{4}{\epsilon} (A - A_o) = \frac{4}{\epsilon} \left(\log \frac{1}{T} - \log \frac{1}{T_o}\right)$$

Then

$$\Delta [S] = \frac{4}{\epsilon} \log \frac{T_o}{T} \qquad (6)$$

Substituting back to (4) one gets:

$$\frac{1}{\Delta t} \frac{4}{\epsilon} \log \frac{T_o}{T} = k_4 [G_o] [E]$$

or

$$\log \frac{T_o}{T} = \frac{1}{4} k_4 \epsilon [G_o] [E] \Delta t = K \Delta t \qquad (7)$$

where:

$$K = \frac{1}{4} \epsilon k_4 [G_o][E] \tag{8}$$

Hence a semilog plot of T vs t should give a straight line with slope -K passing from $T = T_o$ at $t = 0$.

A special attachment on the DU spectrophotometer permits the continuous recording of % transmission versus time. If this record is replotted on semilog paper with T on the log scale, a straight line is obtained. The t_o time might be obtained by extrapolation to $T = T_o$, but the slope K can be evaluated using Equation (9) over the time interval t_1 to t_2, i.e., $\Delta t = t_2 - t_1$ equally well and t_o is not needed.

Therefore:

$$K = \frac{\log \frac{T_1}{T_2}}{t_2 - t_1} \quad \sec^{-1} \tag{9}$$

This K I call the over-all reaction rate constant, the one which has been measured. In other words, K is the change of absorbance per unit time. Relation (9) has been used throughout this study since K is related directly to enzymatic activity.

b. Calculations. In practice, it was decided to use the same dry enzyme preparation throughout this study, to determine k_1, k_4, K_m, and K_{max} (at infinite substrate and donor concentrations) for this preparation, and to use the value of k_4 as a routine check of the above dry HRP preparation (see Appendix 1 for k_1, K_m, and K_{max} determination).

Relation (8) can be written:

$$K = 1/4 \epsilon k_4[G_o][E] = k[E] \text{ or } k = \frac{K}{[E]} \quad (10)$$

where: $k = 1/4 \epsilon k_4[G_o]$

or: $$k_4 = \frac{4}{\epsilon[G_o]} \frac{K}{[E]} = 0.456 \frac{K}{[E]} = 0.456k \quad (11)$$

where: $\epsilon = 26.6 \text{ mM}^{-1} \text{ cm}^{-1}$ at 470 mμ

$[G_o] = 3.3 \times 10^{-4}$ M guaiacol

Therefore, by measuring K for a known [E], k can be established and hence k_4. In practice, however, [E] is not known because of impurities present. Then by weighing the dry enzyme in a microbalance, a solution can be made of concentration C(mg/l) of dry powder added. Thus, it is possible to vary C and to measure the corresponding K's according to (9) above. Then a linear plot of K vs C must be a straight line through the origin with slope $k' = \frac{K}{C}$. The concentration C will be identical to [E] for pure enzyme preparation, in which case k' = k. One can use as a standard the best purified enzyme available. Chance[26] reported a value $k_4 = 2.4 \times 10^5 \text{M}^{-1}\text{sec}^{-1}$ at 25°C. Using this value as a standard for HRP activity, I evaluated k

$$k = k_4/0.456 = 5.26 \times 10^5 \text{M}^{-1}\text{sec}^{-1}$$

This value should be compared with the experimentally determined k' = K/C from Figure 1, which is a plot of K vs C (C being the enzyme concentration in mg/l of the dry preparation[#] used in the Beckman cuvette). C varied from 0.09 to 1.0 mg/l. The value of the ratio k/k' will give a relative index of enzyme purity. From Figure 1, $K = 4.5 \times 10^{-5}$ at C = 1 mg/l for $[G_o] = 3.3 \times 10^{-4}$ M

[#]Dry preparation by Nutritional Biochemicals Corp. of Cleveland, Ohio.

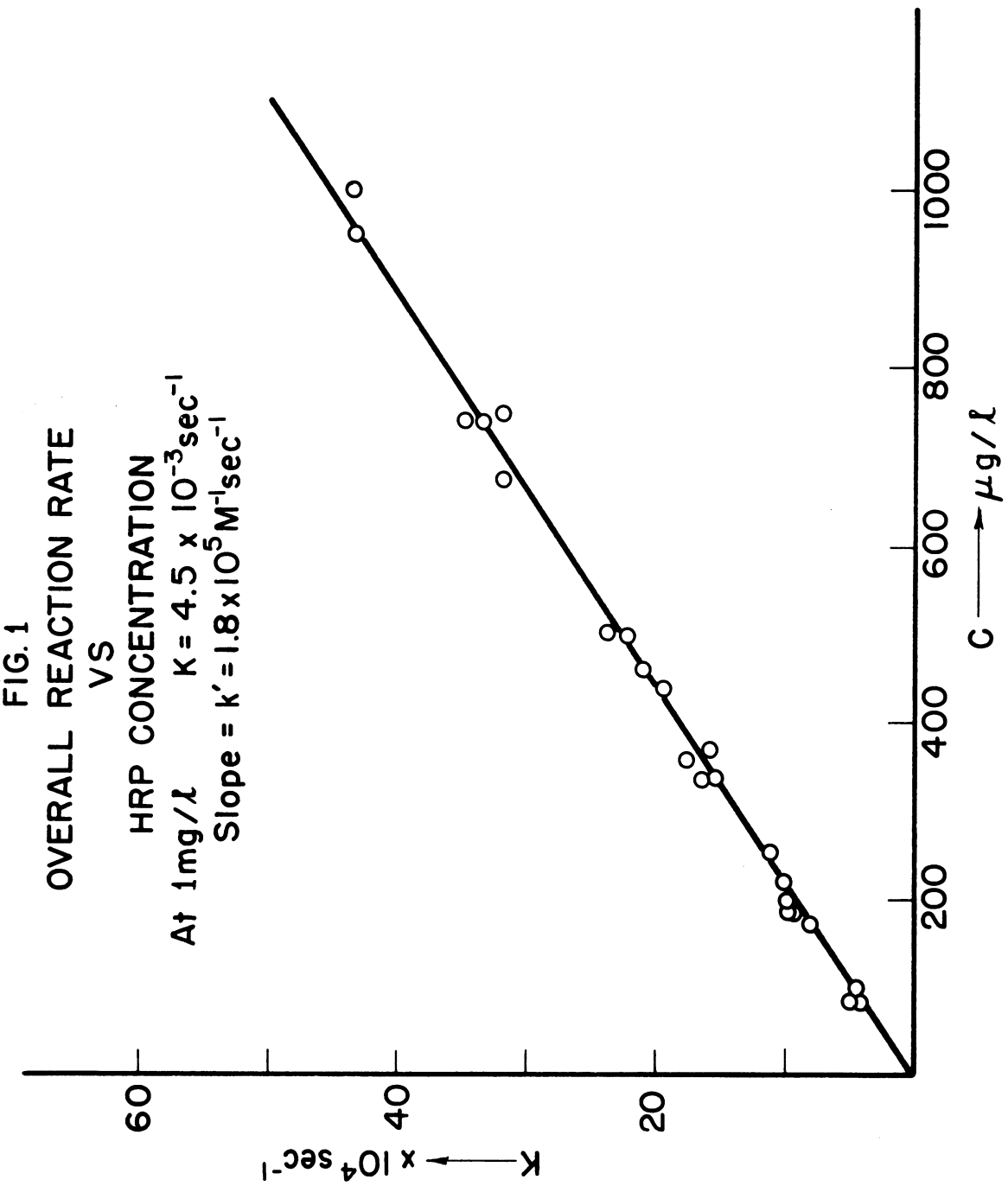
FIG. 1
OVERALL REACTION RATE
VS
HRP CONCENTRATION
At 1mg/l K = 4.5 x 10⁻³sec⁻¹
Slope = k' = 1.8x10⁵M⁻¹sec⁻¹
K ⟶ x 10⁴ sec⁻¹
60
40
20
200
400
600
800
1000
C ⟶ µg/l

(the initial guaiacol concentration [G_o] was kept constant throughout this study). Therefore

$$k' = \frac{4.5 \times 10^{-3} \text{sec}^{-1}}{1 \text{ mg/l}} = \frac{4.5 \text{ sec}^{-1}}{1 \text{g/l}} = \frac{4.5 \times 40{,}000 \text{ sec}^{-1}}{\text{M}} =$$

$$1.8 \times 10^{5} \text{M}^{-1} \text{ sec}^{-1}$$

and $k/k' = 5.26/1.8 = 2.92 \approx 3$

Thus, the enzyme preparation used was less active, by a factor of 3 than the purest enzyme reported in literature, indicating the presence of impurities. These impurities might be inactivated enzyme molecules, heme groups not connected with protein, or other protein residues.

After k' is established, the concentration of any enzyme solution of the same dry enzyme preparation (of course within the range of plot 1) can be evaluated simply by measuring K. If K is in sec^{-1} and C is in M, then:

$$C = K/k' = K/1.8 \times 10^{5} = 5.55 \times 10^{-6} \text{ K}$$

In practice, K's were determined as an average of 4 Beckman runs (at 0.225 mg/l concentration level for the control) for the irradiated sample, for the control under the same physical and chemical conditions, and for the stock solution kept in the refrigerator.[#] Since K is proportional to C, then $K_s/K_c = C_s/C_c$ is the fraction of remaining activity. Next $(1-K_s/K_c) \times 100$ is defined as the per cent of HRP inactivation.

B. Radiation Sources Available

1. Co^{60} γ-ray source

[#]The stock solution measurements were used only to check the control and to confirm the stability of the HRP solution.

The large PML Co^{60} irradiation source was used for preliminary studies. The energy of the emitted γ-rays is 1.17 and 1.13 Mev. Although the photon energies of Co^{60} are so high that the predominant reaction with the target atom is Compton scattering rather than photoelectric absorption, cobalt irradiations are still useful in this study for certain comparative measurements. The high photon intensities, considerable range of dose rates available, uniformity of radiation field throughout the sample, large volumes of radiation space available and the simplicity of operation of the cobalt source made its use very attractive for screening studies. The PML Co^{60} source had an activity of approximately 2000 curies and was calibrated with the Fricke dosimeter. The physical arrangement of the source has been described elsewhere.[7,8]

2. Monochromatic x-ray source

Two General Electric x-ray diffraction units, model XRD-5 operated with a Machlett AEG-50 tungsten target beryllium window x-ray tube were used throughout this study. The power supply of this model provides a voltage range from 10-50 KVP and a current range of 1-50 mA. The output intensity of these units is very high, approximately two million r per minute at the window with maximum voltage and current. The spectrum of the x-ray beam, which will be referred to as the white beam, is the usual continuous x-ray spectrum depending on the applied voltage with the characteristic tungsten lines superimposed. Specialized techniques must be used with this white beam to obtain the highest possible intensity of monochromatic x-rays. The necessity of obtaining a

high beam intensity was one of the early problems which required a considerable expenditure of effort and which resulted in the development of a technique of using fluorescent radiation as the source of monochromatic radiation.

In general, there are two methods for obtaining monochromatic x-ray beams. The first is to utilize the Bragg spectrometer (7,11,13) and a standard crystal with a known lattice constant, high reflectivity and small mosaic spread. High energy resolution can be obtained by using a very narrow collimated beam, but unfortunately the radiation intensity which can be obtained is so low that it cannot be used for the purpose of this study. As successively larger collimator widths are used to obtain higher intensity beams, the energy resolution worsens rapidly. Calculations and an experimental analysis[5] have shown that to obtain the source intensity used by Garsou in his study, for example, the width at half maximum intensity would have to be almost 1000 ev, while it was about 500 ev for the beam used by Emmons.[37] It is apparent that the difficulties of obtaining sufficient intensity with good energy resolution are severe. One possible solution is to use a number of narrow parallel slits close together so that they produce parallel beams with the same incident angle on the crystal. The high resolution standard soller slit[#] suitably modified, was used to collimate the high intensity beam of the AEG-50 Machlett x-ray tube, which is one of the highest intensity tubes available commercially. The spectrogoniometer with a LiF crystal (see Fig. 2) was calibrated by identifying

---

[#]Provided by G.E. (Ref. 105), Direction 11690 C.

K-absorption edges and some of the characteristic emission lines of the tungsten target (see Fig. 3). The resolution of the combined beam, consisting of about ten narrow parallel beams collimated by the above soller slit, was measured[48] by a double spectrometer. The width at half maximum was less than 80 ev at 7.1 Kev photon energy while almost no photons were present outside a $\pm$100 ev region for 14 KVP applied to the tube. As the voltage increases above 15 KVP, second order reflections begin to appear and at 30 KVP, which is the potential used, the second order contamination amounts to 18 per cent of the total.[48] This is the best resolution ever achieved with a relatively high intensity monochromatic x-ray beam. But unfortunately, the dose rate at the sample of the order of 100 rads/hour was still too low and long irradiation times were required (around 140 hours) to obtain the necessary dose. As a result of these difficulties the LiF crystal spectrometer was used in the present work only for supporting studies.

The second method of producing monochromatic x-radiation is to use the characteristic fluorescent x-rays generated when a target atom is excited by high energy photons. The wave lengths of the emitted fluorescent x-rays will be discrete and dependent on the atomic number of the target material. The standard arrangement of the apparatus for fluorescence analysis provided with the XRD x-ray unit (see Figures 4 and 5) was used with the following modifications: 1) the sample was replaced by the particular element whose characteristic radiation was to be used for irradiation and which served as the source of the fluorescent beam

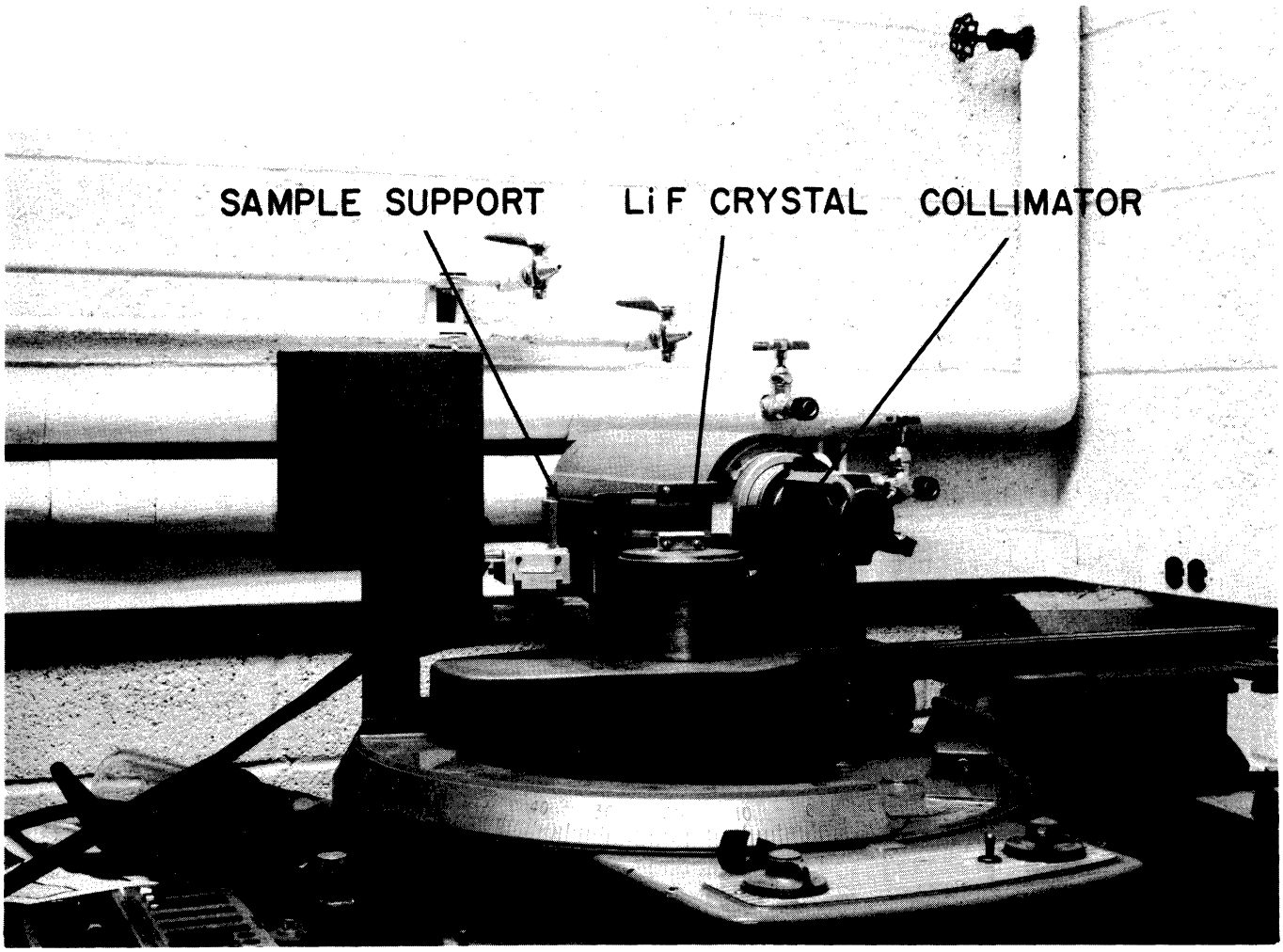

Fig. 2. Photograph of crystal diffraction assembly; the multislit collimator, the crystal, and the sample supporting gauge are in place.

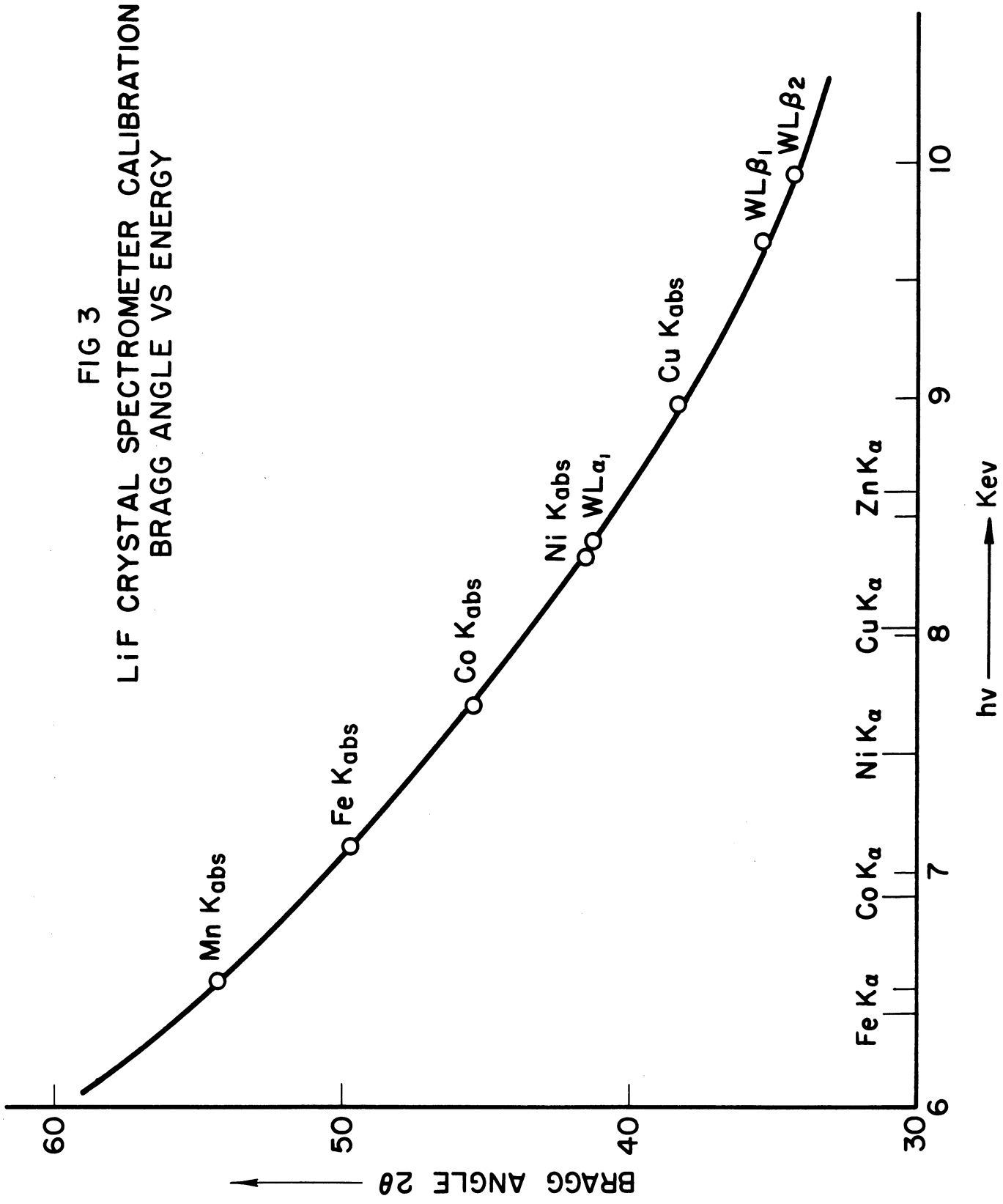
FIG 3
LiF CRYSTAL SPECTROMETER CALIBRATION
BRAGG ANGLE VS ENERGY
BRAGG ANGLE 2θ
60
50
40
30
Mn Kabs
Fe Kabs
Co Kabs
Ni Kabs
WLα1
Cu Kabs
WLβ1
WLβ2
Fe Kα
Co Kα
Ni Kα
Cu Kα
Zn Kα
6
7
8
9
10
hv
Kev

[special plexiglas holders shown in Figure 6 were prepared, and the element was placed so that it presented a 5/4" x 5/4" target area at 45° to the white beam], 2) the exit window of the fluorescent beam was enlarged in an effort to increase the beam intensity, and 3) a special shelf was constructed and fastened to the irradiation box just below the exit window of the fluorescent beam in order to support the sample holder. The geometrical arrangement of the equipment used with the fluorescent irradiation technique is shown in Figures 4 and 5. This modified technique was developed in this laboratory and has been fully described.[5,4,29,37,103,50,27] Thus, the details will not be repeated here.

The resulting radiation was analyzed by crystal diffraction techniques to determine the monochromaticity of the fluorescent beam produced by each one of the radiators used. The results of this analysis indicate that the fluorescent beam consists primarily of K_α emission radiation accompanied by small amount of K_β emission radiation of the particular element used as a radiator. The difference in wave length between K_α and K_β photon energies for any of the five elements used as radiators is less than 11 per cent. The fluorescent beam was contaminated by less than 14 per cent of the total by K_β and less than 2 per cent by continuous radiation (resulting chiefly from Compton and Thompson scattering of the direct beam by the radiator). A filter was used to reduce the K_β contamination when necessary. The filter was a thin absorber of an element with atomic number one less than that of the radiator element. With the filter the K_β contamination was

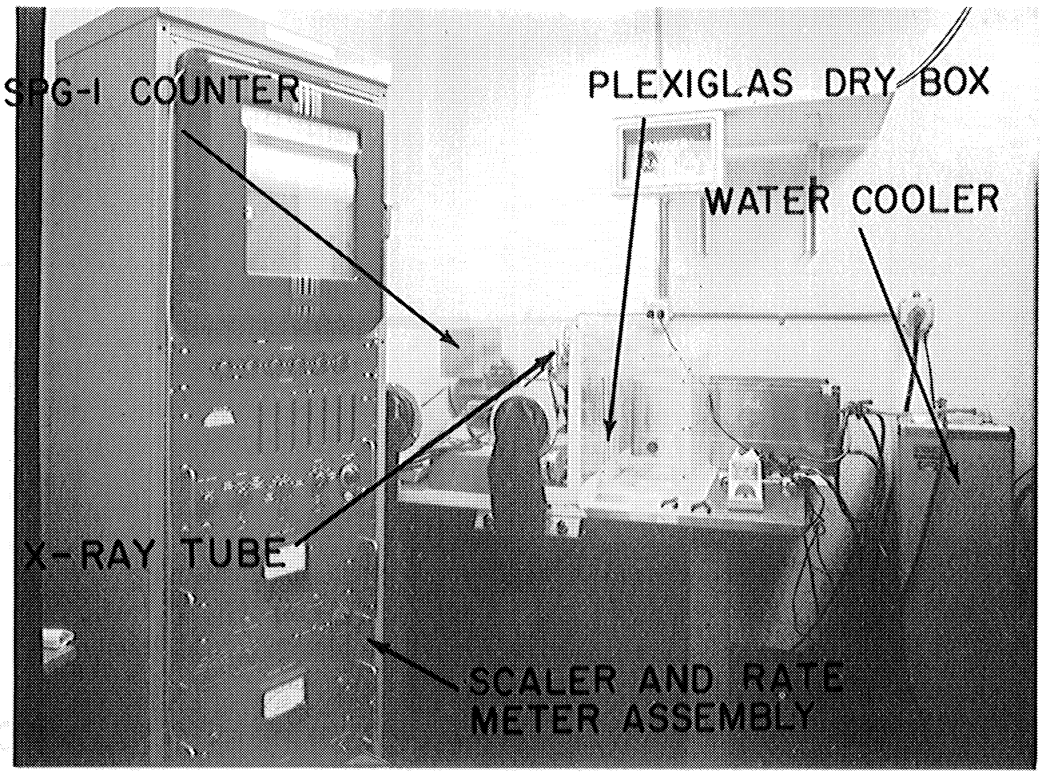

Fig. 4a. Photograph of fluorescent technique assembly; a Plexiglas dry box was made to prevent moisture collection on sample's surface.

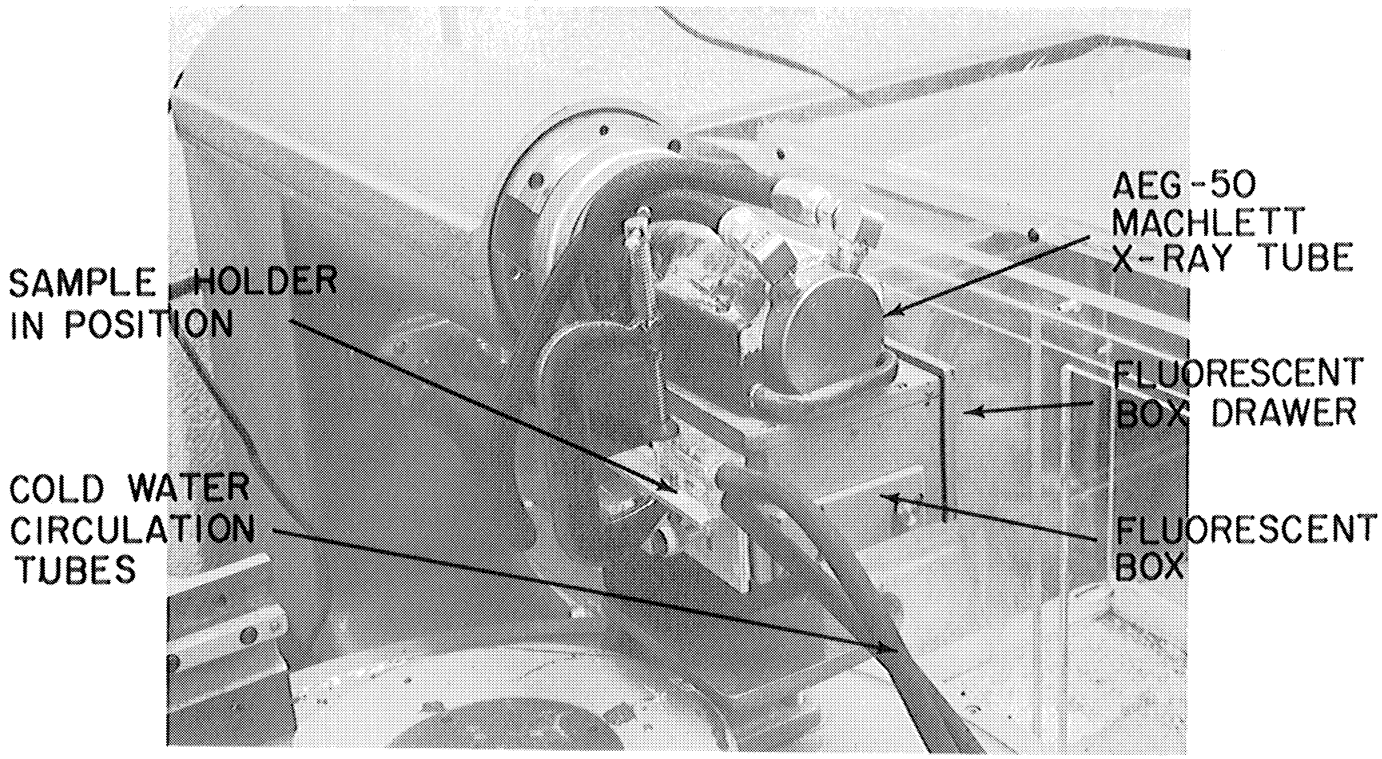

Fig. 4b. Photograph of fluorescent technique assembly; sample and fluorescent box drawer in position.

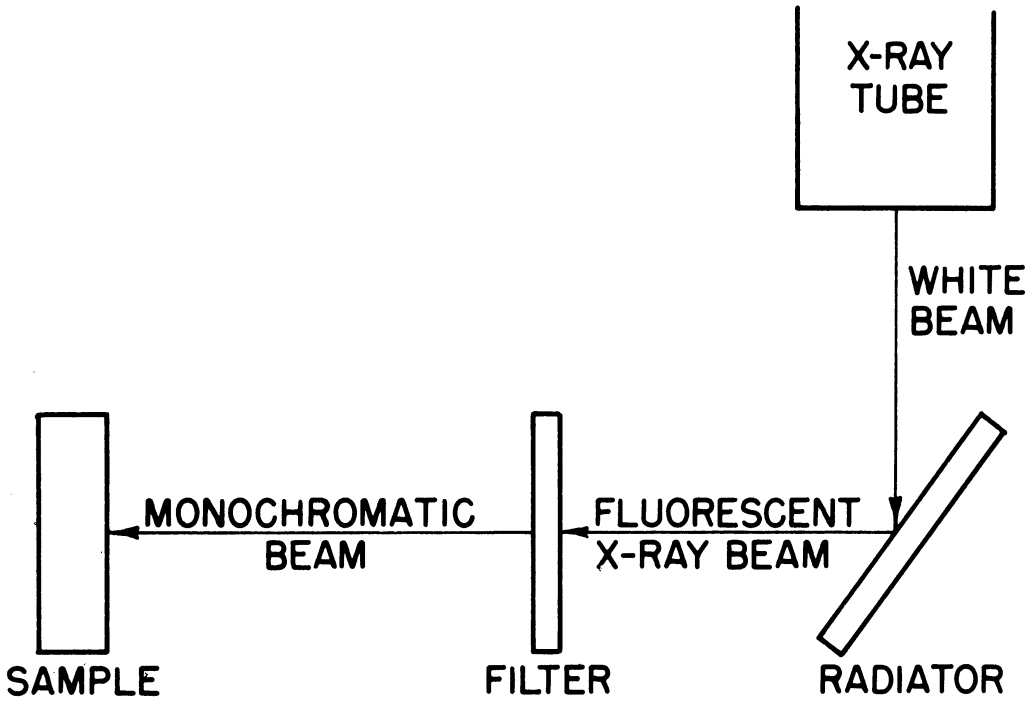

FIG. 5
SCHEMATIC REPRESENTATION OF PRODUCTION
OF FLUORESCENT X-RAY BEAM

reduced to a less than 2 per cent of the total. Therefore, it will be assumed for the purposes of this study that the photon energy of a fluorescent beam is equal to the energy of the K_α emission line for that particular radiator. The intensity of the fluorescent beam is high enough to permit short irradiations (3 hours).

To summarize the two techniques of producing a monochromatic beam, the first offers very good selection of photon energies, but at low intensities, while the second offers high intensities (200-500 times higher), but limited photon energy selection. Thus, the fluorescent technique was adopted for the purposes of this study.

C. Irradiation Procedures

1. Construction of radiators and filters

In general, plastic holders were made out of plexiglas, 1 3/4" x 1 3/4" x 1/4". Grooves were cut of 1 1/4" x 1 1/4" x 1/16" in each of them. Then the elements were placed on the grooves. Five radiators of high grade purity elements were selected with characteristic K_α radiation around the iron K-absorption edge. These were manganese, iron, cobalt, nickel and zinc. Pure metallic foils were commercially available for all except manganese, for which MnO_2 was used at first. Later, pure manganese powder was cast at 1200°C and the fluorescent output of the manganese radiator was increased by a factor of 2. Thin foils and a thin layer of MnO_2 on film were used as filters or absorbers for calibration of the Bragg spectrometer. A .0005" thick pure iron foil filter was used to reduce the K_β contamination

of the cobalt radiator because the energy of the cobalt K_β line was above the iron K-absorption edge and even small contamination of this kind was undesirable. Figure 6 is a picture of some of the radiators; one of them is in position at 45° on the drawer of the fluorescent box.

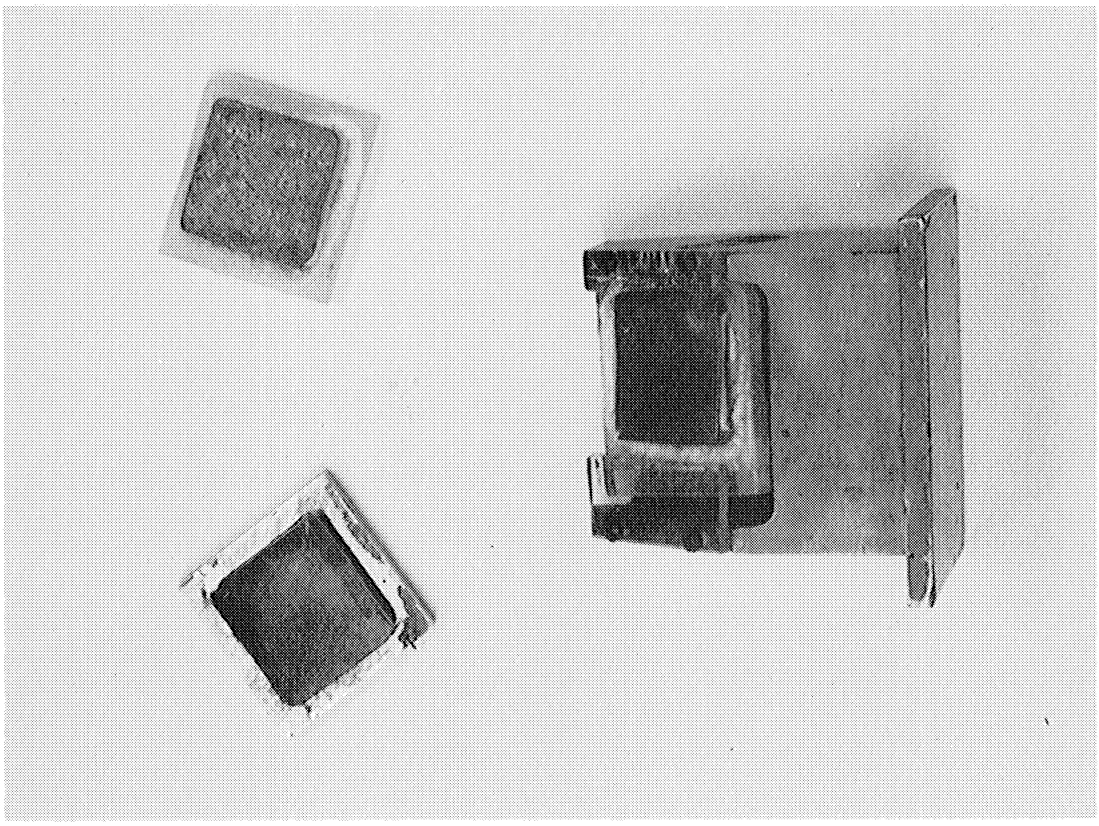

Fig. 4. Photograph of radiators; one of them is mounted in the fluorescent box drawer at 45°.

2. Construction of irradiation cells

The design of the irradiation cell was primarily based on the requirement of a very thin window so that the attenuation of the monochromatic x-ray beam would be as small as possible. Plexiglas proved to be an excellent wall material for the cell. Although the Scotch tape window used by Emmons was simple and permitted cleaning the cell easily, it was disadvantageous because the adhesive was in contact with the enzyme solution. Thin Dupont mylar is commercially available and provides an extremely good material for this purpose: it is highly durable and has very low absorption of soft x-rays. A new type of irradiation sample holder was developed and constructed without the use of any glue or adhesive. On plexiglas of appropriate dimensions two rectangular cavities were cut of a size in accord with the experimental needs. A hole of 1/16" diameter was drilled from the top to the center of each cavity for filling (see Figure 7 and 8).

From one side of the holder and at the back of the cavities, grooves were drilled to permit water circulation for cooling. Next, a plexiglas plate 1/16" thick of the same area was made and two holes of the same dimensions as the cavities were cut through so that the holes and the cavities matched exactly. A piece of 0.00025" thick mylar was sandwiched between two pieces of plexiglas as they were tightened by machine screws. Thus, the enzyme solutions could occupy the cavity volume and could be exposed to the soft x-ray beam through the mylar side of the cavity. The size of the holder depends on the size of the cavities[#]

[#]Which will be called from now on "cells" and the mylar side will be called the "window."

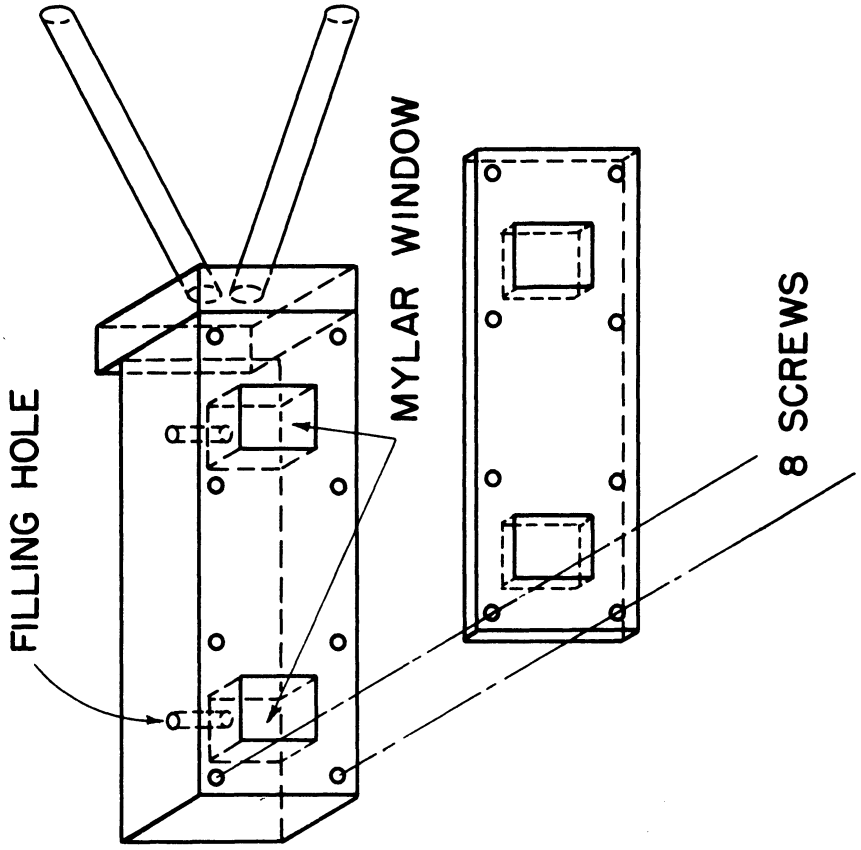

FIG. 7
SCHEMATIC REPRESENTATION
OF TYPICAL SAMPLE HOLDER
USED

which in turn depends on the particular experimental conditions of x-ray beam cross section and uniformity and the requirement to keep the volume of each cell constant and equal to 0.200 ml. Thus, for the fluorescent beam two sizes were chosen, the first, or "standard" size of 6.25 x 8 x 4 mm, and the second of 20 x 10 x 1 mm, and for the spectrometer beam, one size of 18 x 5 x 2 mm. Figure 8 is a picture of some of the sample holders constructed. One cell served for irradiation and was called the "sample," while the second served for checking other factors which might influence the enzyme solution and was called the "control."

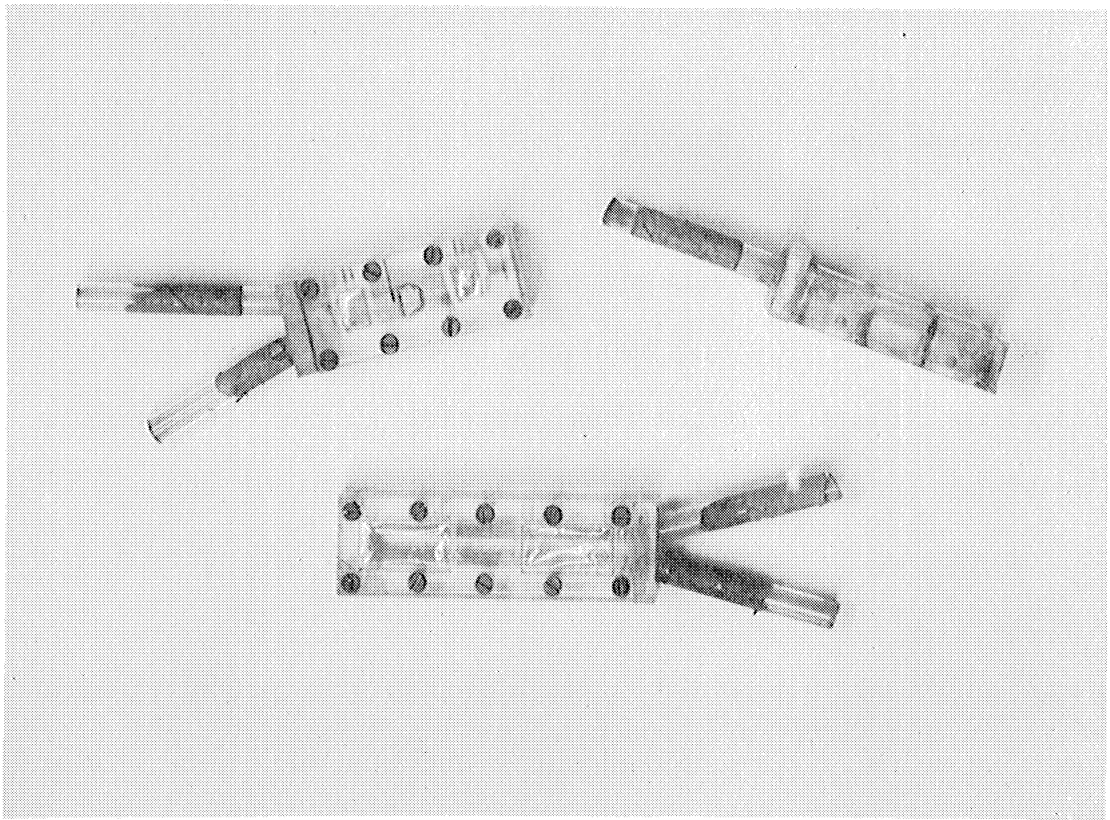

Fig. 8. Photograph of sample holders.

3. Sample-source alignment

The cross sectional area of the monochromatic x-ray beam was determined by photographic film. High sensitivity dental x-ray film was employed for this purpose and was placed at the sample position so that the surface of the film occupied the mylar side of the sample cell. Both the diffracted and the fluorescent beams were horizontal and impinged on the sample surface at right angles. The homogeneity of the beam was determined from the optical densities of the blackening of the film. The diffracted beam had an oval shape and showed large intensity variation with the maximum at the center. The sample was positioned so that the maximum x-ray intensity impinged at its center. The cross section of the sample window, 18 x 5 mm, was chosen so that the intensity variation would be as small as possible for a minimum sample thickness which, by compromise was chosen to be 2 mm. The maximum difference in intensity was from the center to the top or the bottom of the cell along the 18 mm side and amounted to no more than 40 per cent of the maximum intensity while from one side to the other across the 5 mm side amounted to no more than 15 per cent of the maximum. Outside the sample cross sectional area the beam intensity fell off rapidly.

The fluorescent beam just outside the exit from the fluorescent box window had a rectangular shape and was much more uniform than the diffracted beam. Figure 9 represents the relative intensity variation of the fluorescent x-ray beam at the sample position, which was as close as possible to the radiator in order to obtain the highest possible dose rates. The measurements

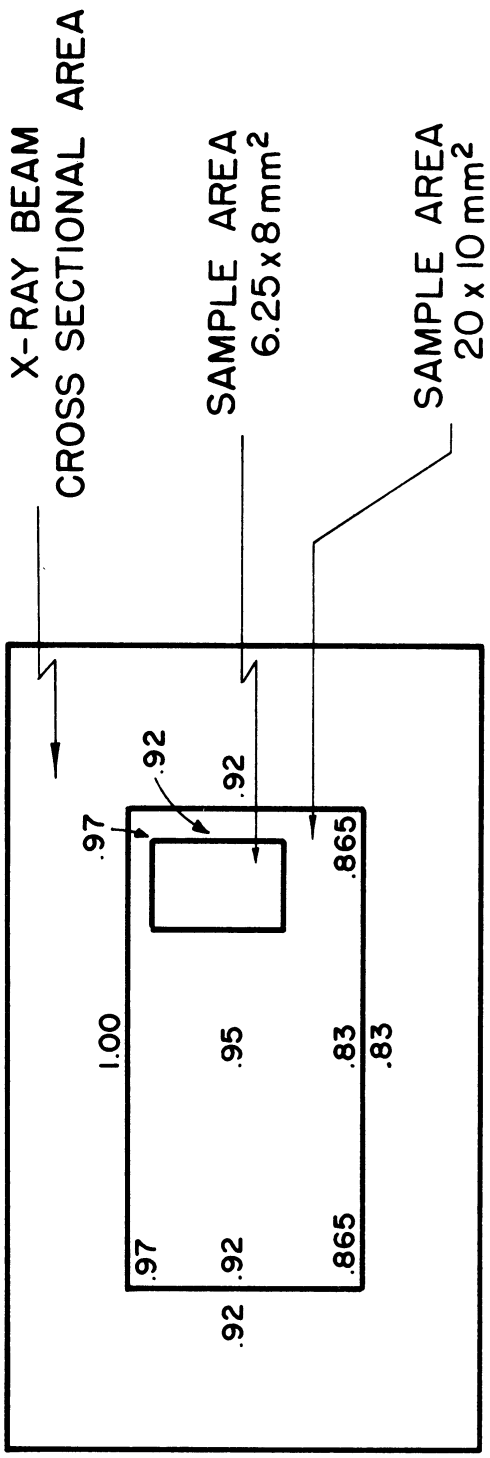

FIG. 9
RELATIVE OPTICAL DENSITY OF FLUORESCENT
X-RAY BEAM PHOTOGRAPHIC IMAGE
(NUMBERS REFER TO O.D.'S NORMALIZED
TO 1.00 FOR THE MAX. O.D. OBSERVED)

indicated that the variation in intensity of the x-ray fluorescent beam was less than 3 per cent in the horizontal direction and less than 17 per cent in the vertical. The standard cell window of 6.25 x 8 mm was positioned so that the maximum impinging intensity was at the left side and top corner and varied by less than 2 per cent across the 6.25 mm side and by less than 8 per cent along the 8 mm side. With this arrangement the lower half of the sample absorbed four per cent less energy than the upper half. The other sample cell with window of 20 x 10 mm was constructed to give maximum cross sectional area and minimum sample thickness. This sample cell was positioned so that the maximum intensity impinged at the center vertical axis and at the top with less than three per cent variation on either side of the center vertical axis in the horizontal direction and less than 11 per cent variation in the vertical direction (see Figure 9).

4. Sample irradiations

After positioning the sample, it was necessary to reproduce the absorbed dose by the sample while the control was properly shielded from the beam. The question was, "What is the difference in absorbed dose in two identical irradiations?" The stability of the x-ray tube output could be continuously monitored by transmission measurements through the sample by the SPG-1 proportional counter[#] in the standard position. A digital printer supplied with the XRD-5[#] unit which prints either interval or cumulative counts for convenient preset periods and was used to monitor long irradiations. In the case of the fluorescent x-ray

---

[#]See G.E. Instruction Manual (105), Direction 11986 B.

beam the goniometer was placed at 0°. The intensity fluctuation of the radiation transmitted through the sample was found to be less than 1 per cent. Other possible factors to influence the delivered dose by the fluorescent beam were the reproducibility of sample and radiator positioning. The radiators could be held rigidly in the fluorescent box drawer, shown in Figure 6, by a spring loaded tongue and could be changed easily. The fluorescent box assembly contained an automatic shutter which shielded the white x-ray beam and which opened only as the sample drawer was fully inserted, thus providing an important safety device. The total reproducibility of the absorbed dose was checked by the ferrous-ferric dosimeter and was found to be within 5 per cent for any of the five radiators used. In the case of the diffracted beam, the sample positioning was the most important factor and since the ferrous-ferric dosimeter could not be used because of the very low dose rates, the SPG-1 monitoring was the only means of checking.

D. Dosimetry

1. Introduction

One of the major problems of the present study was the accurate determination of the radiation dose absorbed by the sample. The most important aspects of the dosimetry problem were:

a) to obtain a simple, accurate and geometrically reproducible system to check routinely the source intensity in everyday measurements.

b) to obtain a system possessing little or known energy dependence which could be used easily and frequently to determine the energy content of a monochromatic x-ray beam.

c) to obtain a system which could be used as an absolute energy absorbed calibration of the other systems.

The SPG-1 proportional counter supplied with the x-ray unit was used with respect to the aims of item (a) above. Because of high counting rates, a lead shield with a pinhole was used to obtain counting rates low enough to avoid large coincidence corrections. A small Fe^{55} source was used as a standard to check and to correct accordingly the response of the counter. The reproducibility of the count rate of any monochromatic beam was better than one per cent. This system was useful for checking any changes in beam intensity by counting the radiation transmitted through the sample during irradiations. This arrangement was especially useful during long irradiations.

The ferrous-ferric dosimeter was successfully used to determine the dose absorbed by the sample. The dosimeter, being liquid and a particularly dilute water solution of ferrous ions, provided a system closely similar to the dilute enzyme system. The energy dissipation in both systems follows exactly the same pattern. The replacement of the enzyme solution by the dosimeter in the sample cell and vice versa offers an ideal comparison and determination of the absorbed dose. The only disadvantage in using this dosimeter was the lack of information regarding its energy dependence in the range of interest around the iron K-absorption edge. Thus, it was necessary to calibrate the ferrous-ferric dosimeter against an absolute dosimeter. This requirement lead to the development of a total absorption calorimeter which was used as a primary standard.

2. The absolute dosimeter[#]

The idea of using a calorimeter for the energy determination of a radiation dose is not new.[53] The radiation energy after being absorbed through ionizations and excitations is converted to thermal energy.

Thus, the temperature of a radiation absorber rises slightly during irradiation. Using thermistors as temperature detectors one can actually measure very small temperature changes. A thermistor is a resister whose resistance changes with temperature. Small resistance changes can be easily detected if the thermistor is part of a Wheatstone bridge circuit. This method has been successfully applied to measure the energy content of an x-ray or γ-ray beam. Atkins and Clendinning[5] at this Laboratory designed and developed a calorimeter, operated at room temperature, for soft x-rays. This preliminary work proved that the construction of a calorimeter sensitive to a power input of the order of 10 μw was feasible.

The calorimeter was redesigned and a new type, operated at liquid nitrogen temperature, was developed. Figure 10 is a picture of the calorimeter assembly, showing the liquid nitrogen container and the Vac-ion pump[##] mounted on the XRD-5 x-ray unit. The absorber consisted of two 0.001" gold plates of about 1 1/4" diameter with a heater coil of 0.001" platinum wire sandwiched between them and two thermistors suitable for operation at liquid

---

[#]For more details see article by H. Gomberg, etc.[49]

[##]Vac-ion model 921-0011. Varian Associates, Palo Alto, California.

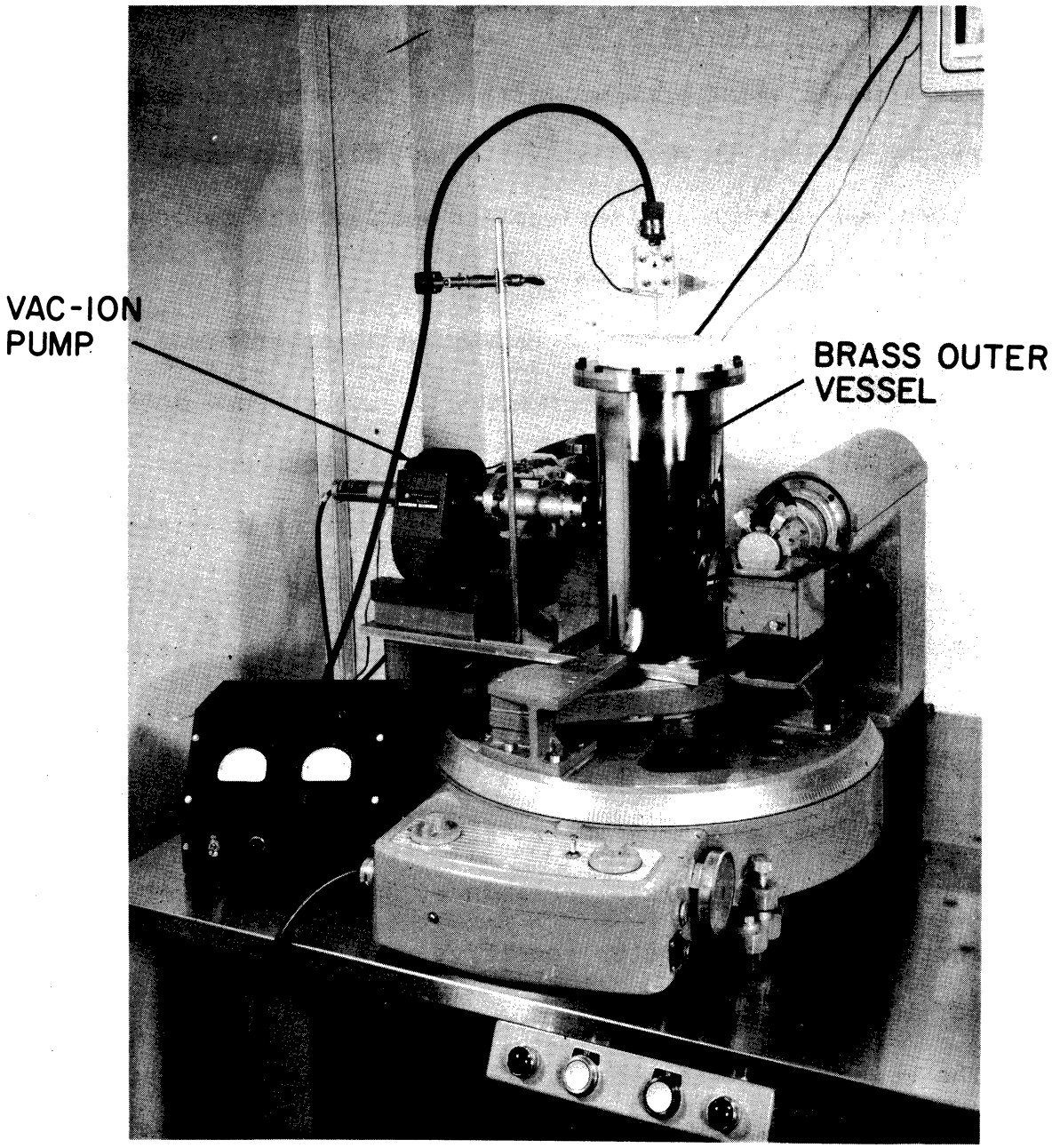

Figure 10. Photograph of calorimeter, showing location on x-ray machine.

nitrogen temperatures attached to the gold plates. The thickness of this absorber was sufficient for total absorption of any fluorescent x-radiation produced by the XRD-5 unit with photon energy below 10 Kev. The absorber was suspended from a plexiglas housing with silk threads (see Figure 11). The plexiglas housing was placed in a small stainless steel vessel called "the calorimetric vessel" with an appropriate window to permit the x-ray beam to strike the absorber. The calorimetric vessel was placed near the bottom of a stainless steel cylinder, or inner vessel, containing liquid nitrogen which in turn was enclosed in another brass cylinder or outer vessel (see Figure 12). The two cylinders constituted the liquid nitrogen container; the space between them and the space inside the calorimetric vessel were maintained at a high vacuum of the order of 10^{-7} mm-Hg by a Vac-ion pump (see Figure 10). A pipe called the beam tunnel with copper inner lining and a 0.0005" thick aluminized mylar window connected the two cylinders (e.g., the calorimetric vessel, and the inner vessel) and permitted the x-ray beam to pass to the absorber with the minimum possible attenuation (less than 2 per cent). The mylar window also served to hold the vacuum. At the other end of the beam tunnel, parallel and 2 cm from the surface of the gold absorber, a 0.005" beryllium window was placed to block out and to dissipate any infrared radiation entering the beam tunnel. The maximum attenuation of any fluorescent beam used, due to the beryllium absorption, did not exceed 10 per cent.

The two leads of the coiled heater, together with the four leads of the two thermistors, were passed through a small stainless steel tube and sealed vacuum tight with Apiezon "Q" wax.

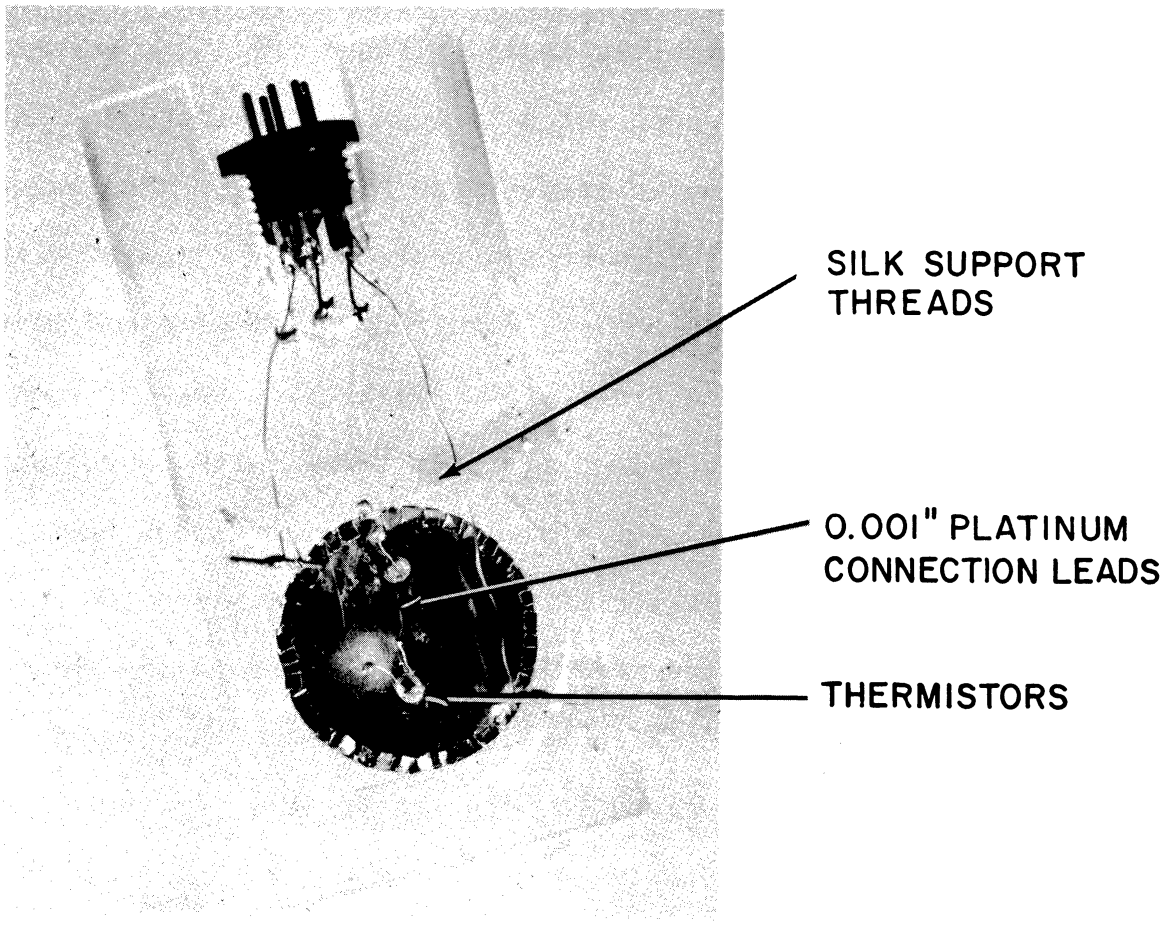

Figure 11 Photograph of gold target for calorimeter.

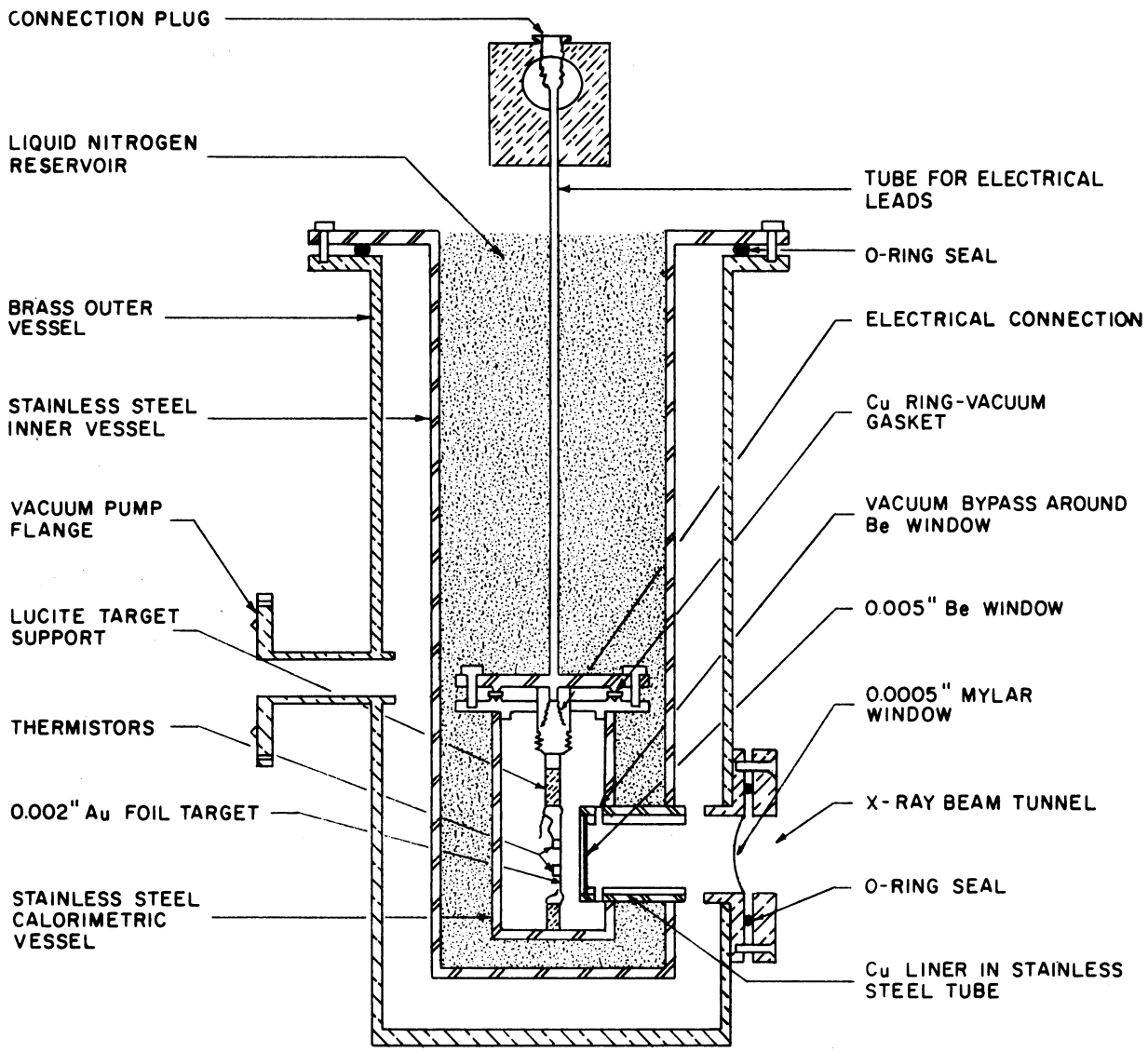

FIG. 12
SCHEMATIC REPRESENTATION OF X-RAY CALORIMETER

The heater leads were connected to a 1 1/2-volt battery through a potentiometer and a micro-microammeter so that currents of the order of 100 μA could provide heating power to the absorber of the order of 10 μW. The thermistor leads were connected with two other resistances to form a Wheatstone bridge in which the thermistors were two opposite arms. Two opposite corners of the bridge were connected to a 6-volt battery through a potentiometer; the other two opposite corners were connected to a microvoltmeter (vacuum tube type electrometer). The bridge was balanced with the help of two high accuracy potentiometers connected in series with one of the resistances (see Figure 13). A signal amplified by the microvoltmeter was recorded by a 10 mV Leeds and Northrup precision recorder.

The criteria for the construction and operation of the calorimeter are given in detail in references (103,14,41,53, and 17) and will not be repeated here.

3. Calorimetric measurements

At the equilibrium temperature, which was close to that of liquid nitrogen, the signal, recorded against time, showed a positive or negative slope at zero power input. The fluctuation of the slope indicated that the temperature of the absorber was not constant, but varied above and below the equilibrium temperature. The period and the amplitude of the fluctuation depended upon the amount of liquid nitrogen present. Thus, by pre-cooling the well-evacuated calorimetric vessel for 4-5 hours, and by afterwards maintaining the amount of liquid nitrogen above a certain level, it was possible to obtain small amplitude fluctuations with periods of the order

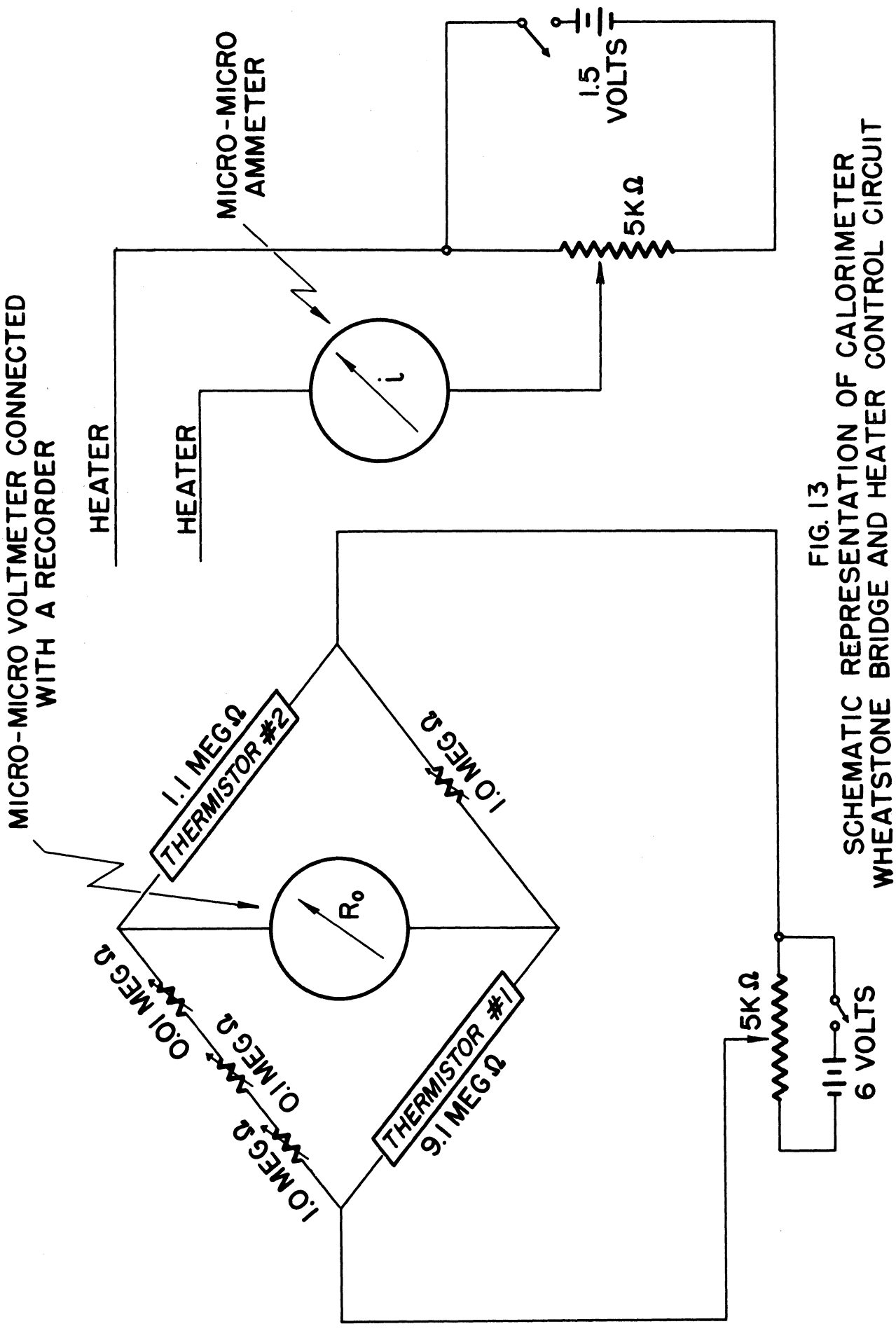

FIG. 13
SCHEMATIC REPRESENTATION OF CALORIMETER WHEATSTONE BRIDGE AND HEATER CONTROL CIRCUIT

of hours. Then by turning on the input power, a positive slope was produced. The slope discontinuity was marked and sharp. The net change of slope, which can be expressed in μ volts per sec, was proportional to the rate of change of the resistance of the thermistors, which in turn was proportional to the rate of change of the temperature of the gold target, which, finally, was proportional to the rate of energy input on the gold target for small temperature changes. Small temperature changes for which the heat losses were negligible were obtained when the heating duration of the gold absorber was less than 1 minute. It was immaterial whether the target was heated by an x-ray beam or by electrical power dissipated in the heater. On the basis of this procedure, a technique was developed for taking and interpreting data with the smallest possible standard deviation. The saw-tooth technique was comprised of a slope versus time curve, such as that shown in Figure 14. A fixed power input was turned on and off periodically at equal time intervals of about 30 sec each. Each portion of the curve is a fairly straight line. An average of the 10 to 12 slope changes produced in one set of saw-tooth curves was taken. This average then constitutes the average slope change for a given power input and is called one run for this particular power level.

The linearity of the calorimeter was established by plotting average slope change versus electrical power input (see Figure 15). Each point of Figure 15 is an average of six runs. The straight line of Figure 15 constitutes the power calibration of the calorimeter (see Table I).

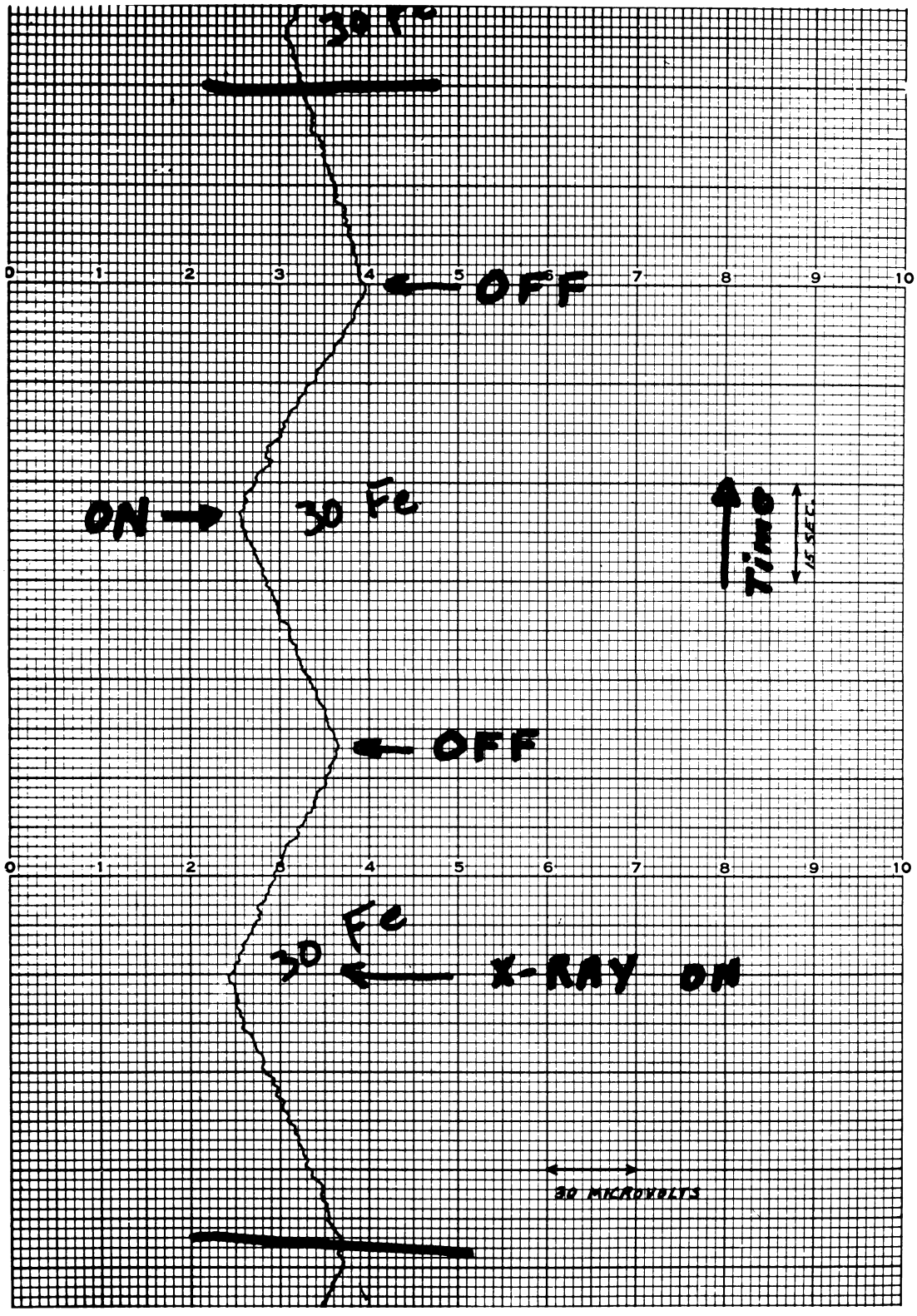

Figure 14 Photograph of typical plot of data output from calorimeter.

TABLE I

CALIBRATION OF THE CALORIMETER BY ELECTRICAL POWER

$\bar{P}$ μW	$\bar{\theta}_1$	$\bar{\theta}_2$	$\bar{\theta}_3$	$\bar{\theta}_4$	$\bar{\theta}_5$	$\bar{\theta}_6$	$\bar{\theta}$ #
3.44	3.4	3.24	3.24	3.0	3.53	-	3.30
7.72	7.5	7.56	6.46	7.52	8.19	7.52	7.43
10.10	9.4	9.63	9.63	9.46	9.13	-	9.45
13.76	12.69	12.50	12.90	12.07	12.89	12.78	
	12.72	12.52	12.10	12.50	12.50	12.20	12.6
	13.20	11.75	12.50	13.50	-	-	
19.80	17.02	17.90	17.90	18.10	18.50	18.60	18.0
25.18	22.20	23.80	22.85	23.25	23.52	23.50	23.21

#Arbitrary units, $\bar{\theta} = \frac{1}{6} \sum_{i=1}^{6} \bar{\theta}_i$, $\bar{\theta}_i$ = average of the 10-12 slope changes produced in the set of saw-tooth curves

TABLE II

X-RAY BEAM ENERGY MEASUREMENTS
AND G VALUE EVALUATIONS

Radiator	$\bar{\theta}$	$\bar{P}$ (μW)	$\bar{P}/S_1$ (ergs/cm^2-h)	$\frac{\Delta A}{hr} \times 10^3$	G ##
Cr	6.9	7.5	$4 \times 10^4 \pm 1.21\%$	$6.1 \pm 3.3\%$	$9.30 \pm 4\%$
Mn	10.25	11.1	$5.85 \times 10^4 \pm 1.75\%$	$9.6 \pm 3.95\%$	$9.60 \pm 4.9\%$
Fe	12.2	13.3	$7.1 \times 10^4 \pm 1.93\%$	$11.9 \pm 2.05\%$	$9.45 \pm 3.5\%$
Co	10.0	10.9	$5.82 \times 10^4 \pm 1.29\%$	$10.6 \pm 1.5\%$	$9.96 \pm 2.9\%$
Ni	11.9	12.9	$6.88 \times 10^4 \pm 1.70\%$	$12.4 \pm 3.2\%$	$9.85 \pm 4.2\%$
Zn	12.1	13.1	$7.0 \times 10^4 \pm 1.81\%$	$13.5 \pm 2.35\%$	$10.10 \pm 3.7\%$

##Number of ferrous ions oxidized per 100 ev absorbed in solution.

Example of G values calculation is given in Appendix 2A.

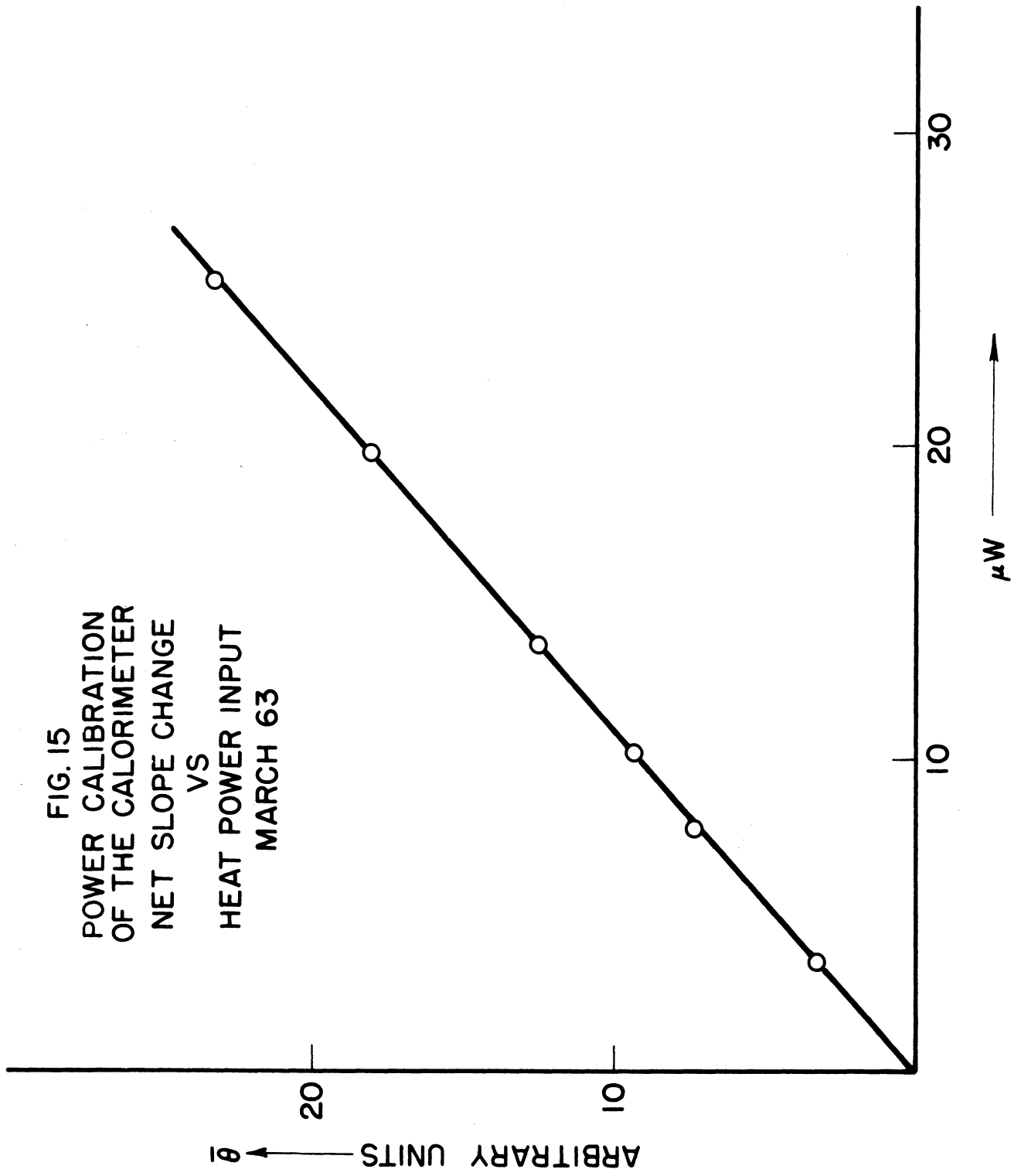

FIG. 15
POWER CALIBRATION
OF THE CALORIMETER
NET SLOPE CHANGE
VS
HEAT POWER INPUT
MARCH 63

By determining the slope change produced by an x-ray fluorescent beam the power of this beam could be determined directly from the power calibration curve. An average of seven runs was used to determine the power content of different x-ray fluorescent beams shown in Table II. In other words, 70 individual slope changes were used to determine each average. The calorimeter served as a primary standard to determine the energy dependence of the Fricke dosimeter at photon energies from 5 to 9 Kev.

4. The Fricke dosimeter

A ferrous-ferric dosimeter was made with about the same area as the gold absorber. This dosimeter consisted of a glass cylinder 1 cm long and about 3 cm in diameter whose ends were sealed by 0.0005" mylar attached to the glass with special cement, and which was filled with ferrous-ferric dosimetric solution.# The dosimeter fitted in a plexiglas housing of the same size as the one used for the gold absorber. This housing was placed at the same position in the calorimetric vessel so that the front mylar surface occupied the position of the gold absorber. This arrangement insured the same incident flux to both the gold absorber and the ferrous-ferric dosimeter. The thickness of both the gold absorber and the ferrous-ferric dosimeter was chosen so that any fluorescent beam used was totally absorbed, thus assuring the same energy absorption in both of them. Since mylar was used for the dosimeter window, it was necessary to remove the mylar window of the calorimeter to avoid any undesirable corrections due to absorption in a second layer of mylar. The removal of the second mylar window was possible, since vacuum was not necessary in this

---

#5×10^{-4} M Fe^{++}, 5×10^{-4} M NaCl, 0.8 N H_2SO_4

type of measurement. The absence of the vacuum resulted in a small attenuation in the x-ray beams due to air absorption. However, the known absorption coefficients in air for the photon energies used, made it possible to correct for the air absorption accurately.

The energy absorped in the dilute aqueous ferrous ion solution oxidized the ferrous to ferric ions. The yield of ferric ions could be measured with a spectrophotometer at 305 or 224 mμ for which the molar extinction coefficients[#] were known (see ref. 53,6,19,20, and 7).

Therefore, a radiation dose could be measured either as heat energy dissipated in the gold absorber or as yield of ferric ions produced in the Fricke dosimeter. Thus, the energy required to oxidize one ferrous ion could be measured, or the conventional G values[##] could be established. An example of ferric ion yield measurements versus time of radiation exposure is given in Figure 16. The fluctuation of the x-ray fluorescent beam, checked with the SPG-1 counter, was found to be less than 1 per cent for the long irradiation exposures required for the ferric ion yield measurements. An example of the calculation of G value is given in Appendix 2A. The G values for 6 fluorescent x-ray beams were evaluated and are presented in Table II. The photon energies for these G values were assumed to be the energies of the K_α emission lines of the radiators. The contribution from the K_β contamination

---

[#] or absorption coefficients per cm of light path.

[##] G value is the number of ferrous ions converted into ferric ions per 100 ev of energy absorbed in the system.

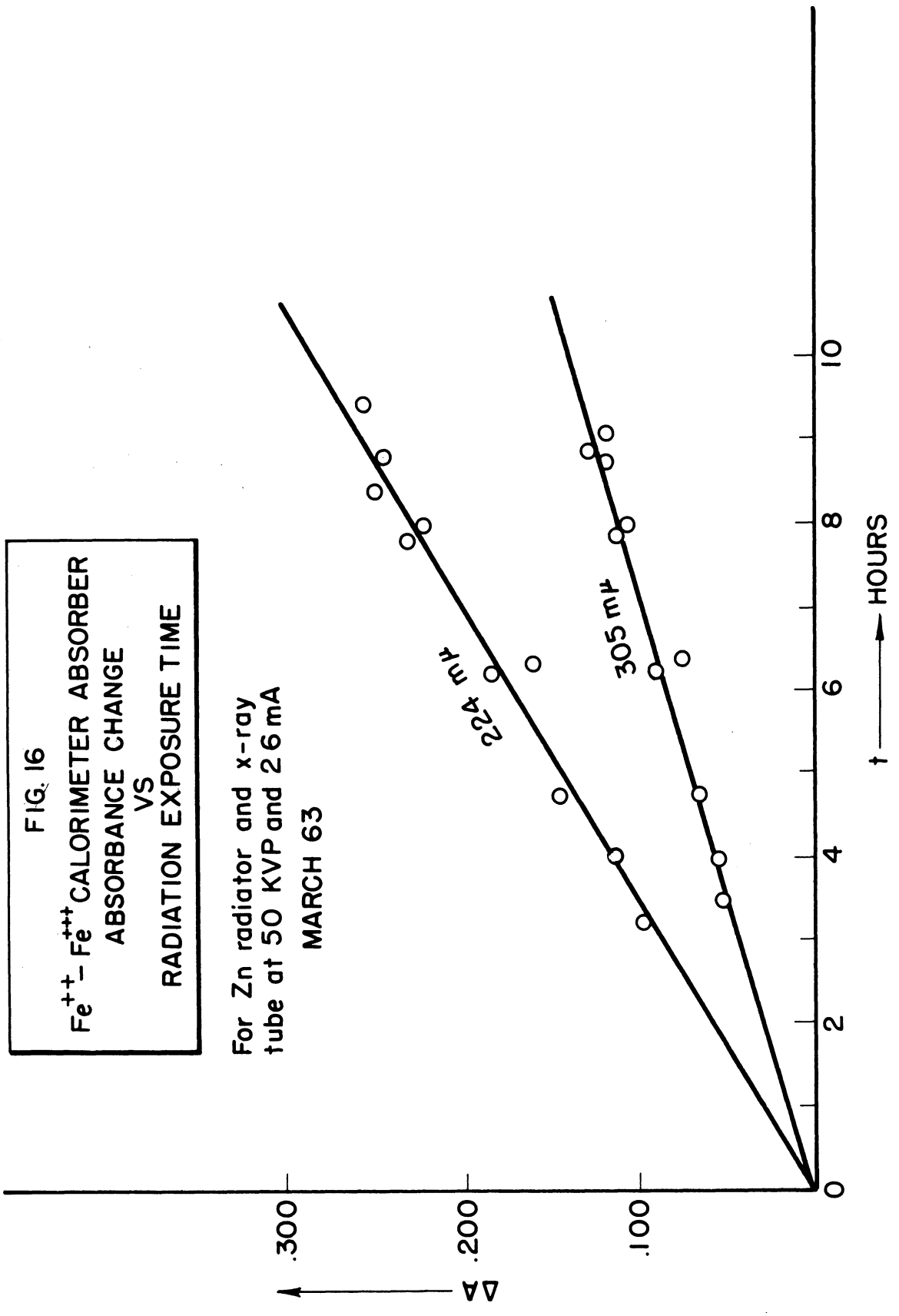

FIG. 16
$Fe^{++} - Fe^{+++}$ CALORIMETER ABSORBER
ABSORBANCE CHANGE
VS
RADIATION EXPOSURE TIME

TABLE III

COMPARISON OF THE THREE SETS OF DATA AVAILABLE

Radiator	Energy of $K\alpha$ line$_{Kev}$	G_1	G_2	G_3	$\overline{G}$#
Cr	5.414	9.52±3.05%	9.89±3.05%	9.30±4%	9.57
Mn	5.896	9.78±5.5%	10.10±4.30%	9.60±4.9%	9.83
Fe	6.408	9.55±5.4%	9.43±15%	9.45±3.5%	9.48
Co	6.930	-	-	9.96±2.9%	9.96
Ni	7.477	9.95±3.4%	10.09±3.53%	9.85±4.2%	9.96
Zn	8.638	10.46±7.2%	11.10±7.18%	10.10±3.7%	10.55

Note: G_1 Data taken by Paraskevoudakis, Dec., 1962.[75]

G_2 Data taken by Wegst, Dec., 1962.[103]

G_3 Data taken by Paraskevoudakis, April, 1963.[75]

#Average number of ferrous ions oxidized per 100 ev absorbed.

TABLE IV

DETERMINATION OF THE DOSE RATES
ABSORBED IN THE SAMPLE

Radiator	X-ray Tube Operation		$\frac{\Delta A}{hr}$	G	Dose Rate# Krads/hr
	KVP	mA			
Mn	50	50	.310	9.7	14.2
Fe	50	37	.400	9.5	18.7
Co	50	50	.390	9.95	17.4
Ni	50	25	.370	9.9	16.4
Zn	50	24	.400	10.3	17.2
Ni	50	50	1.400	9.9	64.0
Ni	50	5	.180	9.9	8.15
Ni	30	1	.014	9.9	0.645

#Example of dose rate calculation in krads/hr is given in App. 2B.

was less than 15 per cent and, therefore, was neglected. For the cobalt radiator a .0005" iron foil was used to filter out the K_β component of the beam because its energy was above the iron K-edge. The same quality of x-ray fluorescent beams was maintained throughout this study. The G value measurements were repeated independently by W. Wegst. Also, the calorimeter was assembled again and the measurements were repeated once more four months later. The results are compared in Table III.

5. Determination of dose rates delivered in sample

The G values of the Fricke dosimeter for the particular energies of interest given in Table III permit the absorbed dose in the sample to be measured accurately.

The primary energy absorption takes place in the water solvent. The ferrous ions are oxidized by the free radicals produced in aerated water by the radiation. The same sample holder used for enzyme solution irradiations, and described in Section C2, Part III, was filled with the Fricke dosimeter solution and placed at the same position as the sample so that it was certain, within experimental error, that both the sample and the dosimeter absorbed the same dose at equal time exposures for the same operating voltage and current applied to the x-ray tube. For each fluorescent beam used, the absorbance change of the dosimetric solution was measured versus time. The relation was linear (see for example, Figure 17 for iron fluorescent radiation) for all fluorescent beams. Therefore, it was possible to determine ΔA change per hour of radiation exposure for all exposures and to apply statistics for error determination (see table in

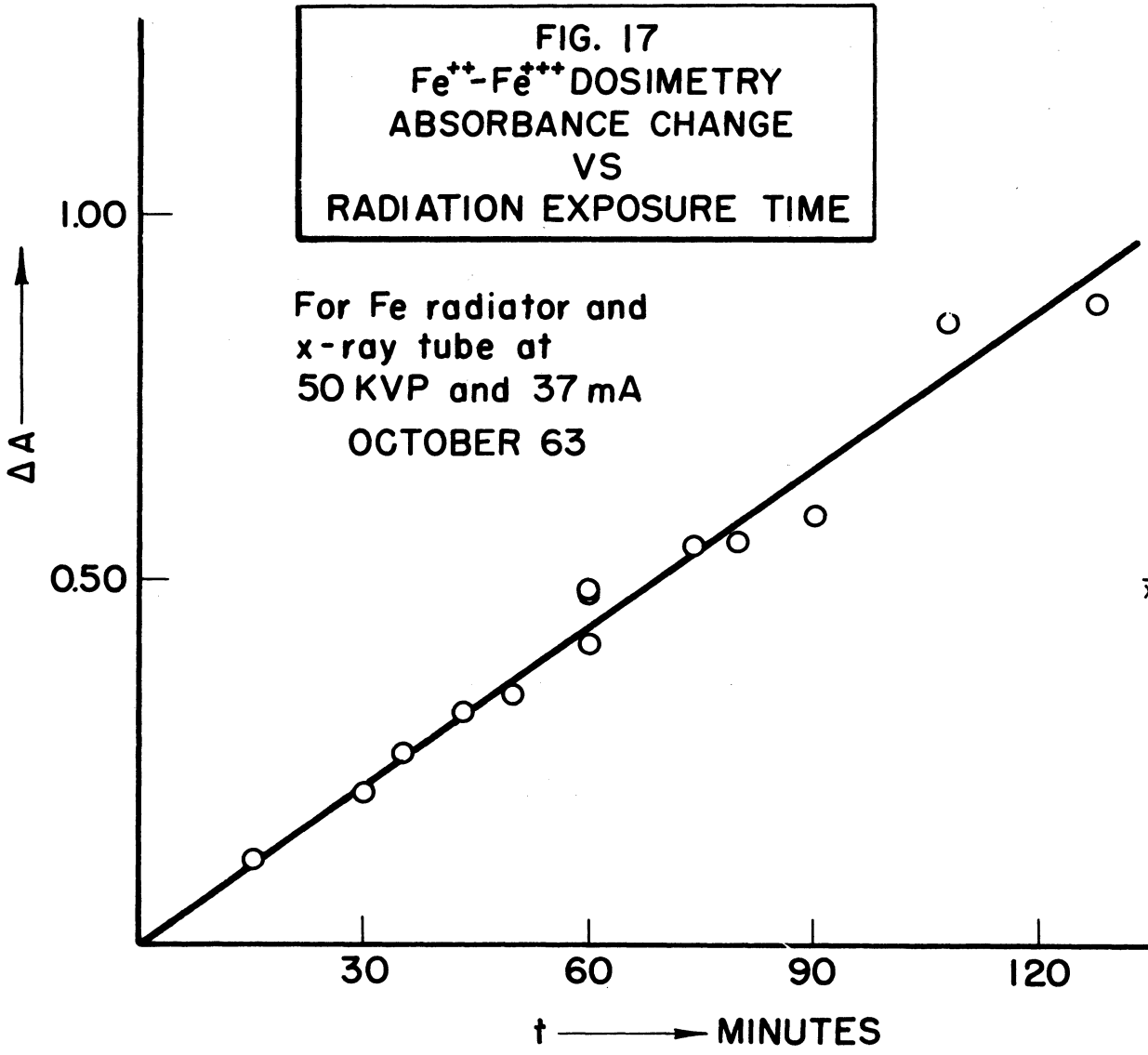

FIG. 17
Fe^{++}-Fe^{+++} DOSIMETRY
ABSORBANCE CHANGE
VS
RADIATION EXPOSURE TIME

For Fe radiator and
x-ray tube at
50 KVP and 37 mA
OCTOBER 63

x_i ΔO.D./h	$x_i - \bar{x}$	$[x_i - \bar{x}]^2$
.449	.013	.000169
.478	.052	.002704
.418	-.018	.000324
.412	-.024	.000576
.392	-.042	.001764
.410	-.026	.000676
.414	-.022	.000484
.460	.024	.000576
.449	.013	.000169
.483	.047	.002209
.454	.018	.000324
.412	.024	.000576
.444	.008	.000064
5.675		$\sum$=.010605

$\bar{x}$ = .436 / h $S^2 = \frac{.0106}{12} = .000885$

$S = .0297$

at 95% for $v=12$, $t=2.17$

$\therefore e_x = 2.17 \times \frac{.0297}{\sqrt{13}} = .0176$

$\therefore x = 0.436 \pm 0.0176$
$= 0.436 \pm 4\%$ Per hour

Figure 17). The voltage applied to the x-ray tube was kept constant at 50 KVP while the current was adjusted so that maximum and approximately equal dose rates were delivered by all fluorescent beams. The results are presented in Table IV, and an example of the conversion of absorbance change per hour into rads per hour is shown in Appendix 2B.

Table IV also contains the dosimetric results obtained for nickel fluorescent radiation at different dose rates.

An attempt was made to apply the above technique and to measure dose rates delivered to samples by crystal diffracted x-ray beams. This was possible, since the variation of G values of the Fricke dosimeter was small in the energy region from 5 to 9 Kev. Assuming linear variation of the G values from 5 to 9 Kev, one can determine all other G values by interpolation in this energy range (see Figure 18). Also, it is normally assumed that the Fricke dosimeter is independent of dose rate at the low dose rate level of the diffracted beams between 5 and 9 Kev. To increase the sensitivity of ferric ion yield benzene (1.3×10^{-3}M) was added to the dosimetric solution.[60] An increase in ferric ion yield by a factor of 3 was observed for Co^{60} irradiations. Also, the extinction coefficient of ferric ion is twice as high at 224 mμ[86] as at 305 mμ. Thus, a total factor of 6 is provided by this extended technique which I duplicated using Co^{60} irradiation and glass containers. Next, the sensitized dosimeter should be calibrated against the regular dosimeter with the fluorescent x-ray beams. Unfortunately, the results of diffracted x-ray beam at 224 mμ were not reproducible and high yields of ferric ions were

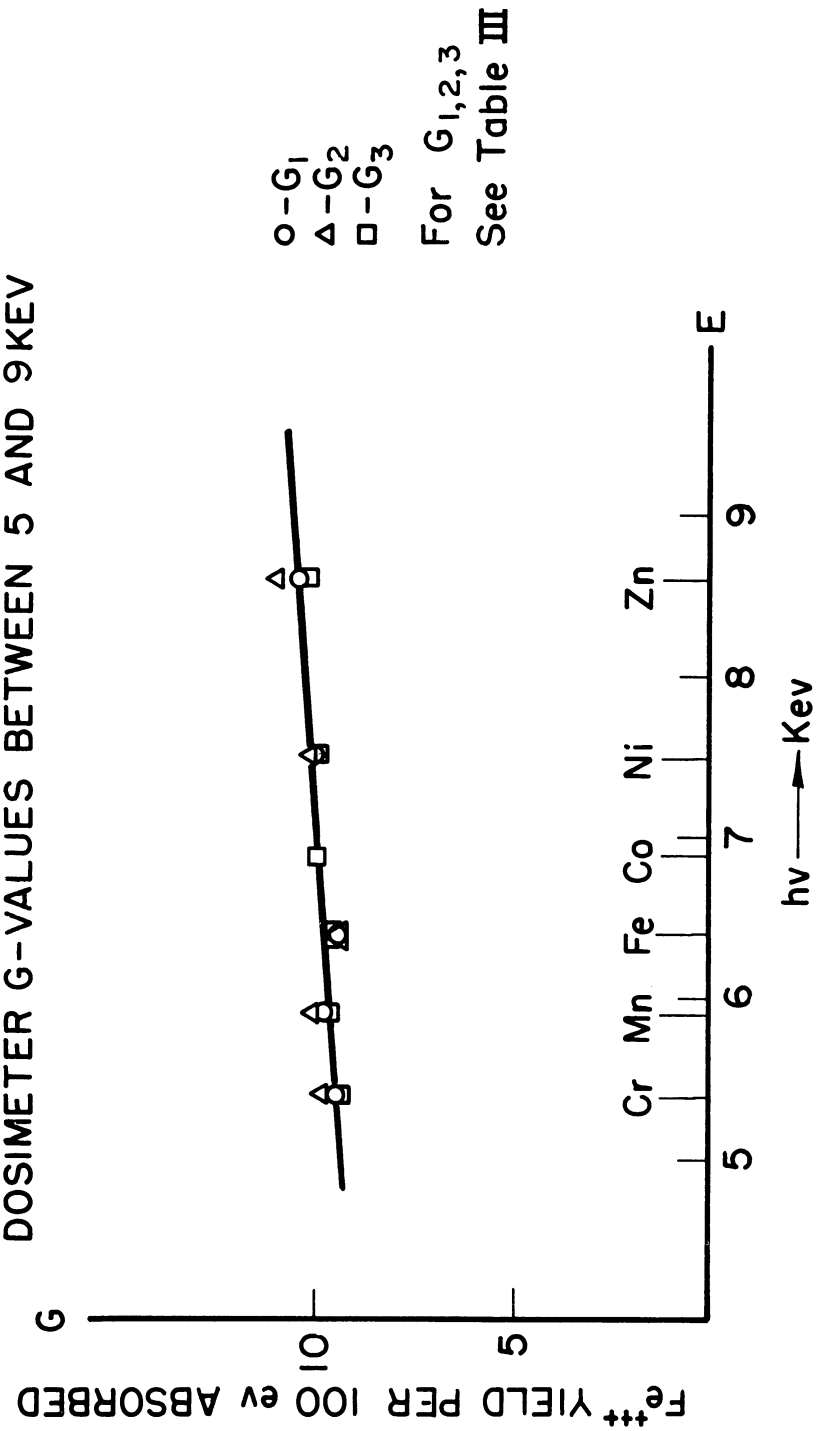

FIG. 18
THE ENERGY DEPENDENCE OF FRICKE'S DOSIMETER G-VALUES BETWEEN 5 AND 9KEV

observed for non-irradiated solutions. Perhaps light helped benzene in oxidizing ferrous ions. Another possible explanation is that benzene can dissolve plexiglas. Since the benzene concentration was low, 1.3×10^{-3}M, its effect on the plexiglas walls of the sample holder and in turn on the ferric ions was not predictable. Thus, the technique was not applicable in the case of low dose rates and plexiglas holders. The thiocyanate method also proved to be inapplicable because of very large variations.[48]

The relative dose rates of the Bragg spectrometer outputs were calculated using data taken with the SPG-1 counter. Examples are given in Appendix 2B. The uncertainty is large, but it is possible to assure equal dosages at different angular settings.

IV. IRRADIATION EFFECTS ON HORSERADISH PEROXIDASE

A. Bragg Spectrometer Technique

The sample holder having 18x5x2 mm cells was used throughout this experiment. Both cells were filled with HRP stock solution and positioned so that one intercepted the diffracted x-ray beam and the other was shielded from scattered x-rays. The x-ray tube was operated at 30 KVP and 50 mA. This resulted[48] in a second order contamination in the radiation diffracted by a LiF crystal of about 18 per cent, a necessary compromise to obtain higher intensities at diffracted x-ray beams.

For different Bragg angle settings each sample received a total number of photons equal to 3×10^{13} measured with the SPG-1 x-ray counter. After irradiation, three 50 μl aliquots of the irradiated, of the control (nonirradiated), and of the stock (kept) in refrigerator) solutions were evaluated for HRP activity. The three aliquots were averaged and a calculation was made of the per cent enzyme inactivated by the radiation (see page 26). The results appear in Figure 19, which is a plot of per cent HRP inactivated as a function of photon energy. There is an indication that the inactivation of HRP is favored at energies greater than the iron $K\alpha$ emission line. The above results are not conclusive because of large uncertainties, especially in the dosimetry. Thus, more emphasis was given to the results obtained with fluorescent technique.

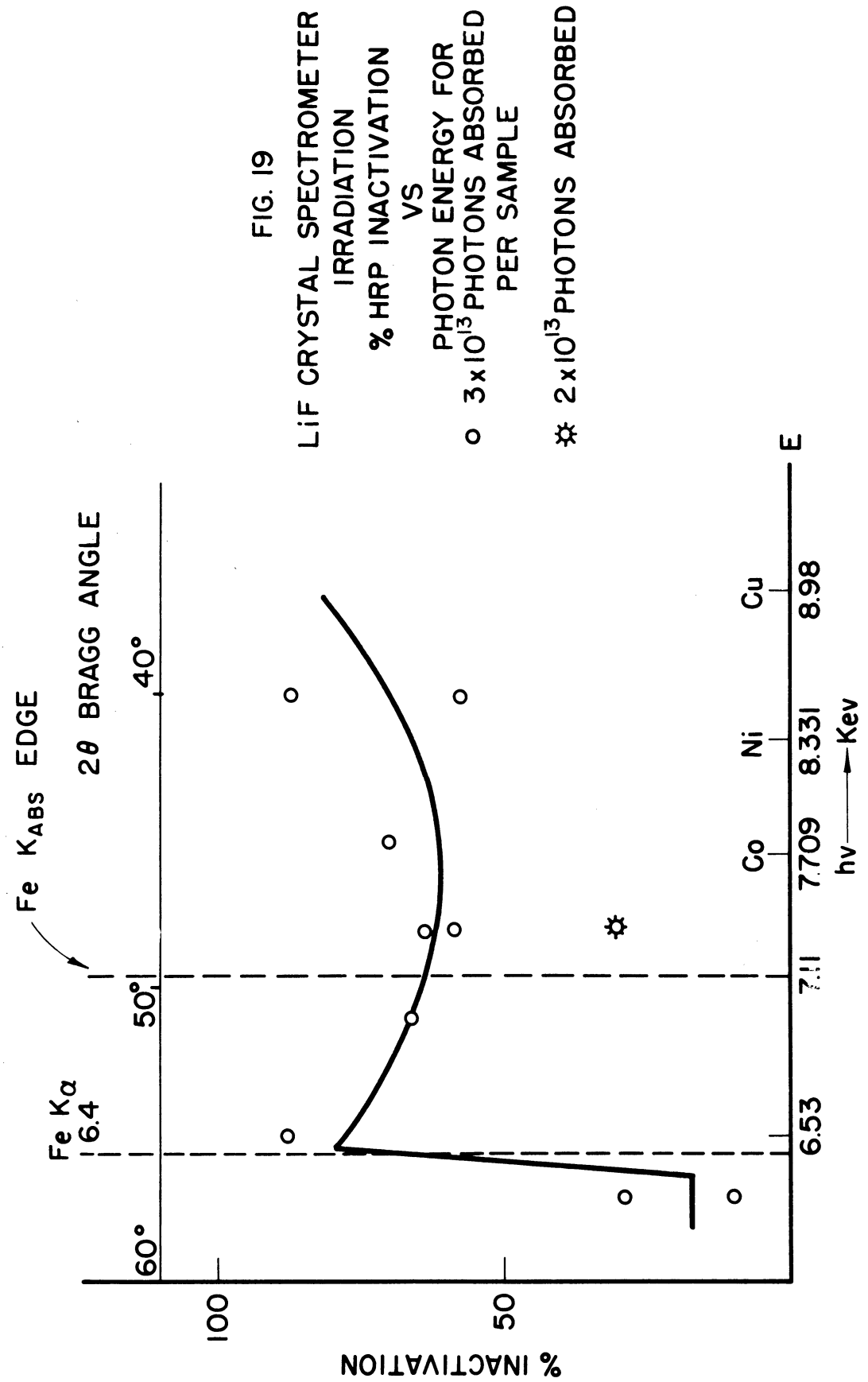

FIG. 19
LiF CRYSTAL SPECTROMETER
IRRADIATION
% HRP INACTIVATION
VS
PHOTON ENERGY FOR
o 3×10^{13} PHOTONS ABSORBED
PER SAMPLE
✲ 2×10^{13} PHOTONS ABSORBED

B. Fluorescent X-Radiation Technique

1. The dose-effect relation

The crystal diffraction technique has presented a definite disadvantage, namely, the very low dose rates and the resulting lack of reliable dosimetry. Therefore, the fluorescent technique has been preferred because it overcame these two difficulties. However, the fluorescent technique suffered from the disadvantage of energy selection. Only discrete photon energies could be produced at approximately 0.5 Kev intervals. It proved to be very useful in studying the particular effect of HRP inactivation around the iron K-absorption edge and the high dose rates made possible the study of the dose effect relation.

For this reason, two sample holders having cells of 6.25 x 8 x 4 mm were used for both enzyme and Fricke solution. Each holder was assigned to one XRD-5 x-ray unit and was positioned so that one of its cells intercepted the fluorescent beam and the other was shielded from radiation (see Figures 5 and 6). The experimental program was designed so that:

1) the applied potential to x-ray tube was 50 KVP and the current was adjusted so that the fluorescent output of all radiators delivered to the sample resulted in approximately equal dose rates as determined by the Fricke dosimeter;
2) a suitable iron filter was used to eliminate the cobalt Kρ fluorescent irradiation;
3) the dosimetry irradiations were repeated at 3-month intervals with occasional checks on the consistency of dose rate in between;

4) the HRP irradiations were thoroughly mixed with respect to photon energy, i.e., the radiators were interchanged for the different runs so that all dose-effect curves progressed simultaneously;

5) for each dose-effect curve the same sample holder, the same x-ray unit (at constant potential and current), and the same radiator were used;

6) the sample holder was cooled by circulating 1°C water through it. Also, the sample holder was prevented from heating by 1/16" air gap between the front surface of the holder and the fluorescent irradiation box. The temperature in the cells was measured by thermocouples inserted in the cells and was found to reach an equilibrium within 15-20 minutes. The temperature of the solutions in the cells never exceeded 12°C.

7) after irradiation for each run, two 50 μl aliquots and one 100 μl aliquot[#] of the irradiated, of the control (non-irradiated), and of the stock (kept in refrigerator) solutions were evaluated for HRP activity. The three values were averaged with a weighting factor of 2 given to the 100 μl value, and the per cent activity remaining after irradiation was calculated (see page 26). The proportionality of the enzyme criterion was necessary to assure that an unknown reaction did not take place.

[#]To be certain that for each run the over-all reaction rate was proportional to the enzyme concentration.

8) for each fluorescent beam, the per cent of HRP activity remaining was studied as a function of exposure time.

The results are shown in Figures 20, 21 and 22. The shape of the curves obtained is not a straight line, thus indicating something other than simple exponential inactivation of the enzyme. The radiosensitivity varied from one curve to another, indicating an energy dependence. The curves represented average per cent of the activity remaining and at certain total absorbed doses the per cent inactivations were evaluated from each curve. Figure 23 is a plot of per cent inactivation as a function of photon energy at various total absorbed dose levels. The energy dependence effect is apparent and need not be emphasized. The per cent HRP inactivation at the cobalt, nickel and zinc $K\alpha$ emission lines is approximately twice as high as at the manganese and iron $K\alpha$ emission lines except at 10 rads.

A question can be raised about the spread of the points on each dose-effect curve and the reproducibility of the results. For a spread $S = \pm 30$ of per cent activity remaining, a standard error of $e_x = \pm 10$ was anticipated on an average value of 10 runs. For that reason, another experiment was designed to test the reproducibility of the above results and to give a better idea of the standard deviation of the measurements.

2. The energy dependent effect

A dose of 30,000 rads was selected to be delivered in enzyme solutions and dosimeter as well. For each of the 5 radiators used, 10 HRP irradiations were performed and 10 dosimeter measurements as well. Special care was taken to interchange the radiators

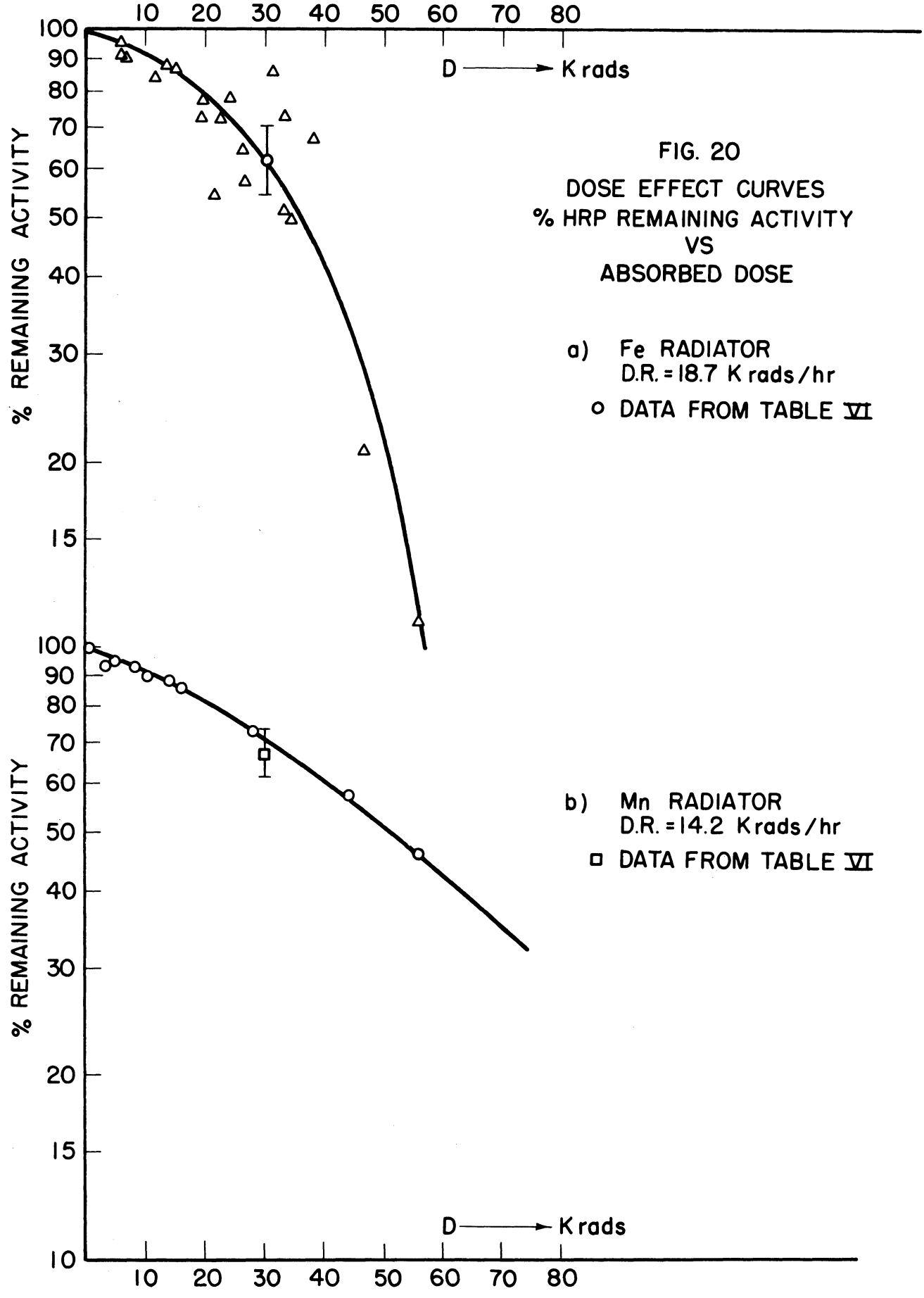

FIG. 20

DOSE EFFECT CURVES
% HRP REMAINING ACTIVITY
VS
ABSORBED DOSE

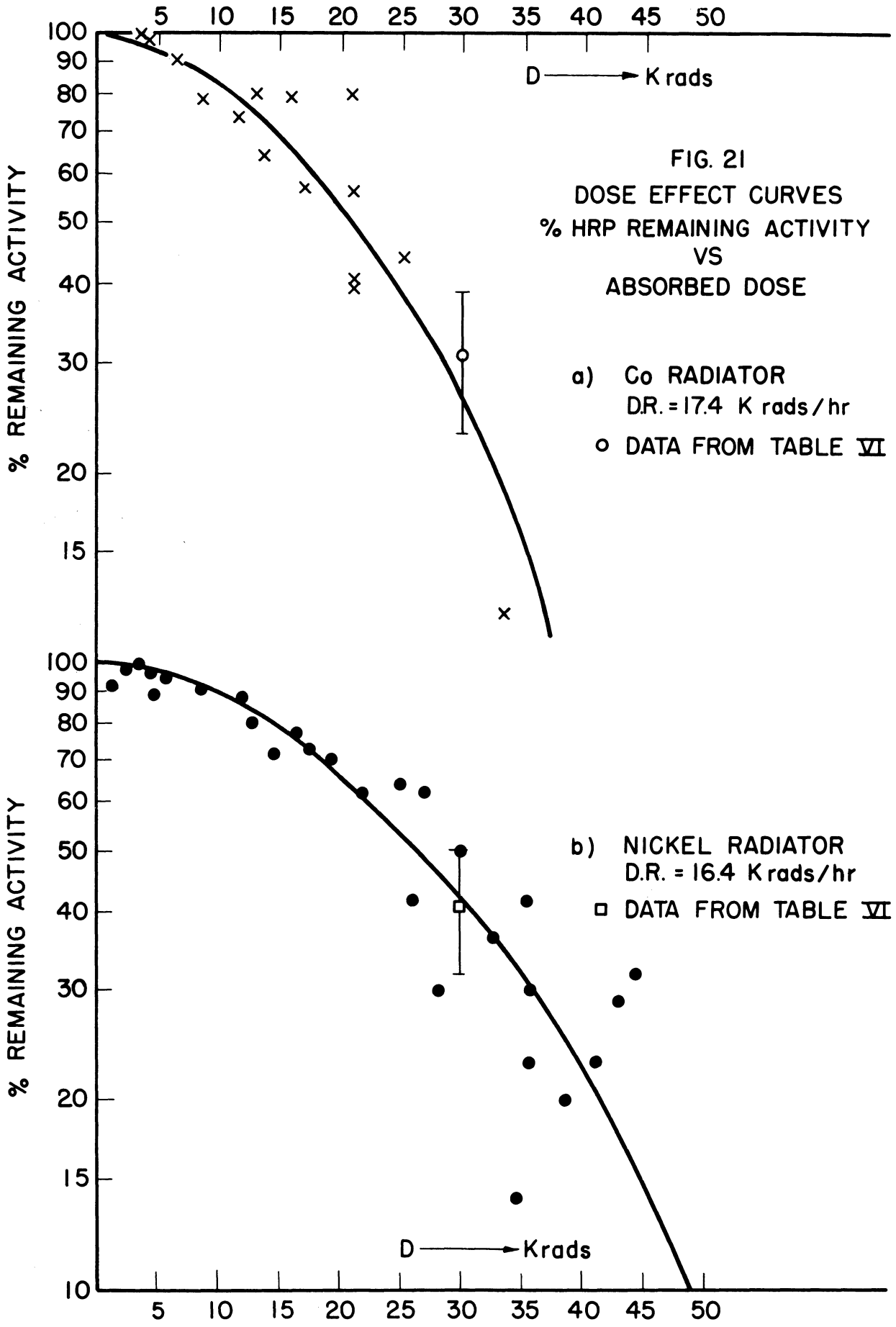

FIG. 21
DOSE EFFECT CURVES
% HRP REMAINING ACTIVITY
VS
ABSORBED DOSE

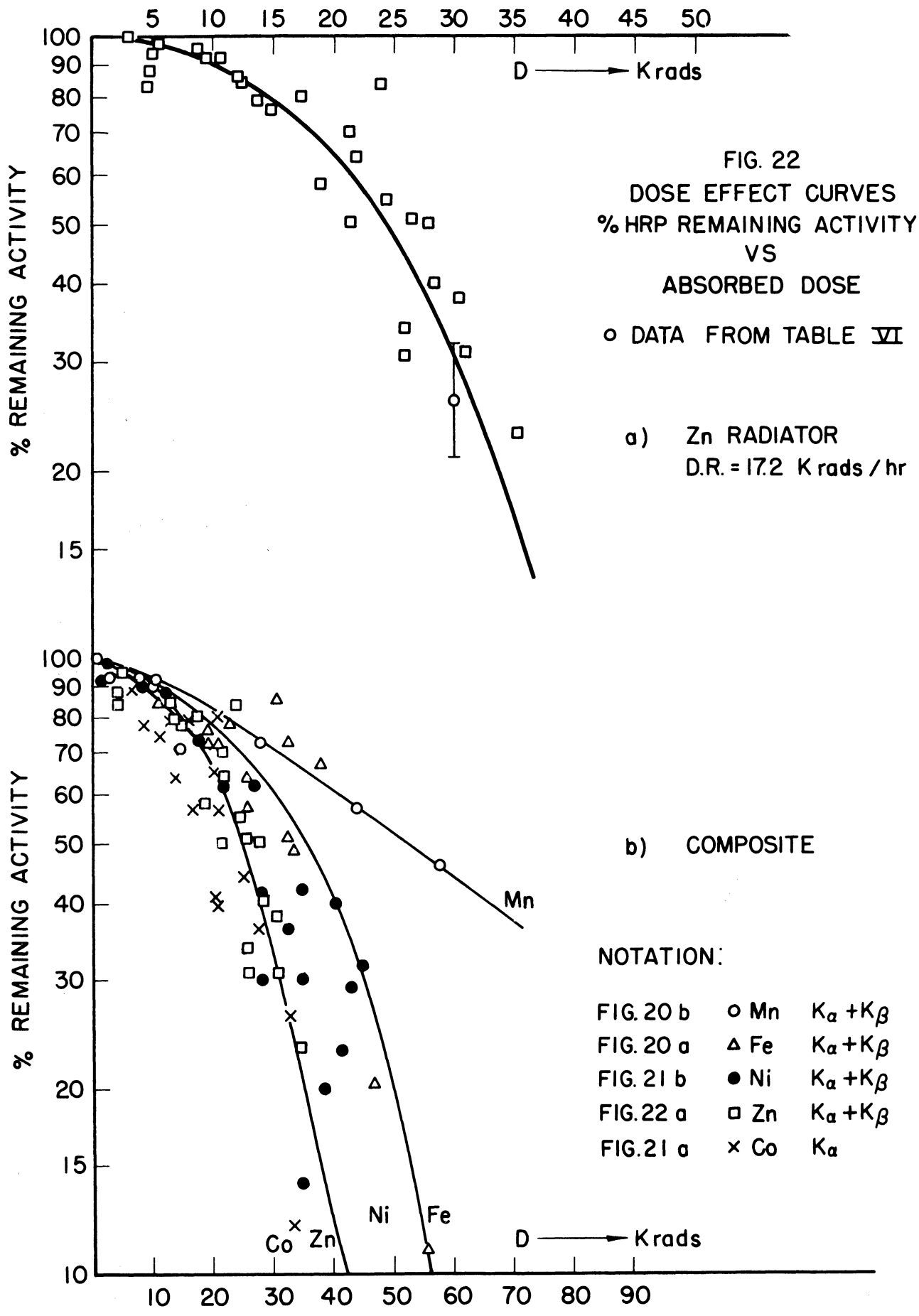

FIG. 22
DOSE EFFECT CURVES
% HRP REMAINING ACTIVITY
VS
ABSORBED DOSE

o DATA FROM TABLE VI

NOTATION:

FIG. 20 b	o Mn	$K_\alpha + K_\beta$
FIG. 20 a	Δ Fe	$K_\alpha + K_\beta$
FIG. 21 b	● Ni	$K_\alpha + K_\beta$
FIG. 22 a	□ Zn	$K_\alpha + K_\beta$
FIG. 21 a	× Co	K_α

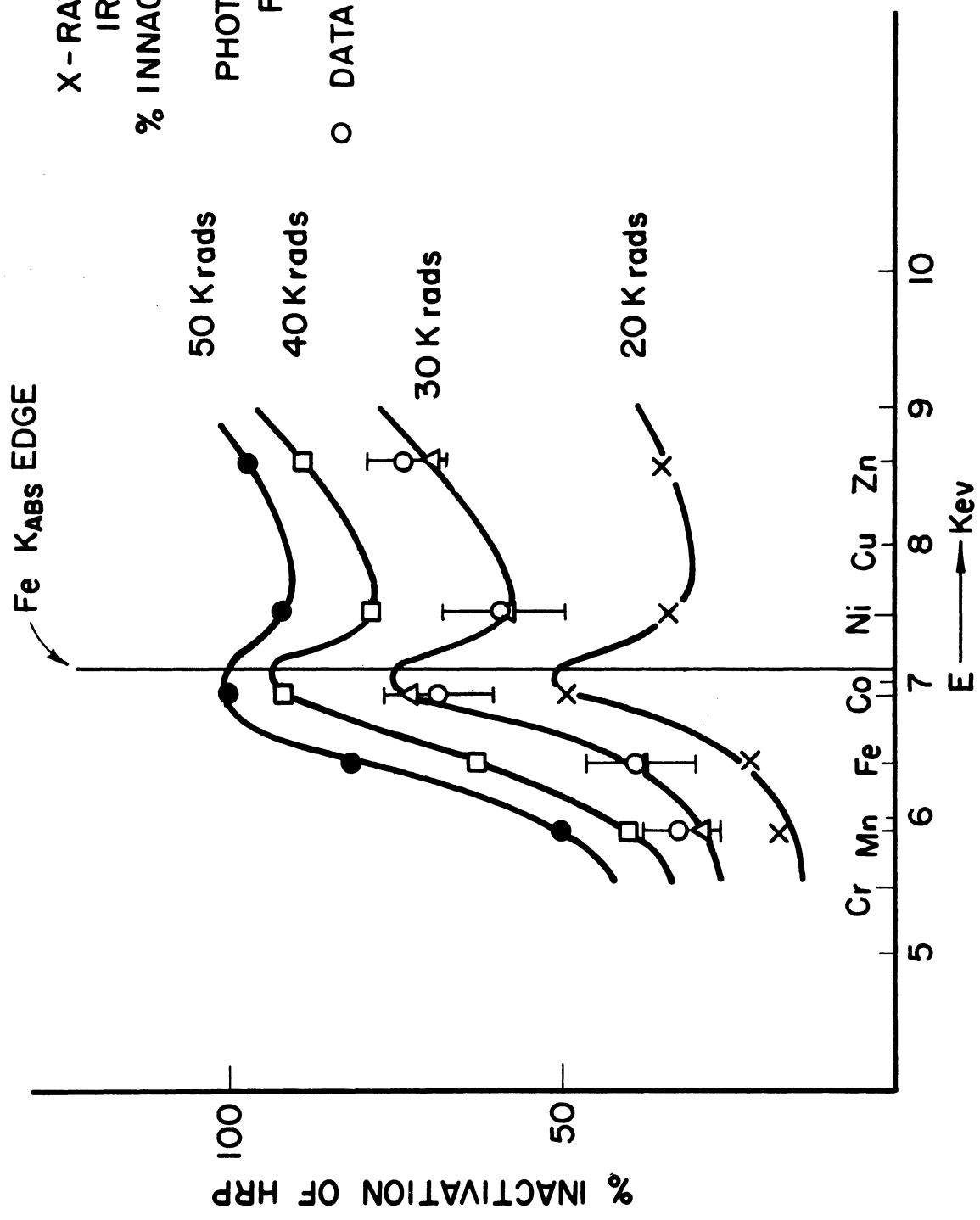

FIG. 23
X-RAY FLUORESCENT IRRADIATIONS
% INNACTIVATION OF HRP
VS
PHOTON ENERGY AT FIXED DOSES

O DATA FROM TABLE VII

and to keep an order so that all the measurements would be completed at the same time. Then an average of the 10 values of per cent activity remaining, was taken and the standard deviation was determined. The results are presented in Fig. 24 and in Table VI. The standard errors at the 95 per cent confidence level are calculated in Table VI and are shown as error bars at each point in Figures 20-24. Figure 25 shows four possible ways of representing the energy dependent effect. The most possible is the step curve because the data shows two distinct levels of radiosensitivity. Furthermore, the results indicated: 1) the complete justification of the results in Figure 23, 2) the reproducibility of the energy dependence effect is within experimental error, and 3) the effect itself is not the result of large error of the method of analysis and technique used. The experimental error was not greater than $\pm$10 of the value of per cent activity remaining and will be discussed separately.

3. The effect of dose rate

Since the dose rates obtained by the spectrometer and the fluorescence techniques differed by a large factor, and since catalase had been found to be dose-rate dependent, it was very important to investigate the effect of dose rate on HRP inactivation. An experiment was designed to utilize monochromatic x-rays. Thereupon, the nickel fluorescent beam was employed because of the high fluorescent output of the nickel radiator. By adjusting the voltage and the current applied to the x-ray tube a variation of dose rates was obtained. The sample holder having 20 x 10 x 1 mm cells was used throughout this experiment. The thickness of 1 mm for the sample was taken as the minimum possible in order to avoid large variation of dose rate within the sample; the half value layer

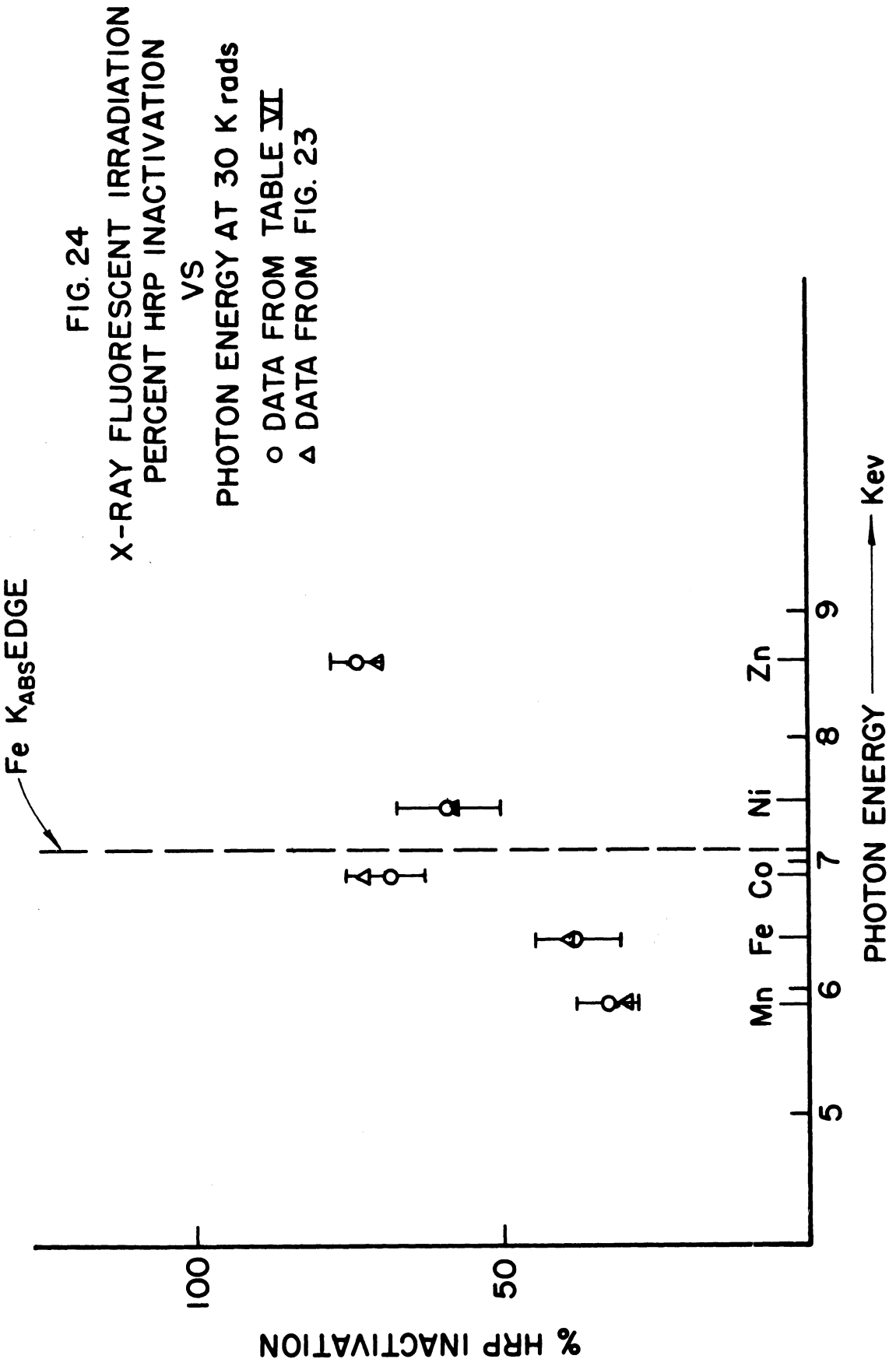

FIG. 24
X-RAY FLUORESCENT IRRADIATION
PERCENT HRP INACTIVATION
VS
PHOTON ENERGY AT 30 K rads
o DATA FROM TABLE VII
Δ DATA FROM FIG. 23

FIG. 25
POSSIBLE WAYS OF REPRESENTING THE ENERGY DEPENDENT EFFECT
% HRP INACTIVATION VS PHOTON ENERGY AT 30 K rads

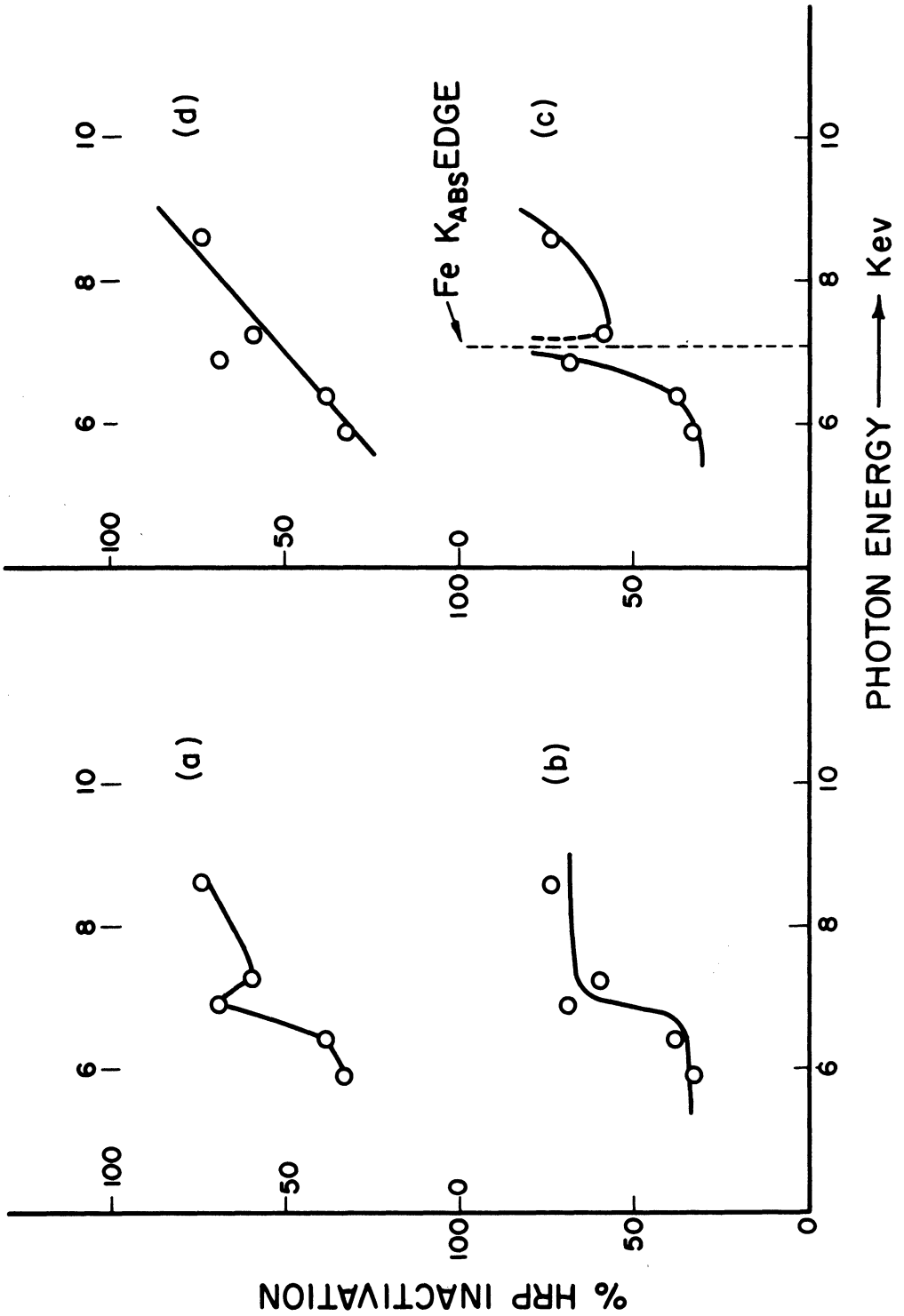

of water (see App. 3) is about 1 mm for 9 Kev photons.[#] Three dose rate levels were selected, including the maximum possible, to represent a dose rate range of a hundredfold. At each dose rate level the dose-effect curves and dosimetry curves were taken in the way described above. Also, the same procedure of HRP activity analysis was followed. The results are presented in Figures 26 and 27 as per cent of remaining activity as a function of absorbed dose at constant dose rate levels. There is not significant difference in the mode of HRP inactivation with respect to dose rate. This result is in accord with the literature, that is "the inactivation of most proteins investigated is independent of dose rate."(6)

4. Some useful computations

Since each irradiated sample consists of 0.200 cm^3 of stock enzyme solution, it is possible to compute the number N of different molecules present.

$$N = C\ V\ N_o \quad \text{mol./sample}$$

where: C = concentration in M (M = 1 gram mole/l)

V = sample volume = 0.200 cm^3 = 2×10^{-4} l

N_o = Avogadro's number = 6.02×10^{23} mol./gram mole

The value of N was calculated for HRP, buffer, and water molecules constituted the sample (see Table V.)

[#]H. E. Johns, "The Physics of Radiation Therapy," Ch. C. Thomas Publ., 1953.

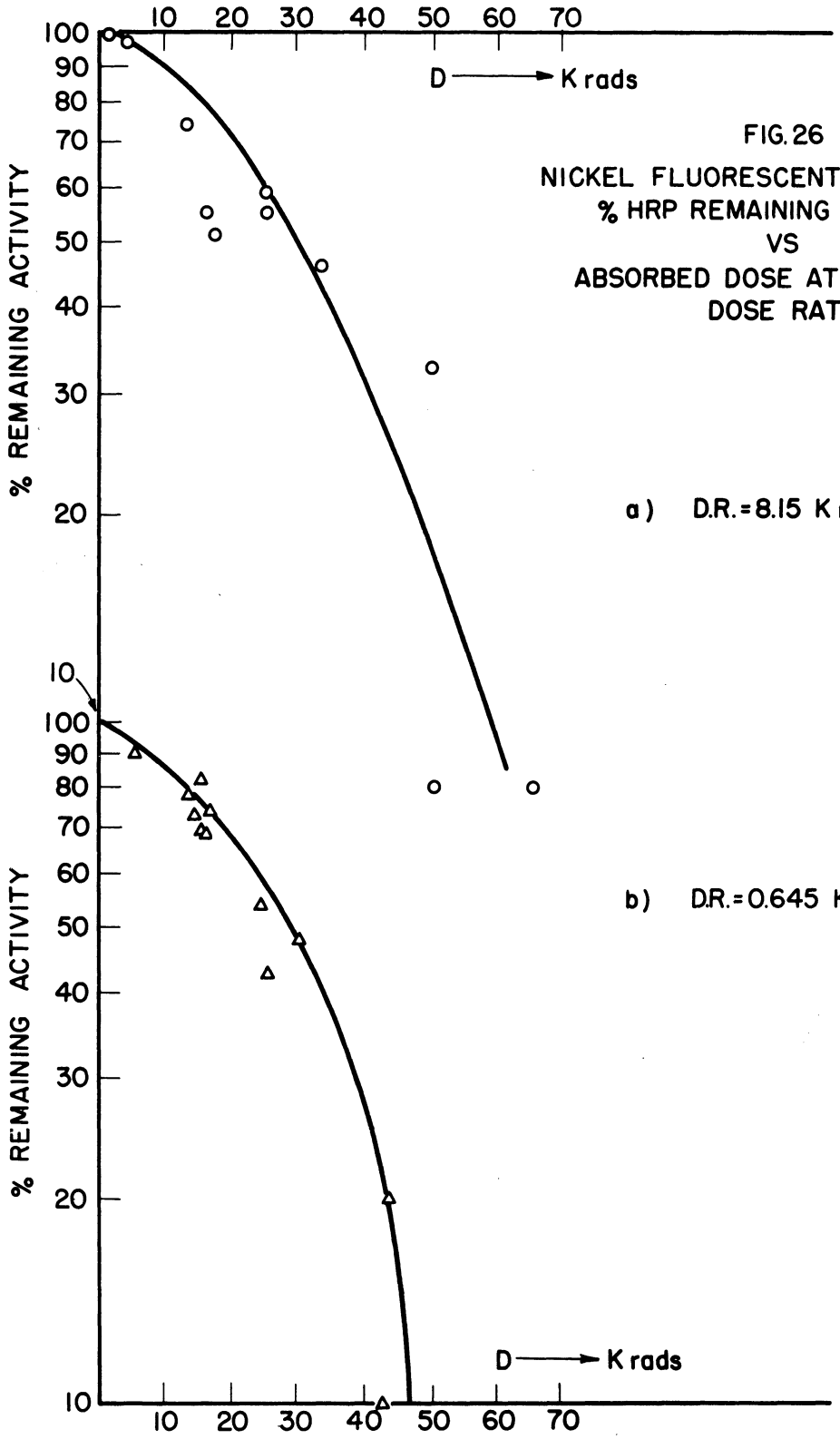

FIG. 26

NICKEL FLUORESCENT IRRADIATION
% HRP REMAINING ACTIVITY
VS
ABSORBED DOSE AT CONSTANT
DOSE RATE

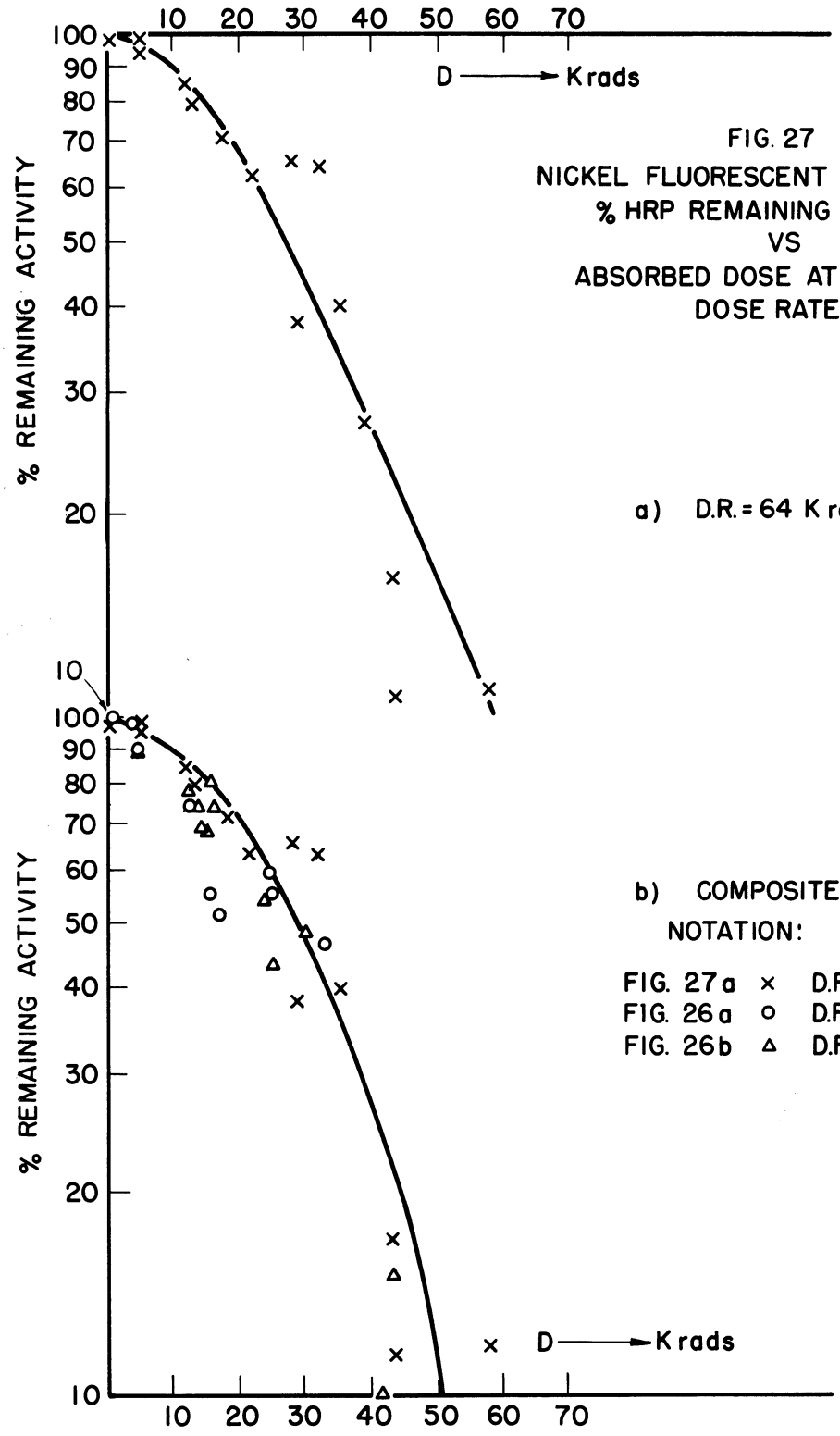

FIG. 27
NICKEL FLUORESCENT IRRADIATION
% HRP REMAINING ACTIVITY
VS
ABSORBED DOSE AT CONSTANT
DOSE RATE

TABLE V

DETERMINATION OF THE NUMBER OF MOLECULES PRESENT IN THE SAMPLE

	Molecular weight	Concentration M	Volume l	N mol./sample
Water	18	55.5	2×10^{-4}	6.7×10^{21}
Buffer		6.6×10^{-2}	2×10^{-4}	8.05×10^{18}
HRP C	40,000	3.3×10^{-7}	2×10^{-4}	3.96×10^{13}
HRP [E]#	40,000	1.1×10^{-7}	2×10^{-4}	1.32×10^{13}

#[E] = active HRP concentration = 1/3 C

(Since the measured reaction rate constants were smaller by a factor of 3 than the ones reported in literature.)

The density of stock solution was $d_w \approx 1$ g/cm^3; thus, each sample weighed about 0.2 g and for an absorbed dose of 30,000 rads, the number of photons absorbed per sample can be evaluated if $h\nu$ is known, by the ratio $D/h\nu$. Where:

$$D = 30{,}000 \text{ rads} = 3 \times 10^4 \times 100 \times 0.2 \times \frac{10^{12}}{1.6} = 3.75 \times 10^{17} \text{ ev } \frac{\text{absorbed}}{\text{sample}}$$

(1 rad - 100 ergs/gm, 1 ev = 1.6×10^{-12} ergs)

The per cent of HRP activity remaining after 30,000 rads were absorbed was determined for each photon energy 10 times. Averages, standard deviations and errors are shown in Table VI. From Table VI the fractions of active molecules inactivated can be computed and hence, the average number of molecules inactivated per sample for each photon energy can be determined. Thus the G values of HRP inactivation or the average number of HRP molecules inactivated per photon absorbed can be evaluated. All these determinations

TABLE VI

STATISTICAL VARIATION OF HRP INACTIVATION BY FLUORESCENT X-RAYS FOR AN ABSORBED DOSE OF 30 Krads. THE NUMBERS REFER TO PERCENT REMAINING ACTIVITY

Mn RADIATOR D.R. = 17.0 K rads/hr			Fe RADIATOR D.R. = 20.4 K rads/hr			Co RADIATOR D.R. = 16.45 Krads/hr			Ni RADIATOR D.R. = 18.8 K rads/hr			Zn RADIATOR D.R. = 17.0 K rads/hr		
x_i	$x_i - \bar{x}$	$[x_i - \bar{x}]^2$	x_i	$x_i - \bar{x}$	$[x_i - \bar{x}]^2$	x_i	$x_i - \bar{x}$	$[x_i - \bar{x}]^2$	x_i	$x_i - \bar{x}$	$[x_i - \bar{x}]^2$	x_i	$x_i - \bar{x}$	$[x_i - \bar{x}]^2$
77	10	100	55	-7	49	23	-8	64	27	-14	196	36	10	100
70	3	9	47	-15	225	31	0	0	48	7	49	22	-4	16
54	-13	169	69	7	49	16	-15	225	34	-7	49	34	12	144
68	1	1	53	-9	81	23	-8	64	40	-1	1	29	3	9
76	9	81	70	8	64	25	-6	36	27	-14	196	18	-8	64
56	-11	121	68	6	36	29	-2	4	40	-1	1	23	-3	9
73	6	36	54	-8	64	43	12	144	63	22	484	22	-4	16
57	-10	100	70	8	64	55	24	576	45	4	16	32	6	36
69	2	4	87	25	625	33	2	4	62	21	441	23	-3	9
70	3	9	59	-3	9	32	1	1	27	14	196	20	-6	36
665		630	623		1266	310		1118	413		1629	259		439
$\bar{x} = 67$		$S^2 = 70$	$\bar{x} = 62$		$S^2 = 140$	$\bar{x} = 31$		$S^2 = 124$	$\bar{x} = 41$		$S^2 = 181$	$\bar{x} = 26$		$S^2 = 48.7$
		$S = 8.4$			$S = 11.8$			$S = 11.1$			$S = 13.4$			$S = 7$
$S_{\bar{x}} = \frac{8.4}{\sqrt{10}} = 2.65$			$S_{\bar{x}} = \frac{11.8}{3.16} = 3.73$			$S_{\bar{x}} = \frac{11.1}{3.16} = 3.51$			$S_{\bar{x}} = \frac{13.4}{3.16} 4.24$			$S_{\bar{x}} = \frac{7}{3.16} = 2.22$		
$e_{\bar{x}} \pm 2.26 \times 2.65 = \pm 6$			$e_{\bar{x}} = \pm 2.26 \times 3.73 = \pm 8.4$			$e_{\bar{x}} = \pm 2.26 \times 3.51 = \pm 7.9$			$e_{\bar{x}} = \pm 2.26 \times 4.24 = \pm 9.5$			$e_{\bar{x}} = \pm 2.26 \times 2.22 = \pm 5$		

At 95% $t = 2.26$ for $v = 9$ $S_{\bar{x}} = \frac{S}{\sqrt{n}}$ $e_{\bar{x}} = \pm t S_{\bar{x}}$

are shown in Table VII. The data of Figure 23 at 30,000 rads were also considered in the final determinations of the G values.

TABLE VII

HRP G VALUES DETERMINATION

Radiator Element	$h\nu_{Kev}$		Photons Absorbed per Sample	% HRP Inactivation			$G^{\#}$	$\bar{Y}^{\#\#}$
				Tabl.V	Fig.23	Avg.		
Mn	5.89	$D = 3.75 \times 10^{17}$ ev/sample	6.36×10^{13}	33	29	31	.0011	.065
Fe	6.40		5.87×10^{13}	38	39.5	39	.0014	.088
Co	6.93		5.42×10^{13}	69	73	71	.0025	.173
Ni	7.48		5.02×10^{13}	59	58.5	59	.0021	.103
Zn	8.63		4.35×10^{13}	74	70	72	.0025	.218

$G^{\#}$ = Number of HRP molecules inactivated per 100 ev absorbed in solution.

$\bar{Y}^{\#\#}$ = Average number of HRP molecules inactivated per photon absorbed in solution.

Since the photoelectric process is the predominant mode of photon absorption at these low energies one may compute the cross section of each atom present in solution by Bethe's corrected[#] formula.[(79)] Assuming the atomic photoelectric cross section to be independent of molecular bonding, one may compute the total cross sectional area of the atoms of one kind present in the sample. Next, the total cross section areas of all the HRP molecules, all the buffer molecules and all the water molecules

---

[#]E. Segre, Ed., "Experimental Nuclear Physics," Vol. I, 310, Wiley, N.Y., 1953.

can be determined. The ratio of the first of the three total cross sectional areas to the sum of the three of them will give the probability that a photon at the iron K-absorption edge will be absorbed by an enzyme molecule. This probability was found to be $\frac{1}{87000} = 1.5 \times 10^{-5}$. Furthermore, the probability of a photon of $h\nu = 7.11$ Kev being absorbed in an iron atom was found to be 0.6×10^{-6}.

C. Absorption Spectrum of Horseradish Peroxidase

Most organic substances absorb light below 250 mμ. Three amino acids exhibit extensive light absorption at wave lengths longer than 250 mμ; phenylalanine, tyrosine, and tryptophan have their absorption maxima at about 260 mμ, 275 mμ, and 280 mμ, respectively. If a protein contains one or more of these amino acids, therefore, an aqueous solution of the protein will absorb light in the region 260 to 290 mμ. Because of unsaturated linkages, the porphyrins have striking absorption bands. A sharp absorption band exists near 400 mμ, and it is usually termed the Soret band. The Soret band is characteristic of the porphyrin ring. Hence HRP, a conjugated hemoprotein may exhibit light absorption maxima near 280 mμ and 400 mμ. Figure 28 is the absorption spectrum of irradiated and nonirradiated HRP aqueous solutions of C = 1 mg/ml = 2.5×10^{-5}M. A dose of 3×10^{5} rads was delivered to the sample by the white x-ray beam (see Fig. 5). The x-ray tube was operated at 50 KVP, 25 mA. The results indicate a marked reduction of the Soret band peak of the irradiated HRP solution. This reduction implies destruction of the porphyrin ring. The increase of light absorption at 277 mμ may be due to irradiation products.

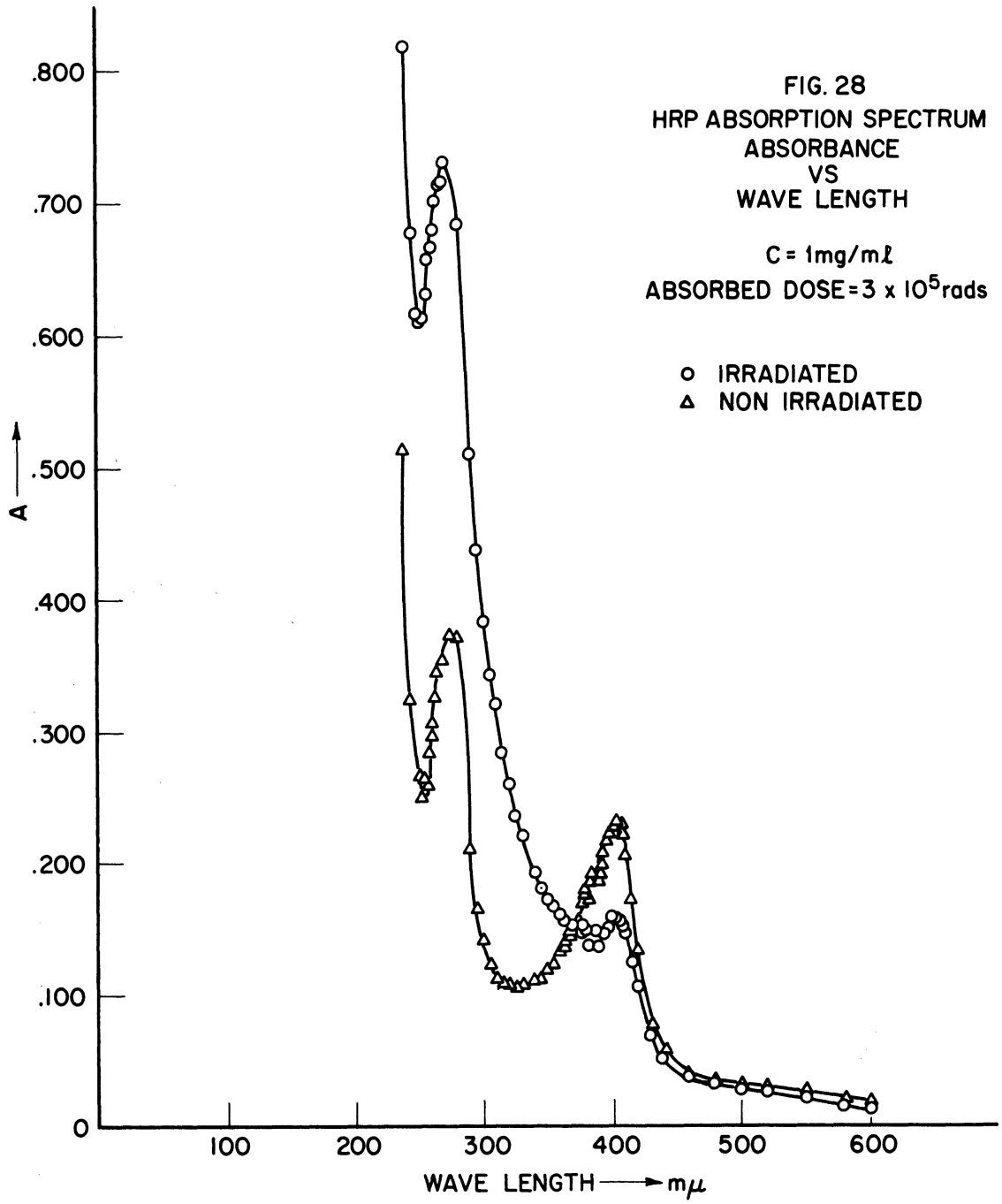
.800
.700
.600
.500
.400
.300
.200
.100
0
A
100
200
300
400
500
600
WAVE LENGTH ⟶ mμ
FIG. 28
HRP ABSORPTION SPECTRUM
ABSORBANCE
VS
WAVE LENGTH
C = 1mg/mℓ
ABSORBED DOSE = 3 x 10^5 rads
o IRRADIATED
Δ NON IRRADIATED

D. Consideration of Errors

1. Introduction

The over-all error of the measurements in this work depends chiefly on the errors of enzyme assay and of dose determination. The HRP activity analysis error depends in turn on errors of 1) weighing the dry enzyme and preparing the stock solutions, 2) transferring the stock solutions to the Beckman cuvette, i.e., the measurement of 50 μl, 3) sample volume, 4) differences in light paths of the cuvettes, 5) Beckman measurements and recording, 6) graphing and calculation, etc. The dose determination error depends in turn on 1) the fluctuation of x-ray beam, 2) the positioning of the sample and the interchange of the radiators, 3) the G values used, 4) the optical density measurements of the ferric ion yield, and 5) the extinction coefficient of the ferric ion. Also, changes may occur in stock solutions which may result in loss of enzymatic activity.

In general, the over-all and some partial errors were evaluated as follows. Each particular measurement, x, was repeated n times and and average, $\bar{x}$, was taken. Assuming normal distribution, one can approximate the standard deviation of one measurement by the square root of the variance

$$S^2 = \frac{\sum (x_i - \bar{x})^2}{n-1}$$

and the standard deviation $S_{\bar{x}}$ of n measurements was taken as $S_{\bar{x}} = \frac{S}{\sqrt{n}}$. Since in most cases n was small, the approximation to the normal distribution was subject to error and the t-distribution correction was applied. Thus, for the evaluation of the 95

per cent confidence limits the t values, taken from tables,[55] for n-1 degrees of freedom, were used instead of $z = 1.96$. In other words, the standard error at the 95 per cent confidence level was taken as $(e_{\bar{x}})_n = \pm t\, S_{\bar{x}}$.

2. Errors of the measurements

The error for HRP activity measurements was determined at $C_1 = .225$ and $C_2 = 1.5$ mg/l enzyme concentration. For 10 runs the error was found to be $(e_{\bar{c}_1})_{10} = 4$ per cent and $(e_{\bar{c}_2})_{10} = 5$ per cent at the 95 per cent level of confidence. From this, the error for 4 runs can be evaluated:

$$(e_{\bar{c}_1})_4 = \sqrt{\frac{10}{4}}\ (e_{\bar{c}_1})_{10} = 1.5 \times 4 = 6\% \text{ for } C_1 = 0.225 \text{ mg/l}$$

The variation of stock solution activity was measured 15 times during a period of 5 months. Each measurement was an average of 4 runs. The variation of stock solution activity over the period of 5 months was found to be less than 3 per cent at the 95 per cent confidence level.

The maximum error in absorbance measurement of the Fricke dosimeter was less than 5 per cent (see table in Figure 17 for example). Also the error of the G values was less than 5.5 per cent (see Table III).#

The per cent remaining activity error is given in Table VI for each photon energy used in this work. The maximum error of per cent remaining activity, 9.5 per cent, was found for the nickel radiator.

#A detailed calculation of G value error is given by Wegst..[103]

V. DISCUSSION

A. Summary of Conclusions

The experimental results of the present investigation indicate that the radiation damage spectrum of HRP in solution displays an energy dependence in the photon energy range from 5 to 9 Kev. The evidence for the existence of such a phenomenon is presented in Figures 19 through 25 of this thesis. The radiation damage sensitivity of dilute HRP solutions to monochromatic x-rays in the above energy range, varies with the energy in a manner best described by a step curve (see Fig. 25b). A photon with energy above 6.9 Kev is capable of producing twice as much radiation damage as a photon with energy below 6.9 Kev. The data neither permit any correlation with the iron K-edge discontinuity nor disproves it with certainty. Furthermore, the experimental error of the average of 10 runs value of per cent activity remaining measurement was found to be less than $\pm$10 of per cent activity remaining at the 95 per cent confidence level for each photon energy used in this work (see Table VI for details).

In the section titled "Effect of Dose Rate," data are presented which indicate that the inactivation of dilute HRP solutions by nickel fluorescent radiations is independent of dose rate in the range from 645 to 64,000 rads/hr (see Figs. 26 and 27).

Finally, in the section titled "Absorption Spectrum of Horseradish Peroxidase," data are presented which indicate that soft x-rays[#] attack and destroy the porphyrin ring.

[#]Soft x-rays = white beam (see Fig. 5) at 50 KVP, 25 mA.

B. Discussion

1. Modes of HRP inactivation

Comparison of the catalase system with the peroxidase system from a biochemical point of view reveals that catalase has four active sites including a porphyrin ring. However, on a percentage basis, the iron content is about the same for both enzymes, since the molecular weight of catalase is more than four times higher than that of HRP. Furthermore, the position of the active site is on the surface of the peroxidase molecule, while it is buried inside the catalase molecule as revealed by substrate specificity measurements.[22] Substrate molecules for peroxidase can have any size from hydrogen peroxide up to cytochrome c while for catalase they must be of small size. Thus, it appears that HRP in solution would be more susceptible to attack by free radicals, i.e., to the indirect effect of radiation, if the major factor in enzyme activity is the porphyrin ring. It is known that the protein itself is not catalytically active. Separation of the protoporphyrin IX from HRP[96] leads to an inactive protein product which becomes active again upon the addition of hematin, thus, both the hematin and the protein are required for catalysis. Also, it is known that a change in the space configuration of the protein molecule leads to its inactivation.[6,59] Therefore, the active site of HRP depends upon the porphyrin molecule, its position on the protein molecule surface, and the tertiary structure of the protein molecule (or space configuration). Any serious perturbation of even one of these factors leads to inactivation.

It is known[6,56,106] that ionizing radiation can bring about inactivation by: a) one or more ionizations produced directly in the enzyme molecule (direct action of radiation), or b) chemical attack of the enzyme by free radicals produced in the surrounding enzyme medium (indirect action of radiation). Therefore, if enough energy is transferred to the active site, or if chemical transformation is produced in the active site, the result appears to be the same: the enzyme molecule loses its function to catalyze a specific reaction. The nature of the perturbation capable of rendering a molecule inactive is not exactly known, but this perturbation must be irreversible. Several possibilities exist:

a) The chemical bond between protein and porphyrin might rupture in an irreversible manner.

b) The porphyrin ring itself might rupture.

c) The disulfide bonds which hold the polypeptide chains together might break, and this leads to an unfolding of the molecule.

d) The hydrogen bonds might break and recombination might result in a different space configuration.

e) Free radicals may attack the active site of the molecule so that the formation of active intermediate complexes might be prevented.

f) Free radicals may attack the protein and cause change of its tertiary structure.

In general, one of the effects of radiation on proteins is the loss of solubility; aggregation seems to take place, presumably by cross-linking of radicals on different molecules, because

precipitation and changes in sedimentation patterns are observed.[6] Also, it is possible that small changes in configuration happen which do not result in inactivation, but the molecule becomes abnormal. This abnormality has been demonstrated[13] by investigating the sensitivity to thermal denaturation of irradiated invertase.

The mechanism by which HRP molecules are inactivated is not known; all or some of the above possibilities may apply.

2. Energy dependence phenomena

The observed energy dependence is of a similar nature to the ones reported previously.

The observed energy dependence phenomena cannot be explained by existing theories. It is not fully understood why a photon with slightly higher energy than another photon is capable of producing more damage. Apparently a process, different than the ones mentioned above takes place; energy absorbed in one molecule can migrate to another. Such a process has been observed previously[67], but the mechanism by which energy is transferred from one molecule to another, several molecular diameters away, is not known.

Since the energy of the photons employed in this research is low, nearly all the primary absorption takes place by the photoelectric process in water molecules. The probability of direct photon absorption by HRP molecules in solution is of the order of 10^{-5} as it was calculated from photoelectric cross section considerations. But the efficiency of inactivation of enzymes by indirect action is lower by a factor

of the order of 10^4 than the efficiency of inactivation by direct action.[6] Thus, even in dilute enzyme solutions, the direct effect is relatively high and of great importance to the total effect. However, what fraction of the total inactivation is due to direct effect is not known for the particular HRP concentration used in this work and the impurities present. The impurities act in favor of the direct effect because the effectiveness of the indirect effect decreases.

The dose required to inactivate 63 per cent of a catalase solution in the frozen state is higher than the dose required to inactivate 63 per cent of the same solution in the liquid state by a factor of 10^2.[74] Also, it is known that one primary ionization that occurs within an enzyme molecule results in its inactivation (average energy required about 100 ev[6]). Thus, one may conclude that 1) primary photon absorption in a water molecule near an enzyme molecule can produce one ionization in the enzyme molecule through a secondary electron. This process is still classified as a direct action of radiation. 2) the energy deposited in an enzyme molecule when a photon is absorbed is far more than enough to inactivate this molecule. Only a part of the primary energy absorbed may escape from the molecule through secondary electrons. The fluorescent yield is very small for low atomic number elements[34] even for iron it is only 20 per cent. Therefore, after photon absorption, Auger transitions predominate.

Therefore, it is possible for a relatively large amount of energy to be localized in an HRP molecule for a very minute time interval, that is, the enzyme molecule as a whole becomes excited.

This excited state has a definite lifetime probably between 10^{-14} sec and 10^{-10} sec.# Several possibilities exist for processes that might take place after the formation of the excited molecule.

1) The excess energy is distributed rapidly in the form of excitational and vibrational energy. Ultraviolet photons are possibly emitted.

2) The energy is transferred by ultraviolet photons through the prophyrin ring to other molecules (fluorescence process). But the fluorescent emission of proteins is reported to be low. Also the efficiency with which ultraviolet photons inactivate enzymes is small and becomes equal to x-ray efficiency for photons with energy greater than 10 ev or $\lambda<1200$ Å.

3) The molecule splits into fragments. The fragments being highly reactive can combine with other enzyme molecules which in turn lose their capability to catalyze the decomposition of hydrogen peroxide.

4) The excess energy is transferred into the water molecules producing free radicals. In this way the indirect action yield is increased.

The energy dependence observed indicates that energy is transferred from one enzyme molecule to others via one of the above processes or combination of two of them. Also, it is

---

#10^{-14} is the time required for an ionization or excitation process and 10^{-10} is the lifetime of an ion or excited molecule.(18)

possible that another energy transfer process may exist. The fourth possibility cannot adequately explain the effect because the free radicals produced in excess are subject to recombination and the efficiency of indirect action is low [100-200 free radicals on the average are required to inactivate one enzyme molecule[6]]. On the other hand, energy transferred by photons gives an adequate explanation only if the photon wave length is less than 1200 Å. This is possible because the efficiency of direct action on proteins is surprisingly high.

The author favors the third possibility because one of the effects of ionizing radiation on proteins, besides inactivation, is the formation of aggregates. This has been demonstrated by the loss of solubility after irradiation and by loss of migrating capability in paper chromatography[34] the author has reproduced Dale's[34] work on catalase). Also splitting of large molecules has been demonstrated (6 p. 180). Thus it is possible that a certain amount of energy is required to cause the splitting of the excited molecule into fragments which are then capable of serving as bridges connecting other enzyme molecules. This amount of energy has to be equal to or greater than the iron K_{α} emission line. The large absorption cross section of an iron atom favors the localization of this large amount of energy. Reporting these possibilities, the author does not feel that a full explanation of the energy dependence effect has been given. But rather a picture of the difficulties, ambiguities and perplexities has been reported.

APPENDIX 1

Horseradish Peroxidase Kinetics

A. Introduction

The determination of individual reaction velocity constants from the kinetics of the over-all enzyme reaction necessitates a rather detailed knowledge of the reaction mechanism and of the denaturing effects of high substrate concentrations. It is generally accepted that the kinetics of the intermediate enzyme substrate complexes follow an extension of the theory of Michaelis and Menten[71] to include the second order reaction of the complexes with the donor. However, there is a question about the existence of a ternary complex (22,23), i.e., a complex of the enzyme the substrate and the donor. There is no positive evidence for such a complex; nevertheless, its existence has not been disproved. Its lifetime may be too short to permit detection by available methods, or no shift of the absorption spectrum may occur upon combination of the enzyme-substrate complex with the donor. Thus, two possible mechanisms of enzyme action have been developed. The "Theorell and Chance"[20,21,22,23,24] mechanism which seems to fit several systems assures that no actual ternary complex is formed and that the enzyme substrate complex reacts with donor to give the corresponding free enzyme and products, and the "Alberty"[23] mechanism, which is an extension of Briggs' and Haldane's[51] original idea, assumes that a ternary complex

is formed followed by chemical change within the complex leading to the dissociation of the "product complex" to yield the products. At the present time HRP data that I have taken can fit either model.

Chance[5,22] concludes that those explanations of enzymatic action based solely upon the kinetics of the over-all reaction are generally inadequate and that full explanations require direct studies of the reaction kinetics of the enzyme-substrate complexes themselves.

B. The "Theorell and Chance" Mechanism

Since in peroxidase both the green and the red compounds participate in a compulsory reaction sequence, the steady state reaction scheme can be simplified as follows:

$$\overset{e-p}{E} + \overset{x}{S} \underset{k_2}{\overset{k_1}{\rightleftharpoons}} \overset{p}{[E\,S]} \qquad (12)$$

$$\overset{p}{[ES]} + \overset{\alpha}{A}H_2 \xrightarrow{k_4} E + SH_2 + A$$

where: (the small letters above the symbols denote corresponding concentrations.)

e, x_o, α_o are the initial enzyme, substrate and donor concentrations; e-p, x and α are their respective values at any time, and p is the concentration of the intermediate complex. It should be noted here that complex [ES] is actually complex $[ES]_{II}$ and it is preceded by the formation of $[ES]_I$:

$$E + S \underset{k_2}{\overset{k_1}{\rightleftharpoons}} [ES]_I + AH_2 \xrightarrow{k_3} [ES]_{II} \qquad (13)$$

In cases where k_3 is measurable, Chance[5,22,24] has found k_3 to be larger than k_1. Thus, with an excess of donor (α) over substrate (s), $k_1 x$ would set the rate of formation of $[ES]_{II}$ and the simplified mechanism of Eqs (12) is justified. Under these conditions, the reaction may be presented by the following non-linear differential equations:

$$
\begin{aligned}
-\frac{dx}{dt} &= k_1 x (e-p) - k_2 p \\
-\frac{d\alpha}{dt} &= k_4 \alpha p \qquad (14) \\
\frac{dp}{dt} &= k_1 x (e-p) - k_2 p - k_4 \alpha p
\end{aligned}
$$

No exact solution in closed form exists for these equations. Under many experimental conditions, a steady state region is observed. At this time, one may make quasi-static approximation that is $dp/dt = 0$. Under this approximation then

$dx/dt = d\alpha/dt$ and

$k_1 x e = k_1 x p + k_2 p + k_4 \alpha p = k_1 p \left(x + \frac{k_2 + k_4 \alpha}{k_1}\right)$ (from the last of equation (14))

$$\text{or } \frac{p_{max}}{e} = \frac{x}{x + K_m} \qquad (15)$$

where $K_m = \frac{k_2 + k_4 \alpha}{k_1}$ is the Michaelis constant or substrate concentration which gives half maximal activity. It is seen that K_m depends on donor concentration and that is directly proportional to α when $k_2 \ll k_4 \alpha$. By combining equations (14) and (15) we get:

$$\frac{dx}{dt} = \frac{d\alpha}{dt} = -k_4 \alpha p_{max} = -k_4 \alpha \frac{ex}{x + K_m} \approx -\frac{e}{(1/k_4\alpha) + (1/k_1 x)} \qquad (16)$$

when $k_4\alpha >> k_2$

Now if $x >> K_m$ the enzyme is saturated by its substrate, i.e., $p_{max} \longrightarrow e$ and k_4 can be measured directly:

$$k_4 = \frac{1}{e\alpha}\left(-\frac{dx}{dt}\right) \qquad (17)$$

And if $x << K_m$ then $p_1 << e$ and k_1 can be measured directly:

$$k_1 = \frac{1}{ex}\left(-\frac{dx}{dt}\right) \qquad (18)$$

In this case the rate of the over-all reaction becomes independent of the donor concentration. Thus, choosing the relative values of $k_4\alpha_o$ and $k_1 x_o$ of equation (16), we can establish a procedure for determining k_1 and k_4. It is clear, however, that the experimental design would have been very difficult had the values of k_1 and k_4 not already been known from direct studies of kinetics of formation and decomposition of the enzyme-substrate complex (Chance[20-24] $k_1 = 0.9 \times 10^7$ $M^{-1}sec^{-1}$, $k_4 = 2.4 \times 10^5$ $M^{-1}sec^{-1}$).

C. Experimental Studies of the Over-all Reaction

In the case where $k_1 x_o >> k_4 \alpha_o$ we have seen (Part III, Section 3) that $k_4 = 0.465 \frac{K}{C}$ where K is the over-all reaction rate constant (in sec^{-1}) and C is the enzyme concentration known from the weight of dry preparation used (in mg/l of protein content. See page 22). A comparison of the value of $\frac{K}{C}$ with the one given in literature (i.e., $\frac{K}{e} = \frac{k_4}{0.465}$) will give an indication of the purity of the preparation used. A more complete picture will be obtained if one compares corresponding values of k_1 or K_{max} and K_m. In

the case where $k_1 x_o << k_4 \alpha_o$ the enzyme is not saturated with substrate; p<<e and K is independent of α_o (since $\alpha_o >> x_o$ and the donor concentration does not change appreciably during the reaction). This K is designated by K' to avoid any confusion with previous case. Therefore

$$\frac{\Delta x}{\Delta t} \approx k_1 x_o e \tag{19}$$

since

$$\Delta x = \frac{4}{\epsilon} \log \frac{To}{T} \quad \text{(see Eq. 6, p. 22)}$$

can be written:

$$\log \frac{To}{T} = \frac{1}{4} k_1 x_o e \epsilon \Delta t = K' \Delta T \tag{20}$$

where

$$K' = \frac{1}{4} k_1 x_o e \epsilon \tag{21}$$

Also, Equation (20) can be written in the form:

$$K' = \frac{\log \frac{T_1}{T_2}}{t_2 - t_1} \tag{22}$$

which is equivalent to Equation (9) of the text (see p. 23) and gives the numerical value of the over-all reaction rate in this case.

Ten runs were taken of an enzyme solution of C = .225 mg/l = 5.5×10^{-9} M and the K_1' were evaluated using Equation (22) above. The average value of K_1' was

$$K' = 13.7 \times 10^{-4} \text{ sec}^{-1} \pm 6\%$$

Therefore k_1 can be determined from Eq. (21) above.

$$k_1 = \frac{4}{\epsilon x_o}\frac{K'}{C} = \frac{4}{26\times10^3 \times 1.4\times10^{-5}}\frac{13.7\times10^{-4}}{5.5\times10^{-9}} =$$

$$11.0\times2.5\times10^5 = 2.75\times10^6 \text{ sec}^{-1}$$

This value of k_1 is to be compared with the value given in literature. From direct spectrophotometric measurements, Chance[20-24] evaluated, with his rapid flow appartus, $k_1 = 0.9\times10^7$ sec^{-1}.

Thus, the ratio $\frac{0.9\times10^7}{2.75\times10^6} = 3.25$ gives an index of enzyme purity. This value compares very well with the equivalent calculated from measurements of k_4 (see p.24)

The Michaelis constant for the enzyme preparation used can be determined assuming $k_2 << k_4\alpha_o$ after Chance's determination of $k_2 = 5$ sec^{-1}. Hence:

$$K_m = \frac{k_2+k_4\alpha_o}{k_1} \approx \frac{k_4}{k_1}\alpha_o = \frac{.825 \times 10^5}{.275 \times 10^7} \times 3.3\times10^{-4} = 9.9\times10^{-6}\text{M}$$

K_m compares very well with the value of $K_m = 12\times10^{-6}$ obtained using literature values of k_1 and k_4. This value is 14 times smaller than $x_o = 1.4\times10^{-4}$ M.

The maximum reaction rate constant at infinite substrate and donor concentration can be determined from the double reciprocal plots. Since HRP requires a hydrogen donor to decompose its substrate, both the substrate and the donor concentration should be varied.

Varying the guaiacol (hydrogen donor) concentration the over-all reaction rate constants K were evaluated at constant hydrogen peroxide concentration. The reciprocal of K was plotted versus the reciprocal of guaiacol concentration and the resulted

straight line was extrapolated to intercept the $\frac{1}{K}$ axis (see Figure 29). The interception gave the reaction rate constant K_i^* at infinite guaiacol concentration at a constant substrate level. The above experiment was repeated for different hydrogen peroxide concentrations, and the K_i^*s were evaluated (see Figure 29). The reciprocal K_i^* was plotted versus the reciprocal H_2O_2 concentration and the resulted straight line was extrapolated (see Figure 30) to obtain the reaction rate constant K_{max} at infinite H_2O_2 and at infinite guaiacol concentration. All the above experiments were performed at constant enzyme level 3 = 0.22 mg/l = 5.5×10^{-9} M in the Beckman cuvette. This analysis indicated that HRP follows Michaelis-Menten kinetics with $K_{max} = 4.54 \times 10^{-3}$ sec^{-1} at infinite H_2O_2 and infinite guaiacol concentration for the above enzyme concentration. The same results are obtained if $[H_2O_2]$ is varied at constant [G] levels (see Figures 31 and 32).

D. The Alberty Mechanism[102]

Alberty's theory has not yet been applied to a HRP system. C. S. Vestling[102] worked out Alberty's most general reaction scheme for the rat liver LDH[##] system. Since both can be considered as two substrate systems, a similar treatment may be applied to HRP. The explicit assumptions of the general mechanism are:

1) There are binding sites for both substrates.[#]
2) Either substrate may bind whether the other substrate is present or absent.

[#]Hydrogen donor, is regarded here as a second substrate.
[##]LDH = Lactate De-Hydrogenase.

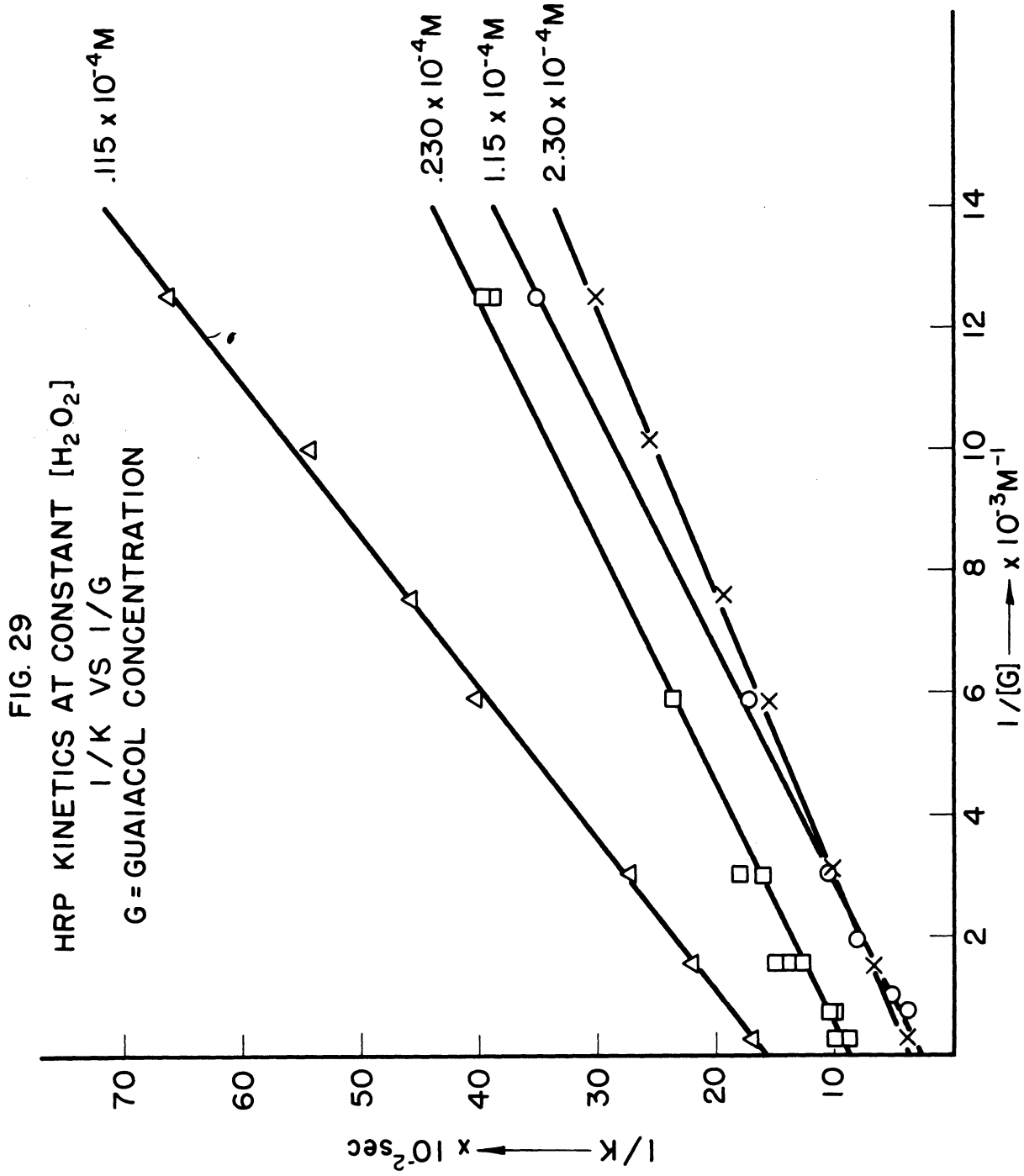

FIG. 29
HRP KINETICS AT CONSTANT $[H_2O_2]$
1/K VS 1/G
G = GUAIACOL CONCENTRATION

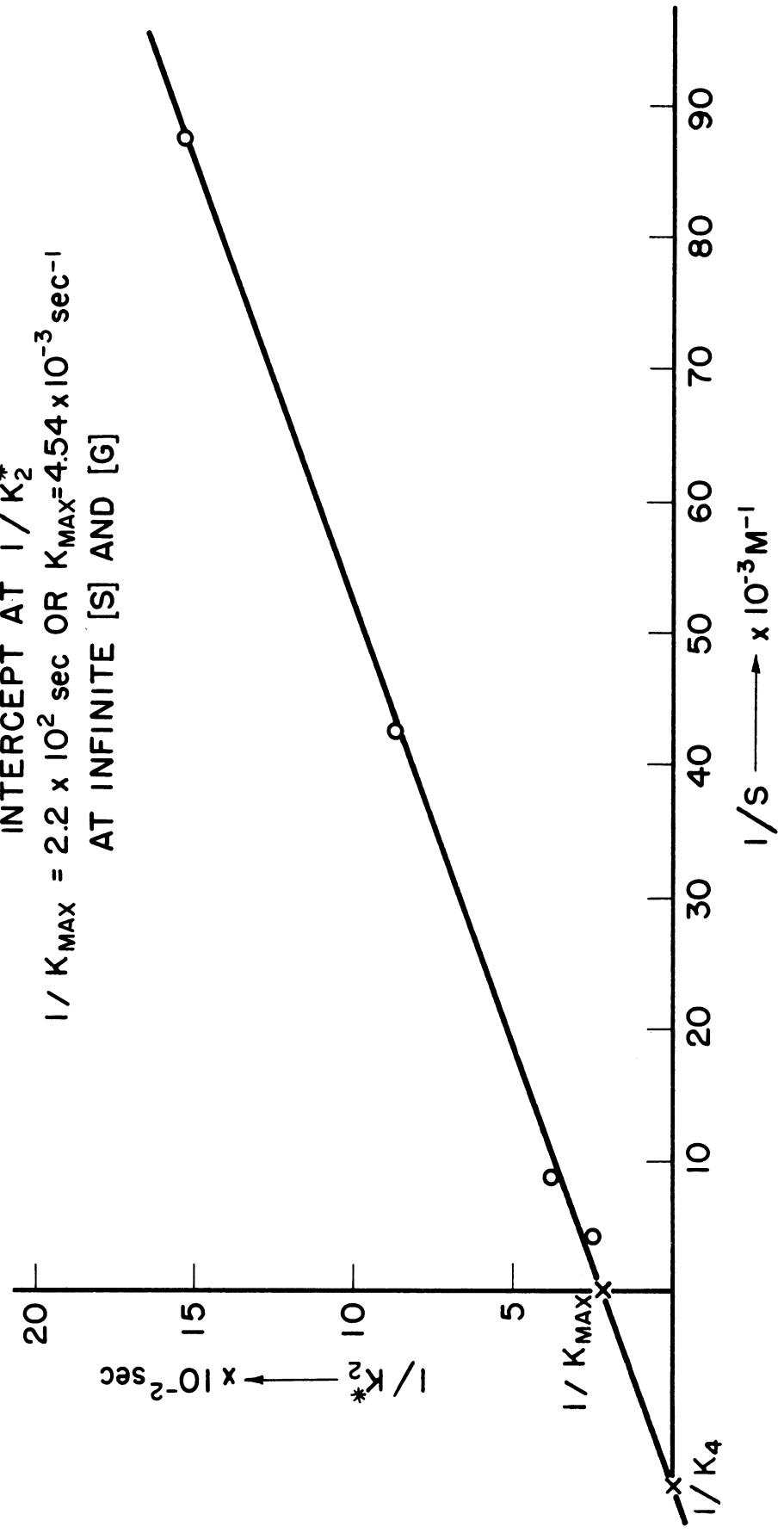

FIG. 30

HRP KINETICS AT INFINITE [G]

$1/K_2^*$ VS $1/S$

INTERCEPT AT $1/K_2^*$

$1/K_{MAX} = 2.2 \times 10^2$ sec OR $K_{MAX} = 4.54 \times 10^{-3}$ sec^{-1}

AT INFINITE [S] AND [G]

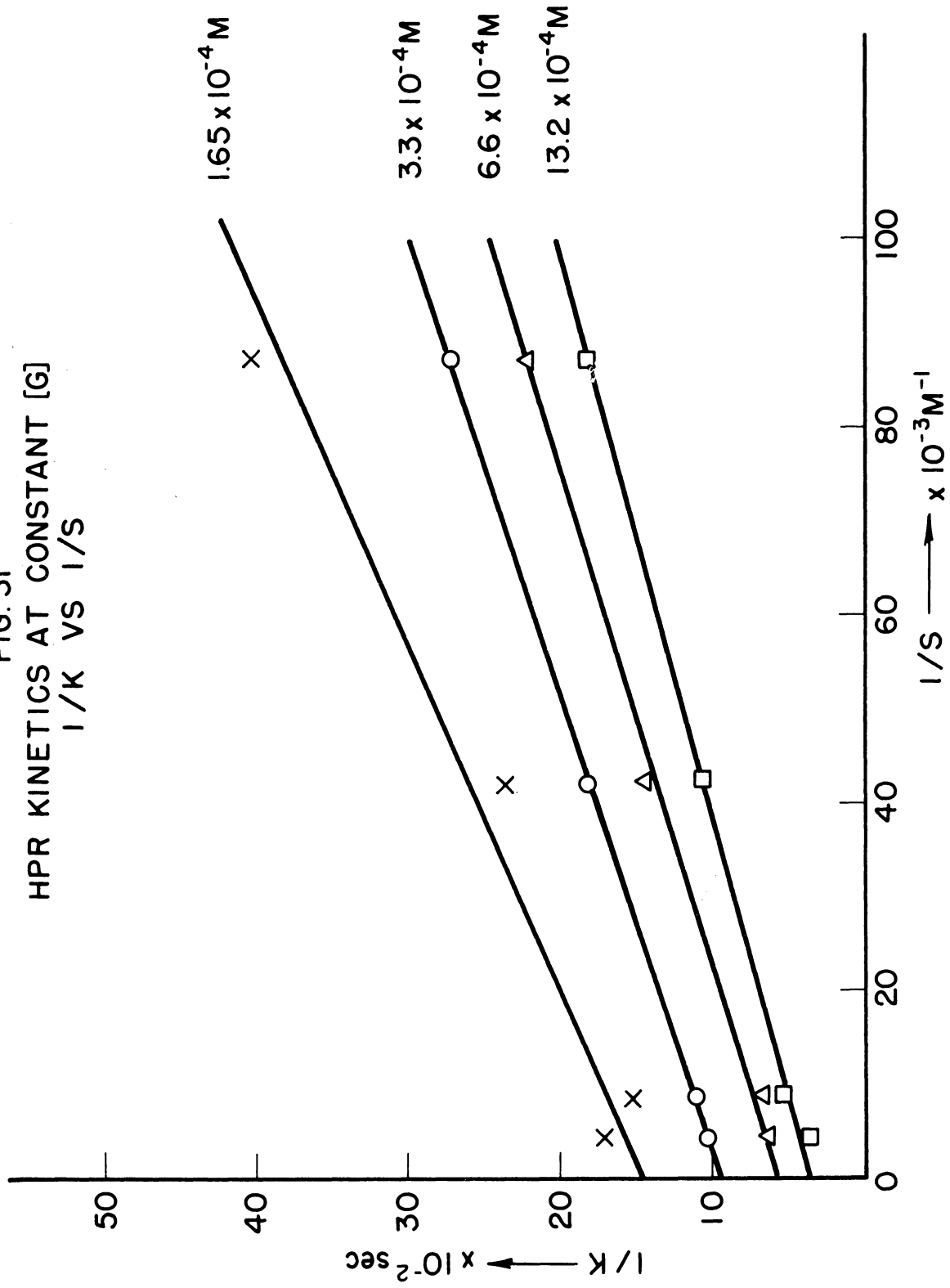

FIG. 31
HPR KINETICS AT CONSTANT [G]
1/K VS 1/S

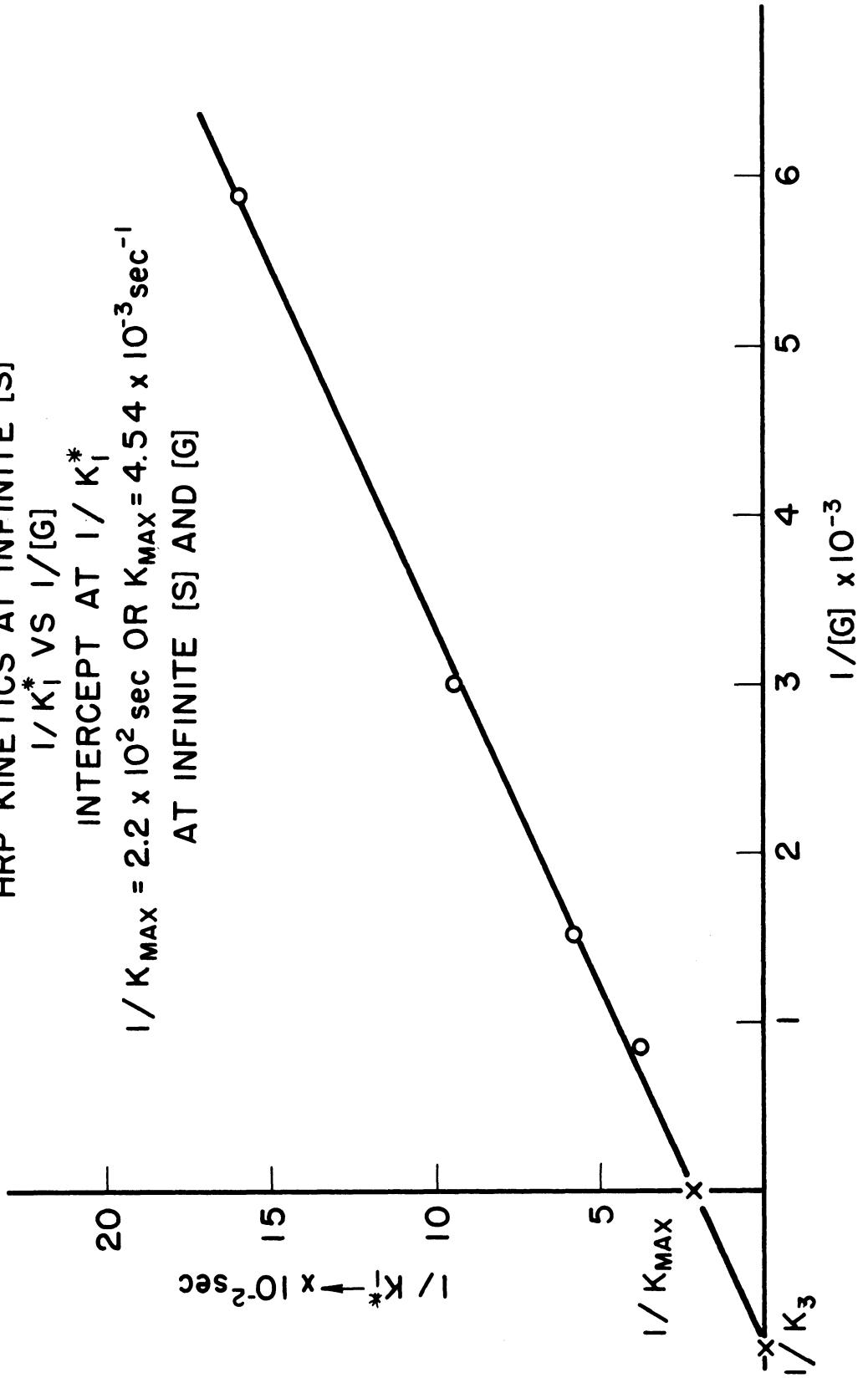

FIG. 32
HRP KINETICS AT INFINITE [S]
$1/K_1^*$ VS 1/[G]
INTERCEPT AT $1/K_1^*$
$1/K_{MAX} = 2.2 \times 10^2$ sec OR $K_{MAX} = 4.54 \times 10^{-3} sec^{-1}$
AT INFINITE [S] AND [G]

3) A ternary complex is formed which has a finite existence.

4) Events within the ternary complex are rate limiting.

5) The "product ternary complex" dissociates to yield the products.

The over-all reaction can be represented:

$$S + AH_2 \xrightleftharpoons{HRP} SH_2 + A$$

$E + S \rightleftharpoons E.S$ $\qquad K_1 = [E][S]/[E.S]$

$E + AH_2 \rightleftharpoons E.AH_2$ $\qquad K_2 = [E]\,[AH_2]/[E.AH_2]$

$ES + AH_2 \rightleftharpoons E.S.AH_2$ $\qquad K_3 = [E.S]\,[AH_2]/[E.S.AH_2]$

$EAH_2 + S \rightleftharpoons E.S.AH_2$ $\qquad K_4 = [E.AH_2]\,[S]/[E.S.AH_2]$

$$E.S.AH_2 \underset{k_2}{\overset{k_1}{\rightleftharpoons}} E.SH_2.A \qquad K_5 = k_2/k_1 = Keq$$

$E.SH_2.A \rightleftharpoons E.SH_2 + A$ $\qquad K_6 = [E.SH_2]\,[A]/[E.SH_2.A]$

$E.SH_2.A \rightleftharpoons E.A + SH_2$ $\qquad K_7 = [E.A]\,[SH_2]/[E.SH_2.A]$

$E.SH_2 \rightleftharpoons E + SH_2$ $\qquad K_8 = [E]\,[SH_2]/[E.SH_2]$

$EA \rightleftharpoons E + A$ $\qquad K_9 = [E]\,[A]/[E.A]$

$V_f = k_1\,[E]_T$ $\qquad$ When $[S] = [AH_2] \longrightarrow \infty$

$V/V_f = [E.S.AH_2]/[E]_T$ = Fractional initial reaction velocity where

$[E]_T = [E] + [E.S] + [E.AH_2] + [E.S.AH_2]$ = total enzyme concentration.

Writing the rate equation and using the above values of the dissociation constants one may develop a system of two equations which can be solved graphically by plotting the double reciprocal forms of the rate equation and the values of all the above constants

can be determined. The author feels that an extensive work to determine all the constants is beyond the scope of the present research. However, from the double reciprocal plots already given (see Fig. 29, 30, 31 and 32), one-half of the above constants can be determined since V_f coincides with K_{max} and V_1^* and V_2^* coincides with K_1^* and K_2^*. The general rate equation is:

$$V = \frac{V_f}{1 + K_4/[S] + K_3/[AH_2] + K_1K_3/[S]\,[AH_2]}$$

The double reciprocal forms of the rate equation are:

$$\frac{1}{V} = \frac{K_4 + K_1K_3/[AH_2]}{V_f} \cdot \frac{1}{[S]} + \frac{1 + K_3/[AH_2]}{V_f}$$

$$\frac{1}{V} = \frac{K_3 + K_1K_3/[S]}{V_f} \cdot \frac{1}{[AH_2]} + \frac{1 + K_4/[S]}{V_f}$$

When the above slope-intercept lines are plotted, the intercepts are the reciprocals of the particular maximum velocities V_i^*, corresponding to fixed concentrations of one of the substrates.

Then: $$\frac{1}{V_1^*} = \frac{1}{V_f} + \frac{K_3}{V_f} \cdot \frac{1}{[AH_2]}$$

$$\frac{1}{V_2^*} = \frac{1}{V_f} + \frac{K_4}{V_f} \cdot \frac{1}{[S]}$$

and when $1/V_1^* = 0$ $\quad K_3 = -[AH_2]^{\#}$

$1/V_2^* = 0$ $\quad K_4 = [S]^{\#}$ } Michaelis constants

that is $[S] = [AH_2] \rightarrow \alpha \quad V_1^* = V_2^* \rightarrow V_f = K_{max}$

From Fig. 4 $\frac{1}{[G]} = 0.9\times10^{3}\,M^{-1}$ therefore $K_3 = \frac{1}{900} = 1.1\times10^{-3}\,M$

#See Figures 29, 30, 31 and 32.

From Fig. 2 $\frac{1}{[S]} = 15\times10^{3}M^{-1}$ therefore $K_4 = \frac{1}{15000} = 6.6\times10^{-5}M$

And from both Figures 2 and 4 $\frac{1}{V_f} = \frac{1}{K_{max}} = 2.2\times10^{2}$ sec

or

$$V_f = 4.54\times10^{-3} \text{ sec}^{-1}$$

$$k_1 = \frac{V_f}{[E]_T} = \frac{4.54\times10^{-3}}{5.5\times10^{-9}} = 0.825\times10^{6} \text{ M}^{-1} \text{ sec}^{-1}$$

APPENDIX 2

A. G Value Determination

The impinging energy flux $\mathcal{F}$ of the x-ray beam on the gold absorber or the ferrous-ferric dosimeter can be determined as follows:

$$\mathcal{F} = \frac{P}{S_1} = \frac{N_o \; f \; V \; \Delta A}{\epsilon \delta \; G \; S \; t} \; e^{\mu x} \qquad (23)$$

where:

$\mathcal{F}$ = the incident energy per unit area per unit time in ergs/cm^2 per hour.

P = the power of the beam in watts.

S_1 = area of the gold absorber = 6.75 cm^2

N_o = Avogadro's number = 6.02 x 10^{23} atoms/gram mole

ϵ = extinction or absorption coefficient of ferric ion at 25°C = 2174 M^{-1} cm^{-1} at 305 mμ

δ = light path through the solution = thickness of Beckman cuvette = 1 cm

G = number of ferrous ions oxidized per 100 ev absorbed in solution

V/S = 1.1 cm = $\frac{\text{volume}}{\text{area}}$ of the dosimeter

Δ A = absorbance change after exposure to x-ray beam of power P for time t in hours

f = energy units convertion factor = 100 ev = 100x1.6x10^{-12}ergs

$e^{\mu x}$ = air absorption correction factor

μ = air absorption coefficient

x = air path

Solving Equation (23) for G and replacing the numerical values of the symbols taking into consideration that 1 ev = 1.6×10^{-12} ergs one gets:

$$G = \frac{N_o f}{\epsilon \delta \Phi} \frac{V}{S} \frac{\Delta A}{t} e^{\mu x} = \frac{6.02 \times 10^{23} \times 1.6 \times 10^{-10} \times 1.1}{2174 \times 10^3 \text{ cm}^3} \frac{\Delta A/t}{\Phi} e^{\mu x}$$

or $$G = 4.87 \times 10^7 \frac{e^{\mu x}}{\Phi} \frac{\Delta A}{t} \frac{\text{ferric ion yield}}{100 \text{ ev absorbed}}$$

example: $\Phi = P/S_1 = 5.16 \times 10^4$ ergs/cm^2 hr (measured by gold absorber)

$\frac{\Delta A}{t} = 8 \times 10^{-3}$ per hour (measured by Fricke dosimeter)

$e^{\mu x} = 1.259$ for Cr fluorescent radiation

(x-ray tube operated at 50 KVP, 50 mA, chromium radiator was used.)

$$G = 4.87 \times 10^7 \times \frac{1.259}{5.16 \times 10^4} \times 8 \times 10^{-3} = 9.52 \frac{\text{ferric ion yield}}{100 \text{ ev absorbed}}$$

B. Dose Rate Determination

1. LiF Crystal Spectrometer Technique

A sensitive G.M. tube (G.E. SPG-1 Counter (105)) was used to count the number of photons incident in the sample. A window $1 \times 0.3 = 0.3$ cm^2 defined the area of the beam which was counted. Initially the count rate was far beyond the range recommended by the manufacturer. To reduce the count rate a lead shield was used with a pinhole centered at the above window. The thickness of the lead shield was selected so that all the fluorescent radiation was absorbed. Thus, the counter counted only x-rays that could pass through the pinhole and enabled us to determine a geometrical factor g. The factor g was determined experimentally at 10 KVP, 1 mA where the beam intensity was the lowest possible.

If the dose rate, D.R., is defined as the number of photons absorbed in the sample per hour, then:

$$D.R. = (C.R.)\ \frac{g}{\epsilon}\ \frac{S_1}{S_2}\ \times 3600 \times e^{-\mu x}\ \text{photons per hour per sample}$$

where:

C.R. = count rate in cps through the pinhole

g = geometrical factor reducing the count rate, i.e.,

$$g = \frac{C.R.}{C.R.\ \text{through pinhole}} \approx 700$$

ϵ = counter efficiency given in ref. (105), counts per photon

S_1 = sample area in cm^2

S_2 = counter window area = 0.3 cm^2

$\bar{e}^{\mu x}$ = absorption factor of the sample

μ = absorption coefficient in water

x = thickness of sample

2. Fluorescent radiation technique

The Fricke dosimeter was used with the HRP sample holder. The dose rate, D.R., is defined here in rads/hr

$$D.R. = \frac{No}{\delta\epsilon}\ \frac{f}{G}\ \frac{\Delta A}{t}\ \text{rads/hr}$$

where:

No = Avogadro's number = 6.02×10^{23} atoms/gram mole

δ = light path through the solution = thickness of Beckman cuvette = 1 cm

ϵ = extinction or absorption coefficient of ferric ion at 25° C = 2174 $M^{-1}\ cm^{-1}$ at 305 mμ

$No/\delta\epsilon$ = number of ferric ions per unit absorbance per liter

G = the G value as measured with the calorimeter = number of ferric ion yield per 100 ev absorbed in solution

$\frac{\Delta A}{t}$ = absorbance change after exposure to x-ray beam for time t in hours

f = energy units conversion factor = 100 ev = $100 \times 1.6 \times 10^{-12}$ ergs

$$D.R. = \frac{6.02 \times 10^{23}}{2174 \times 10^{3}\ cm^{3}} \quad \frac{1}{G} \quad \times \frac{1.6 \times 10^{-10}}{100 \times 1\ gm/cm^{3}} \times \frac{\Delta A}{t} =$$

$$= 4.44 \times 10^{5} \quad \frac{\Delta A/h}{G} \quad rads/hr$$

since:

1 ev = 1.6×10^{-12} ergs, 1 rad = 100 ergs/gm. 10^{3} being the conversion factor from 1 to cm^{3}, and 1 gm/cm^{3} = density of water.

BIBLIOGRAPHY

1. Ackerman, E., Biophysical Science. Prentice-Hall, Inc., 1962.

2. Allen, A. O., The Radiation Chemistry of Water and Aqueous Solutions. Van Nostrand, 1961.

3. Andrews, H. L. Radiation Biophysics. Prentice-Hall, 1961.

4. Atkins, Marvin C. "The Energy Dependence of X-Ray Damage in an Organic Mercury Compound." Ph.D. thesis, The University of Michigan, 1960.

5. Atkins, M. C. and Clendinning, W. E., "Sources of Monochromatic X-Radiation." Technical Report No. 3, UMRI, 1960.

6. Bacq and Alexander, Fundamentals of Radiobiology. Pergamon Press, New York, 1961.

7. Barr, N. etc., "Use of the Fricke Dosimeter to Measure Photoelectric Absorption." Rad. Research, 14, (1961) 291.

8. Barron, E.S.G., "The Role of Free Radicals and Oxygen in Reactions Produced by Ionizing Radiations." Radiation Research, 1, (1954) 109.

9. Barron, E.S.G., "The Effect of Ionizing Radiations on Systems of Biological Importance." Annals of the New York Acad. of Sci. R. W. Miner (ed.), Vol. 59, Art. 4, p. 574.

10. Baum, J., "Catalase Inactivation by 4.9 to 7.5 Kev Fluorescent X-Radiation." Ph.D. thesis, The University of Michigan, 1964.

11. Bethe, H. A. and Ashkin, J., "Passage of Radiations through Matter" in E. Segre (ed.). Experimental Nuclear Physics, Vol. 1, 166. Wiley, N.Y., 1953.

12. Blois, M. E. etc. (eds.), "Free Radicals in Biological Systems." Academic Press, New York, 1961.

13. Braams, R., "Partially Damaged Molecules after Irradiation of Dry Invertase." Int. J. Rad. Biol. 6, No. 3 (1963), 297.

14. Burch, P. R. J., "Calculations of Energy Dissipation Characteristics in Water for Various Radiations." Rad. Research, 6 (1957), 289.

15. Burhop, E. H. S., The Auger Effect and Other Radiation less Transitions. Cambridge: University Press, 1952.

16. Burton, M. B., Hamill, W. H., and Mager, J. L., "A Consideration of Elementary Processes in Radiation Chemistry." Second Geneva Conf. Paper, A/CONF 15/P/916 (1958).

17. Burton, M. B., Comparative Effects of Radiation. J. Wiley and Sons, Inc., New York, 1960.

18. Butler, J. A. V. and Katz, B. (eds.), Progress in Biophysical Chemistry, Vol. 10. Pergamon Press, New York, 1960.

19. Chance, B., Science, 92 (1940), 445.

20. Chance, B., "The Kinetics of the Enzyme-Substrate Compound of Peroxidase." J. Biol. Chem., 151 (1945) 553.

21. Chance, B., "The Properties of the Enzyme-Substrate Compounds of Peroxidase and Peroxides." I. Spectra. Archives of Biochem. 20 (1949) 416.

22. Chance, B., "The Enzyme-Substrate Compounds of Horseradish Peroxidase and Peroxides." II. Kinetics. Archives of Biochem. 22 (1949) 224.

23. Chance, B., "Horseradish Peroxidase Kinetics." Arch. Biochem. and Bioph. 41 (1952) 416.

24. Chance, B. and Maehly, A. C., Methods in Enzymology. Vol. 2, p. 771. Academic Press, New York, 1955.

25. Chance, B., "Velocity Constants in Enzyme Reaction." Arch. Biochem. Biophys, 71, 130 (1957).

26. Chance, B., "Investigation of Rates and Mechanisms of Reactions." Article in Technique of Organic Chemistry. A. Weissberger (ed.) Vol. VIII, Part II, p. 1314. Interscience Publ. Inc., New York, 1963.

27. Clark, G. L., Applied X-Rays. McGraw-Hill, 1955.

28. Claus, W. D. (ed.), Radiation Biology and Medicine. Addison-Wesley, 1958.

29. Clendinning, W. R., "A Study of the Free Radical Yield Produced in 1-Bromobutane by Irradiation with Monochromatic X-Rays." Ph.D. thesis, The University of Michigan, 1960.

30. Compton and Allison, X-Rays in Theory and Experiment. C. Van Nostrand, New York, 1946.

31. Crook, E. M. (ed.), Metals and Enzyme Activity. Cambridge: University Press, 1958.

32. Dainton, F. S., "Chemical Effects of Radiation." Rad. Research Supplement, 1 (1959), 1-25.

33. Dale, W. M., "The Effect of X-Rays on Enzymes." Biochem. J., 34 (1940), 1367.

34. Dale, W. M. and Russel, C., "A Study of the Irradiation of Catalase by Ionizing Radiations in the Presence of Cysteine, Cystine, and Glutathione." Biochem. J., 62 (1956), 50.

35. Dixon, M. and Webb, E. G., Enzymes. Academic Press, New York, 1958.

36. Dosimetry, Assimilation of Articles on Dosimetry. Nucleonics, 17, No. 10 (1959), 58.

37. Emmons, A. H., "Resonance Radiation Effects of Low Energy Monochromatic X-Rays on Catalase." Ph.D. thesis, The University of Michigan, 1959.

38. Evans, R. D., The Atomic Nucleus. McGraw-Hill, 1955.

39. Feldman, C., "Range of 1-10 Kev Electrons in Solids." Phys. Rev., 117, No. 2 (1960), 455.

40. Fine, S. and Hendee, C. F., "X-Ray Critical-Absorption and Emission Energies in Kev." Nucleonics, 13 (March, 1955), 36.

41. Fricke, H. and Morse, S., "The Chemical Action of Roentgen Rays on Dilute Ferrosulfate Solutions as a Measure of Dose." Am. J. Roent., 18 (1927), 430.

42. Fruton and Simmonds, General Biochemistry. J. W. Wiley, New York, 1954.

43. Garsou, J., "Contribution a l'etude de l'efficacite des rayons x monochromatiques sur quelques systemes d' halogenures organizues solides et liquides." Ph.D. thesis, Univ. of Liege, Belgium, 1959.

44. George, P., "The Nature of the Second Hydrogen Peroxide Compound Formed by Cytochrome, Peroxidase and Horseradish Peroxidase." Biochem. J., 54 (1953), 267.

45. George P., "Intermediate Compound Formation with Peroxidase and Strong Oxidizing Agents." J. Biol. Chem. (1953), 413.

46. Gomberg, H. J., "Resonance in Radiation Effects." Technical Report No. 1, UMRI, 1960.

47. Gomberg, H. J. et al., "Resonance in Radiation Effects." Technical Report No. 5, UMRI, 1960.

48. Gomberg, H. J., "Resonance in Radiation Effects." Technical Report No. 1, Puerto Rico Nuclear Center, 1963.

49. Gomberg, H. J., "Total Absorption X-Ray Calorimeter." Phoenix M. L., The University of Michigan, 1964. (To be published.)

50. Gullity, B. D., Elements of X-Ray Diffraction. Addison-Wesley, 1956.

51. Haldane, J. B. S., Enzymes. Longmans Green, London, 1931.

52. Henri, V., Lois generales de l'action des diastases. Hermann, Paris, 1907.

53. Hine and Bronwell (ed.), Radiation Dosimetry. Academic Press, 1956.

54. Hirs, C. H. W., "Inside the Protein Molecule." BNL 649 (T-208) No. 3, 1.11.61.

55. Hoel, P., Elementary Statistics. J. Wiley and Sons, Inc., New York, 1960.

56. Hollaender, A., Radiation Biology. McGraw-Hill, New York, 1954.

57. Hollaender, A., Radiation Protection and Recovery. Pergamon Press, New York, 1960.

58. Huennekens, F. M., "Investigation of Rates and Mechanisms of Reactions." Article in Technique of Organic Chemistry. A. Weissberger (ed.) Vol. VIII, Part II, p. 1231. Interscience Publ. Inc., New York, 1963.

59. Hutchinson, F., "Radiation Effects on Macromolecules of Biological Importance." Article in Annual Review of Nuclear Science." E. Segre (ed.), Vol. 13 (1963), 535.

60. Keilin, D. and Mann, T., Proc. Ray. Soc., London, B122 (1937), p. 119.

61. Kusnetsova, S. S. and Sokolova, I. K., "Improvement of Ferrous Sulfate Dosimeter." Translated from Radiobiologiya 2, No. 4 (1962) AEC-tr-5431, p. 175.

62. Laughlin, I. S. and Gonna, S., "Calorimetric Methods." Art in Radiation Dosimetry, Hine and Bronwell (eds.), Academic Press, New York, 1916.

63. Lea, D. E., "The Dependence of the Biological Effect of Radiation on Intensity and Wavelength." Am. J. Roentgend, 45 (1941), 605.

64. Lea, D. E. Actions of Radiations on Living Cells. Cambridge: University Press, 1955.

65. Liebhafsky, H. A. et al., X-Ray Absorption and Emission in Analytical Chemistry. J. Wiley and Sons, New York, 1960.

66. Maehly, A. C. and Chance, B., "The Assay of Catalases and Peroxidases." Article in Methods in Biochemical Analysis. D. Glick (ed.), Vol I, p. 357. Interscience Publ. Inc., New York, 1954.

67. Magee, J. L. K., Martin D. and Platoman, R. L., "Physical and Chemical Aspects of Basic Mechanism in Radiobiology." Nat'l Acad. of Sciences, Nat'l Research Council Publ., 305 (1953).

68. McGinnies, R. T., "X-Ray Attenuation Coefficients from 10 Kev to 100 Mev." Supplement to NBS Circular, 583 (1959).

69. Manoilov, S. E., "Importance of the Ionization of Iron Containing Compounds During X-Irradiation of an Organism." Proc. All-Union Conf. on Radiation Chemistry, 1st Moscow, 1957, Pt. 4, 189-191 (Engl. Transl., 1959).

70. Manoylov, S. Ye., "Concerning the Question of the Direct Action of X- Rays on Animal Organism." Works of All-Union Conf. on Medical Radiology, Moscow, 1957 (Engl. Transl.) AEC-tr-3661 (Book 1), 65-68.

71. Michaelis, L. and Menten, M. L., Biochem. Z., 49 (1913), pp. 333.

72. Miller, N., "Radical Yield Measurements in Irradiated Aqueous Solutions." Radiation Research, 9 (1958), 633.

73. Nickson, J. J. (ed.), Symposium on Radiobiology. J. Wiley and Sons, 1952.

74. Paraskevoudakis, P., "Temperature Effect on the Inactivation of Catalase Solutions During Irradiation by Cobalt-60 ν-Rays." M.S. Thesis, The University of Michigan, 1960.

75. Paraskevoudakis, P., "Progress Reports." The University of Michigan, School of Public Health, Ann Arbor, 1962-63.

76. Patt, H. M., "Biochemical Aspects of Basic Mechanisms in Radiobiology." Nat'l Acad. of Sci, Nat'l Res. Council Publ., 367, Washington, D. C., 1954.

77. Paul, K. G., et al., "The Assay of Peroxidase with Mesidine." Acta Chem. Scand., 8, No. 4 (1954), 649.

78. Pauly, H., "Uber eine Kalorimetrische Methode zur Intensitätsmesung weicher Röntgenstrahlen." Strahlentherapie, 110.

79. Platzman, R. L. and Frank, J., "A Physical Mechanism for the Inactivation of Proteins by Ionizing Radiation." Symposium on Information Theory in Biology, Pergamon Press, New York, 1958.

80. Pollard, E. C., "Ionizing Radiation Methods for Determining Biological Structure." Annals of the New York Acad. of Sci., R. W. Miner (ed.), Vol. 59, Art. 4, p. 469.

81. Pollard, E. C., et al., "The Direct Action of Ionizing Radiation on Enzymes and Antigens." Art. in Progress in Biophysics, etc." p. 72, J. A. V. Butler (ed.), Pergamon Press, New York, 1955.

82. Pullman B., The Modern Theory of Molecular Structure. Dover Publ., Inc., New York, 1962.

83. Reid, C., Excited States in Chemistry and Biology. Academic Press, New York, 1957.

84. Roos, C. E., "K-Fluorescence Yield of Several Metals." Phys. Rev., 105, No. 3 (1957), 931.

85. Roughton, F. J. W. and Chance, B., "Rapid Reactions" in Technique of Organic Chemistry. (A. Weissberger, et al., editors), Vol. VIII, Part II, Ch. XIV., Interscience Publ., Inc., New York, 1963.

86. Scharp, K. and Lee, R. M., "Investigation of the Spectrophotometric Method of Measuring the Ferric Ion Yield in the Ferrous Sulfate Dosimeter." Rad. Research, 16 (1962), 115.

87. Seely, G. H., "Photochemistry of Prophyrins." US AEC UCRL 2417 (1953), 120.

88. Serment, V. and Emmons, A. H., "Data and Graphs on the Dose Rates In and Around the 5000 Curie Co-60 Source." Unpublished report, Phoenix Memorial Laboratory, The University of Michigan (1958).

89. Setlow, R. B., "The Radiation Sensitivity of Catalase as a Function of Temperature." Proc. Nat'l Acad. Sci., U. S., 38 (1952), 166.

90. Setlow, R. B., "Radiation Studies of Proteins and Enzymes." Annals of the N. Y. Acad. of Sci., R. W. Miner (ed.), Vol. 59, Art. 4, p. 471.

91. Setlow, R. B. and Pollard, E. C., Molecular Biophysics. Addison-Wesley, Reading, Mass., 1962.

92. Siegbahn, K., Beta and Gamma-Ray Spectroscopy. Interscience, New York, 1955.

93. Slater, E. C., "The Physical Chemistry of Enzymes." Disc. Faraday Soc., No. 20 (1955), 231.

94. Sutton, H. C., "Effects of Radiations on Catalase Solutions." I. Kinetic Studies of Inactivation, Biochem. J., 64 (1956) 447: II. The Protecting Action of Complexing Agents, Biochem. J., 64 (1956), 456.

95. Tarasov, B. N., "Principles of Biological Action of Radioactive Radiation." U. S. Dept. of Commerce, 59-11230.

96. Theorell, H., "About the reversible split of hemeprotein in HRP." Arkive Kemi. Mineral. Geol. B14, No. 20 (1940).

97. Theorell, H., Enzymologia, 12 (1941), 250.

98. Theorell, H., "The Reversible Split of Heme-Protein in HRP." Enzymologia, 10 (1942), 250.

99. Theorell, H., Arkiv. Kemi. Mineral Geol. A16, No. 2, No. 3 (1942).

100. Theorell, H., Advances in Enzymol., 21 (1958), 31.

101. Vannotti, A., Porphyrins: Their Biological and Chemical Importance. Hilger and Watts, Ltd., London, N. W. 1 (1954).

102. Vestling, C. S., "Determination of Dissociation Constants for Two-Substrate Enzyme Systems." Article in Methods of Biochemical Analysis, David Glick (ed.), Vol. X, p. 137. Interscience Publ. Inc., New York, 1962.

103. Wegst, W. F. J., "Wavelength Dependent Effects of Low Energy X-Rays on Mammalian Tissue Cells. Ph.D. thesis, The University of Michigan, 1963.

104. West, E. S., Textbook of Biophysical Chemistry. Macmillan, New York, 1956.

105. XRD-5 Instruction Manual, General Electric X-Ray Dept., Milwaukee, Wisconsin.

106. Zimmer, K. G., Studies on Quantitative Radiation Biology. Oliver and Boyd, Ltd., London, 1961.